Technische Universität München
Fakultät für Physik

Max-Planck-Institut für Biochemie
Abteilung Membran- und Neurophysik

Chemical Synapses on Semiconductor Chips

Rahul Alexander Kaul

Vollständiger Abdruck der von der Fakultät für Physik der Technischen Universität München zur Erlangung des akademischen Grades eines

Doktors der Naturwissenschaften

genehmigten Dissertation.

Vorsitzender:		Univ.-Prof. Dr. Manfred Kleber
Prüfer der Dissertation:	1.	Hon.-Prof. Dr. Peter Fromherz
	2.	Univ.-Prof. Dr. Andreas Bausch

Die Dissertation wurde am 05.02.2007 bei der Technischen Universität München eingereicht und durch die Fakultät für Physik am 08.03.2007 angenommen.

Abstract

The nervous system's computational power largely depends on its interconnectivity. Chemical synapses between individual neurons represent the minimal computational units of the brain. Interfacing single chemical synapses with semiconductor devices to control and monitor their activity non-invasively would provide a tool to understand the dynamics underlying neuronal network function.

This thesis project evolved around all aspects of neuron-semiconductor hybrids from synaptically connected cell-cell to cell-chip interactions. A complete experiment - a so-called loop - would consist of chip driven stimulation of the presynaptic cell, the triggering of synaptic transmission, and the recording of postsynaptic activity by chip. The chips featured two-way contacts to control and monitor these small neuronal networks: Electrolyte-Oxide-Semiconductor (EOS) capacitors for stimulation and field-effect transistors (FETs) for recording.

At the single cell level, the 100 μm large, identified neurons from *Lymnaea stagnalis* led to extracellular electrical signals up to tens of millivolts due to their increased adhesion area compared to mammalian neurons. Close contact to the chip verified through cell-substrate distance measurements contributed to the increased signal amplitudes. On the other hand, the usage of the artificial cell-adhesion molecule poly-L-lysine diminished neuronal excitability causing oscillating patterns of activity and quiescence. The introduction of two novel artificial cell adhesion molecules allowed cell culture of chemical synapses on chip without oscillatory behavior.

Recent results demanded a comparison between ramp and square pulse stimuli for the stimulation of presynaptic activity. To create cellular activity on chips coated with a thin SiO_2 layer, repetitive bursts of multiple square-shaped pulses proved to be the most reliable minimal invasive method.

The three snail neurons VD4, LPeD1, and RPeD1 formed groups of neuronal pairs interconnected via excitatory or inhibitory synapses on chip. The activity of both types of synapses could be triggered and monitored through chip stimulation and recording. A specific pulse protocol potentiated the excitatory synapse VD4-LPeD1 to demonstrate chip induced and supervised neuronal learning.

While studying inhibition as a function of a decrease in postsynaptic firing rate, chip induced stimulation of postsynaptic RPeD1 completely prevented synaptic inhibition through presynaptic cell VD4.

A chip controlled double loop experiment with one excitatory and one inhibitory synapse between VD4-LPeD1 and VD4-RPeD1 proved the technique's scalability.

This semiconductor chip technology therefore provides a tool for simultaneous observation and control of multineuronal network dynamics at the resolution of single nerve cells.

Contents

Chapter 1

Introduction

I could paint a picture with a pen
But a song will only scratch the skin
And there are still places I haven't been
Because I know what's in there is already in the air

Oh yeah, there's a storm on the way
And it's comin' no matter what I say

- Gnarls Barkley, *A Storm Coming* (2006)

"Chemical Synapses on Semiconductor Chips" - a description inspiring the imagination of scientists and fiction authors alike. Thinking about its meaning, the first picture appearing before the inner eye looks like "Connecting the brain to the computer".

Taking a closer look at an envisioned brain-computer link, we see, it can work both ways. Either the computer communicates with the brain, or the brain with the computer. The brain receives inputs and creates outputs mediated through sensors and actuators, which help to perceive the environment and to create physical interactions - like, for example, focusing on a soccer ball with an eye while moving to kick a pass. How does the computer fit into this scheme?

Although our imagination could spread wings and envision its interplay everywhere - replacing defunct sensory organs, bridging damaged neuronal contacts or even moving artificial legs - today's research has to stay down to earth to make the very first basic crawling efforts.

But what is it *really* about? What are the topics actually investigated in today's scientific labs? And how do they relate to the ideas mentioned above? Undoubtly this thesis will not report on the creation of artificial eyes or limbs - they seem too much fiction to be true. So do scientific facts exist to bolster these ideas?

Often investors, scientifically apt amateurs or the media ask: 'What can you do with this kind of research?' Depending on the inquirer's interest, we can provide one to all of the three possible answers: biosensorics, creating a tool for neuroscience research or working on computational aspects of cell-chip interactions. During the reply, one can actually feel the imaginative strain the audience then goes through to stretch at least one of the given answers to fit their own ideas about "Chemical Synapses on Semiconductor Chips".

Let's start with what it is all about, before painting an ill-fitting or even misleading picture.

We extract biological tissue and put it on electronic devices created from the semiconducting material silicon: So not chip in the brain, but brain on a chip. The biological material investigated in this thesis project, was taken from an animal model for neuronal interactions in cell culture, the sweet water snail *Lymnaea stagnalis*. So there are no human cyborgs, but maybe we can create robo-snails?
The answer is no, since individual neurons are placed on small semiconductor devices on the chip in close contact to each other. Even though whole animals are involved in the process of extracting the nerve cells, only single cells get in touch with the chip.
During overnight incubation cells stay on the chip, a chemical synapse, the basic neuronal cell-cell contact, forms between groups of two nerve cells. To protect the electronics from the salt solution - the electrolyte - needed for the survival of the nerve cells, a thin layer of silicon dioxide, commonly known as glass, covers the semiconducting material. This oxide layer has a thickness of 10 nanometers.

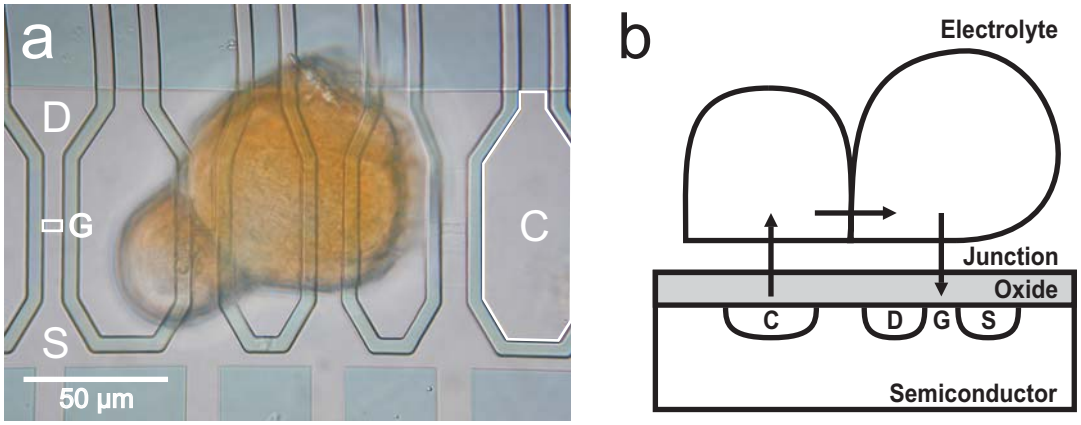

Figure 1.1: *Nerve cells on semiconductor chips.*

(a) A situation typical for the research presented in this thesis: A micrograph with a top view on a group of 2 nerve cells in close contact to each other. The picture was taken after 16 hours in cell culture on a semiconductor chip. After this time a chemical synapse formed between the two neurons. On the chip two structures have been highlighted: The small frame on the left hand side shows the gate G, the voltage-sensor of the field-effect transistor: a gate voltage change due to nerve cell activity modulates the current that runs between source S and drain D. The large frame on the right hand side encircles the capacitor pad C used for stimulation of single nerve cells.
(b) A schematic side view of the situation depicted in (a): the arrows indicate signal flow during a typical experiment. An externally created voltage pulse applied to the capacitor C underneath the left nerve cell triggers synaptic transmission that leads to activity in the right neuron - a voltage signal, which the transistor consisting of Source S, Drain D, and Gate G underneath that cell picks up and transmits to the outside. Note, that the schematic is not drawn to scale: Both junction and oxide are 10.000 times smaller than the neurons.

The cells as well as the electronic structures are in the range of 1/100th to 1/10th of a millimeter, or in other units 10 to 100 micrometers, so small that they are barely visible to the eye. The 10 nanometer thick oxide layer, which actually is amongst the thinnest structure found in this cell-chip system, serves another purpose besides protecting the chip from the cells and vice versa. It not only creates a physical barrier, but also defines two different electronic components on the chip side: Field-effect transistors for recording and capacitors for stimulation of nerve cell activity. Figure 1.1 introduces the major components. As can be seen from panel (b), the layers electrolyte, oxide and semiconductor (EOS) define an EOS field-effect transistor (FET), which has its text book analogy in a metal-oxide-semiconductor (MOS) FET. MOS-FETs form the basis of all modern computers found in almost everyone's home, these EOS devices created on the chip don't compute digitally like commercial chips.
Neuronal activity qualifies as an analog signal: If a nerve cell becomes active, it fires a so-called action potential, a signal spanning a voltage range of 100 millivolts. The Gate G (panel a), the voltage sensitive area of the field-effect transistor, picks up a fraction of that signal, depending largely on the distance between cell and chip. The thickness of the so-called junction measures around 50 nanometers or below.

The signal detection works as follows: A constant current runs through the conducting structures Source and Drain defining the transistor on the chip together with the gate area. Only when the gate G, situated in a narrow region in between the two conducting lines (see Figure 1.1a), 'senses' the voltage of the action potential, this current changes according to the shape and amplitude of the voltage signal in the junction. After converting the analog cellular signal into the digital language of computers, it displays the neuronal activity on its screen for an external observer.
For the stimulation, the capacitors on the chip evoke nerve cell activity through electrical voltage pulses. The same observer can send a pulse from the computer to the capacitor underneath the first cell to trigger the synapse. The activated synapse can then be recorded by a transistor underneath the second cell, which will be visible subsequently on the computer screen.
In a complete experiment, an observer sends a signal from the computer to the first cell, then via the synapse to the second cell and back into the computer to the observer. This complete circuit can be interpreted as a closed feedback loop, the simplest circuit imaginable built from the available biological and electronic parts.

Coming back to the main theme of this introduction: How does this fictitious experiment relate to the three reasons - biosensorics, creating a tool for neuroscience research or working on computational aspects of cell-chip interactions - for this kind of research?

Chemical synapses are the main targets for medication in the central and peripheral nervous system with a scope ranging from the reduction of synaptic transmission in the case of pain [Sch02] to neurodegenerative disorders like Parkinson's disease ([Kan00b], on side effects of drug use see [Ola06]). Therefore this project can be

interpreted as basic research on an automated system for two potential applications: the large-scale screening of potential drugs as well as the testing of side-effects of drugs which have targets outside of the brain in long-term neuronal cell culture.

When it comes to creating a tool for neuroscience research, a look at the techniques available for stimulation and recording of neuronal activity helps to understand the significance of this method: On the stimulation side, there exist very few mechanisms of creating neuronal activity besides the use sharp intracellular electrodes. In general, the available methods fall either into the category of electrical or optical stimulation.
Alexei Verkhratskz [Ver06] wrote a vivid review on the history of electrophysiology. In his review he quotes Ling [Lin49] as one of the first researchers having conducted measurement with sharp intracellular electrodes in 1949, while the usage of extracellular electrodes became known through experiments made by the Dutch natural scientist Jan Schwammerman as early as the 1660s. Amongst the successes of the extracellular stimulation technique were observations on long-term synaptic changes in sedated, but alive rabbits [Bli73]. The intracellular recording technique's successes culminated in the low-noise recording of currents through the smallest cellular conducting units, the ion channels, by Hamill et al. in 1981 [Ham81].
Gustafsson and Jankowska [Gus76] compared parameters needed to evoke intra- versus extracellular stimulation. They found the largest excitability around the region joining the axon to the cell body for mammalian spinal cord neurons. Experiments like the long-term potentiation mentioned above [Bli73] demanded large voltage amplitudes to see lasting effects. Unfortunately these pulses do not only create cell activity close to the stimulated neurons, but also in a large area surrounding the electrode. This example can be seen as the prototype of extracellular electrode-tissue contacts, which come in various shapes and sizes, as well as medical applications like deep brain stimulation in patients suffering from Parkinson's disease [Bre04]. Unfortunately, if the stimulus amplitude exceeds a critical limit, the cells in direct contact to the extracellular electrode suffer irreversible damage. This issue is usually considered irrelevant for most experiments using this technique, but important for long-term effects of a patient's treatment.

On the optical side of stimulation, direct approaches like the release of caged compounds with UV flashes to trigger cellular activity exists [Par02]. Since the compounds need to be previously introduced into the cells through microelectrodes, this technology cannot be applied independently from intracellular contacts. There another emergent technology to create cellular activity with photons exists: Through light application onto a conducting surface, this process increases locally stimulating currents; therefore the technique was named photo-stimulation [Col01]. Unfortunately, only little is known about the exact mechanisms underlying the extracellular stimulation [Col06, God06]. Still, a high-density array for photo-stimulation as well as recording created in a different research lab already exists for quite some time [Buc01b, Buc01a].

On the recording side, quite a few electrical or magnetic detection methods for extracellular recording exist. Most of them average over large patches of active nervous tissue, like electroencephalography (EEG, [Rit06]), magnetoencephalography (MEG, [Ioa06]) or functional magnetic resonance imaging (fMRI, [Log04]) - although the latter two methods use magnetic fields, they still detect electrical currents.

Optical methods of detection mostly rely on the effect, that the fluorescence of a certain group of dyes depends on the localization of an electrical charge along the molecule. If several of these molecules get incorporated into the membrane of a nerve cell all aligned in the same direction, the electrical field across a neuron's membrane can increase the voltage-sensitive dye's fluorescence intensity during neuronal activity. Their high spatial and temporal resolution lets them qualify for optimal probes for single cell activity. Yet the selective staining of exclusively neuronal membranes remains an issue of active research [Hin06].

How does stimulation with capacitors and recording with field-effect transistors fit into the zoo of available techniques? Both for stimulation and recording the spatial as well as temporal resolution is fine enough to evoke and record neuronal activity on a single cell level and even below: The size of the devices defines whether whole cells [Ste97] or only parts [Ulb05, Wei96] of them get excited or probed. Only one technique, the use of inert metal electrodes for both stimulation and recording work on the same scale as the chips created in this department ([Gho06] - just one of many applications, e.g. hippocampal brain slice stimulation and recording). The main difference, the existence of the metal layer between the stimulation and recording circuits, also create issues when trying to understand the system on a theoretical level: The oxide barrier between electrolyte and electronics present in our system creates a defined interface for modeling. Electrical pulses applied to metal electrodes on the other hand not only create electrical, but also electro-chemical signals rendering the theoretical description of its interactions with cells more difficult.
Problematic on the other hand is fitting both types of probes into living tissue, which is a major advantage of the large scale integrative approaches like EEG, MEG or fMRI, which all three are completely non-invasive and can be used on human beings. The neuron-silicon contact demands a minimal distance between cell and chip to even record any nervous activity at all.

None the less, already first projects try to incorporate this kind of design into living tissue (Figure 1.2, [Zre02]). Along these lines, we come to the last and most vague issue: the investigation of computational aspects of cell-chip interactions. Whether thinking about single cell self-excitation [Ulb01], computing with single neuronal contacts [Kau04] as well as bridging neuron-neuron contacts with silicon 'axons' [Bon02], all these facets might qualify for the computational aspects of cell-chip interactions.
In the long run, which potential applications wait at the end of the road? Bridging broken nerves, monitoring neuronal computations as well as influencing the outcome of these 'computations' would be conceivable even though barely realisable - ethical

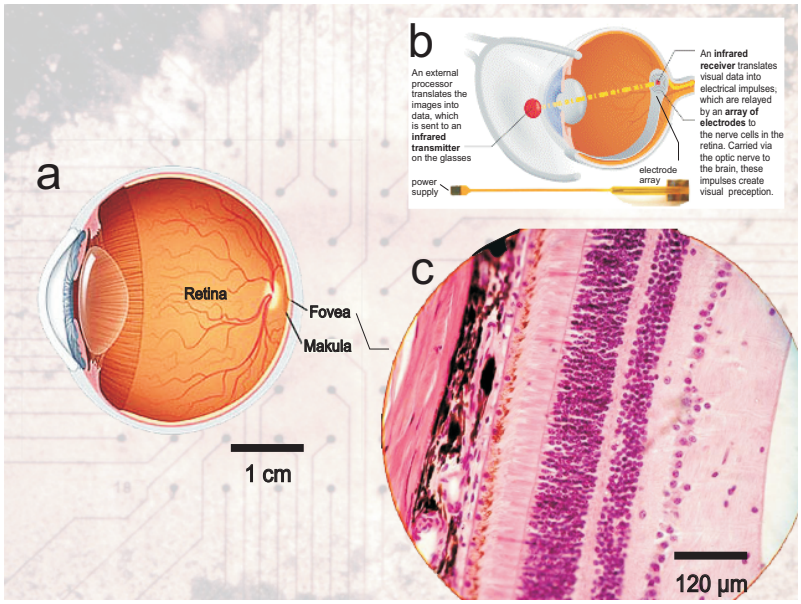

Figure 1.2: *Application of cell-chip contacts - retinal implant.*

Illustration of one example for a cell-chip contact realized with a similar, but different chip technology. (a) shows a lateral view of the human eye, with the retina at the back-side of the eye's glass body. The fovea, the area with the highest density of photo-receptors, the converters of light into electrical signals, is the target of the chip. The macula, a blind spot due to the bundling of millions of axons there, indicates the location where the optical nerve exits the eye. (b) A cartoon of the retina implant as planned by the group around Prof Zrenner from the University of Tübingen: A pair of glasses shines a light beam coding for visual information on the chip located in the fovea. The electrode array converts these data packets into stimulation patterns, replacing the degenerated photo-receptors (see c). The signals then propagates along the remaining retinal network and the optical nerve towards the brain. (c) In the case of the degenerative disease of retinosis pigmentosa, which leads to a drastic decrease of photo-receptor density. Thus the conversion of light into electrical signals fails. The close-up shows a 400x amplification of a stained retina - note that the layout is mirrored as compared to the eye shown in (a) - with the thicker purple layer being the photo-receptors in a healthy eye. The thinner purple layer on the right belongs to the network of neuronal cells that need to be present for the chip to work.
Sources of the files:
(a) http://www.mayoclinic.org/retinal-diseases/index.html,
(b) http://www.mtbeurope.info/news/2006/601007.htm,
(c) http://biology.clc.uc.edu/fankhauser/Labs/Anatomy_&_Physiology/A&P202/Special_Senses/Eye/Histology_EYE.htm.

reasons aside - due to the issue of close contact mentioned above. Therefore all these aspects have to remain on a model system level, unless more is known about the long-term effects of cell-chip contacts on both tissue and device.
The case of eye defects caused by *retinosis pigmentosa*, for example, an inherited disease leading to complete degeneration of the photoreceptive layer and thus to blindness in adult humans, creates a real-life challenge to put these results to the test. Even though the technique chosen for implantation was that of metalized micro electrode arrays (MEAs), the issues encountered remain the same as for field-effect transistor arrays: Low yield of cell-chip contacts necessary to create an signal large enough for transmission along the optical nerve, the problem of power supply for the implanted device, as well as unknown long-term side-effects with these inorganic implants.

The retina, a model system not only for sensory perception but also 'neuronal computation', forms a highly interconnected network that extracts dynamic patterns from the light stream that enters the eye. It breaks down the light patterns into chunks like light-dark borders or the movement of such borders across the two-dimensional photo-receptive layer.
Considering the first ongoing trials of implanting such a device into a human eye which restored crude light-dark vision to a few otherwise blind people, it could create a feeling of awe considering the successes of modern technology. Only the high adaptability of the biological network though, allowed the visual system to extract these patterns from a rudimentary electrical pulse stream that barely resembles the complex signal obtained from the photoreceptors. Therefore this milestone remains more a success of nature to adapt to a yet different external input then a technological breakthrough. The chip does not extract visual information, it merely converts light into electrical signals.
After this first contact, the question remains, how can we interact more specifically with the retinal network?

Introducing electronic structures like MEAs or semiconductor chips to replace the photo-receptive layer, the focus should not only be on the creation of electrical activity in response to optical patterns alone, but also on electrical feedback from the biological network. The higher levels of visual information processing have as many if not even more connections to the retina as vice versa. An implanted chip needs to be able to detect these 'downstream' patterns as well.
If the detection process of the network activity does not take place - along with appropriate actions due to changes in e.g. the excitability of the interneuronal cell layer - this implant technology solely relies on the adaptability of the neuronal network to cope with this alien, static input.
If we could do better by stimulating in response to the recorded signals, why not make use of the technology available? Only when making two-way contacts to the biological network, we can even start claiming to 'communicate' with the brain, instead of just talking without listening.

The here investigated neuron-semiconductor chip hybrids might give the impression of being less technically advanced than the implantable devices. This misconception comes from a difference in scientific approaches: following the reductionist's way to unravel the mechanisms at work behind it, this line of research always preferred complete understanding of the basic mechanisms to gaining insight through creating technical applications. Both approaches form a complementary set of experiences - the combination of well-understood cell-chip interactions along with the expertise on deploying these devices within organisms might create novel implants with the additional functionality of bidirectional communication.

Thus we come back to the comparatively basic issue of interfacing single chemical synapses with semiconductor chips. The structure of the thesis follows that of a scientific publication with introduction, materials & methods, results, and summary section.
After these preliminary thoughts about the larger context of neuron-semiconductor hybrids, a chapter explaining the cell culture, chip handling, and theoretical model of the cell-chip contact follows. The methodological part emphasises the animal model, since the nerve cell preparation has changed considerably as compared to previous thesis projects, reducing the presentation of the other methods to a minimum required to reproduce the given experiments.
The structure of the results part separates the section into investigations at the single neuron level, on single synapses of excitatory and inhibitory nature as well as on experiment on multiple neurons. Although the outline of thesis project mostly evolved around the synaptic interactions, only recent insights into the long-established cell-chip interactions made these experiments possible.
A short summary of the major findings in each results subsection as well as an outlook on a few next experimental steps based on the observations presented herein round off this report.
During the review of literature regarding recording and stimulation techniques, a quote by Luigi Galvani in [Ver06] in the context of his investigation on the electrical excitability of frog muscle contractions caught not only the eye, but also the mood for the upcoming parts of the thesis:

> *I am attacked by two very opposite sects*
> *— the scientists and the know-nothings.*
> *Both laugh at me — calling me "the frogs' dancing-master".*
> *Yet I know that I have discovered one of the greatest forces in nature.*
>
> - Luigi Galvani, 1791.

Chapter 2

Materials and Methods

All work and no play
That's the way it is, ain't it?
...

- Gnarls Barkley, *The Last Time* (2006)

2.1 Cell Culture

Within this chapter the choice of model animal for chemical synapses in cell culture will be motivated along with the external conditions that need to be satisfied to guarantee a reliable, high yield of healthy neurons. In the remaining sections then the extraction and placement of the cells will be described.

2.1.1 *Lymnaea stagnalis*, Model Animal for Cell Culture of Individual Central Neurons

The Nobel Prize awarded to Eric Kandel in 2000 [Kan00a] for his work on unraveling the molecular processes involved in behaviour relevant memory formation and consolidation, put the spot light on the sea slug *Aplysia californica*, which became known as one of the model animals for investigating synaptic activity on a cellular level.

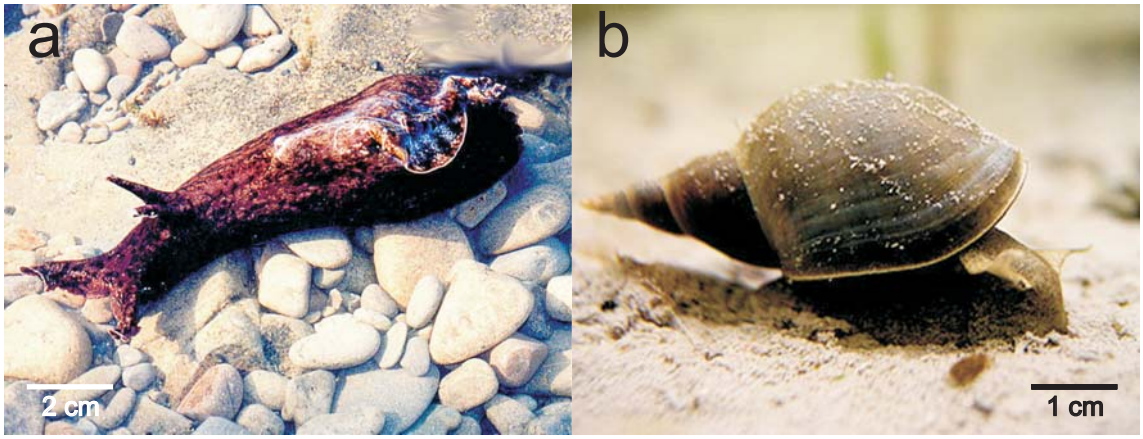

Figure 2.1: *Two model organisms for cell culture of single neurons.*

a.) shows Aplysia californica, *the Californian sea slug, a model animal for long-term studies on changes of synaptic connectivity in the peripheral nervous system, b.)* Lymnaea stagnalis, *the large pond snail, a model animal for cell culture of synaptically coupled central neurons.*

None the less only one laboratory associated with the work of Eric Kandel, the lab of David Schachtner [May92, Eli94] is working with *Aplysia* nerve cells in culture. The studies were carried out on a single peripheral sensory-motor synapse.

At the same time it had been known that the lab of Naweed Syed had created a small neuronal network *in vitro* consisting of three central interneurons, that were putatively necessary and sufficient to drive the breathing cycle of the pond snail *Lymnaea stagnalis* [Sye90]. Especially during the last few years, more knowledge had been published regarding the chemically connected *Lymnaea* neurons VD4 (*V*isceral

*D*orsal 4) [1] and LPeD1 (*L*eft *P*edal *D*orsal 1)[Ham99, Smi01], as well as the neurons RPeD1 (*R*ight *Pe*dal *D*orsal 1) and VD4 [Fen97], making these cells the most likely candidates for experiments on chemical synapses out of two reasons, easy identification and reliable synapse formation: Either, like in the case of LPeD1 and RPeD1, their size of around 100 μm makes them prominent amongst their neighbors, or in the case of VD4, the cell distinguishes itself from its surroundings due to its colouring, therefore their identification becomes possible. Additionally, since VD4 forms an excitatory synapse on LPeD1 and an inhibitory synapse on RPeD1 both *in vivo* [Sye91] and *in vitro* [Woo99, Sye90], these three neurons are the most likely candidates for creating both classes of synaptic contacts. Literature regarding the cell culture of *Aplysia* neurons on the other hand has become more scarce during the last few years: No additional neurons that would form chemical synapses in cell culture were identified and tested.

Considering the long-term goal to record from larger groups of neurons as well as the fact that *Lymnaea* - a sweet water slug as compared to *Aplysia* as a seawater animal - is kept and bred much easier in the lab, the decision to use the latter for the first experiments with chemical synapses in culture was obvious. Especially since the previous work of Prinz [Pri00], Jenkner [Jen01] and Zeck [Zec03] was based on using a group of motoneurons from Lymnaea for their research projects, some experience for keeping these animals was present in this department. It became known during the last few years though, that it would not be possible to link VD4 to multiple LPeD1 [Mun03], and vice versa (Syed, personal communication). Therefore the number of possible ways to interconnect these cells was limited more drastically than anticipated.

None the less, neurons from the pond snail *Lymnaea stagnalis* were the best choice for forming individual synapses in cell culture in a reliable manner. But before being able to conduct experiments on the chemical synapses between large, identified neurons, more about the maintenance and breeding of *Lymnaea stagnalis* had to be learned as will be presented in the following section.

2.1.2 Prerequisites for Cell Culture of Chemical Synapses

The main bottle neck during this doctoral research was achieving and maintaining a high yield of healthy synapses. The expertise in this lab before was to extract cells from *Lymnaea* brains from a cluster of motoneurons, which are known to form electrical synapses in vitro and in vivo [Sye89]. Due to the large number of available neurons and due to the extraction method devised to gain large numbers of cells, the demand on animal culture was totally different: The snails were kept in fish tanks containing snails of all ages. Even though the conditions were sufficient to get large numbers of A-Cluster neurons, the demand on the animal culture became higher by focusing on the large, identified neurons needed for chemical synapse formation

[1] the numeral N denotes the N'th largest cell in that part of the snail brain

and that can be found only once per animal: Besides the demand to keep animal culture conditions constant during the whole animal life, animals had to be selected strictly by age either for successful cell extraction or the creation of brain-conditioned medium, as will be described in the following subsections.
As a result, although the genotype *Lymnaea stagnalis* in culture remained the same, these conditions putatively lead to a substantially different phenotype of snails as compared to 5 years ago.

Culture Conditions and Breeding of the Pond Snail *Lymnaea stagnalis*

While before the snails were kept in 120 l fish tanks at different animal densities and in mixed ages, animals derived from an imported stock of *Lymnaea stagnalis* from the Vrije Unversiteit Amsterdam[2] are now kept in 15 l plastic basins containing 200 animals of the same generation under the following conditions: 12-12 hours light-dark cycle, 20°C water temperature sustained with self-regulating fish-tank heaters, water-flow in such a manner that $20 - 25$ l were added during 24 hours. A pump added air to the water at a moderate rate, not to perturb the water too much. The snails were alternately fed either with lettuce or a highly nutritious vegetarian fish food three times a week in two day intervals. The amount of food was chosen to be enough to last until noon the next day.

After a day without food during the weekend the animals begin mating, a behavior of lesser priority than eating. Like this on Mondays freshly laid egg masses could be collected from containers with a smooth, intransparent surface that had been added to the basins the same day. The egg masses were transferred into 0.5 l plastic containers left then undisturbed to develop. Like this each week a new generation of animals can be created from an existing stock of *Lymnaea*.

Animal Development and Selection

After the transfer into a small plastic container filled with a water volume of around 0.5 l, 12-15 egg masses take 14 days before the first animals will hatch. Therefore just after 12 days the fully developed egg masses (see Figure 2.2c for an example) are transferred into a new 15 l basin with bubbler and heater. The freshly hatched snails will then - when kept at constant temperature and fed sufficiently - grow at a rate of 1 cm per month until the grow into adult sized animals after 2.5 months (Figure 2.2a). At this age the snails will also be mature enough to start mating and to create new egg masses.

For the experiments with large, identified neurons two ages were of special interest. For the cell extraction sub-adult animals of size $16 - 21$ mm were needed (see Figure 2.2d), since the snail brains grow significantly during the last month of development: Both the diameter and the number of neurons increases rapidly during that time.

[2]the author is indebted to the gracious donation of numerous *Lymnaea* snails by Carool Popelier

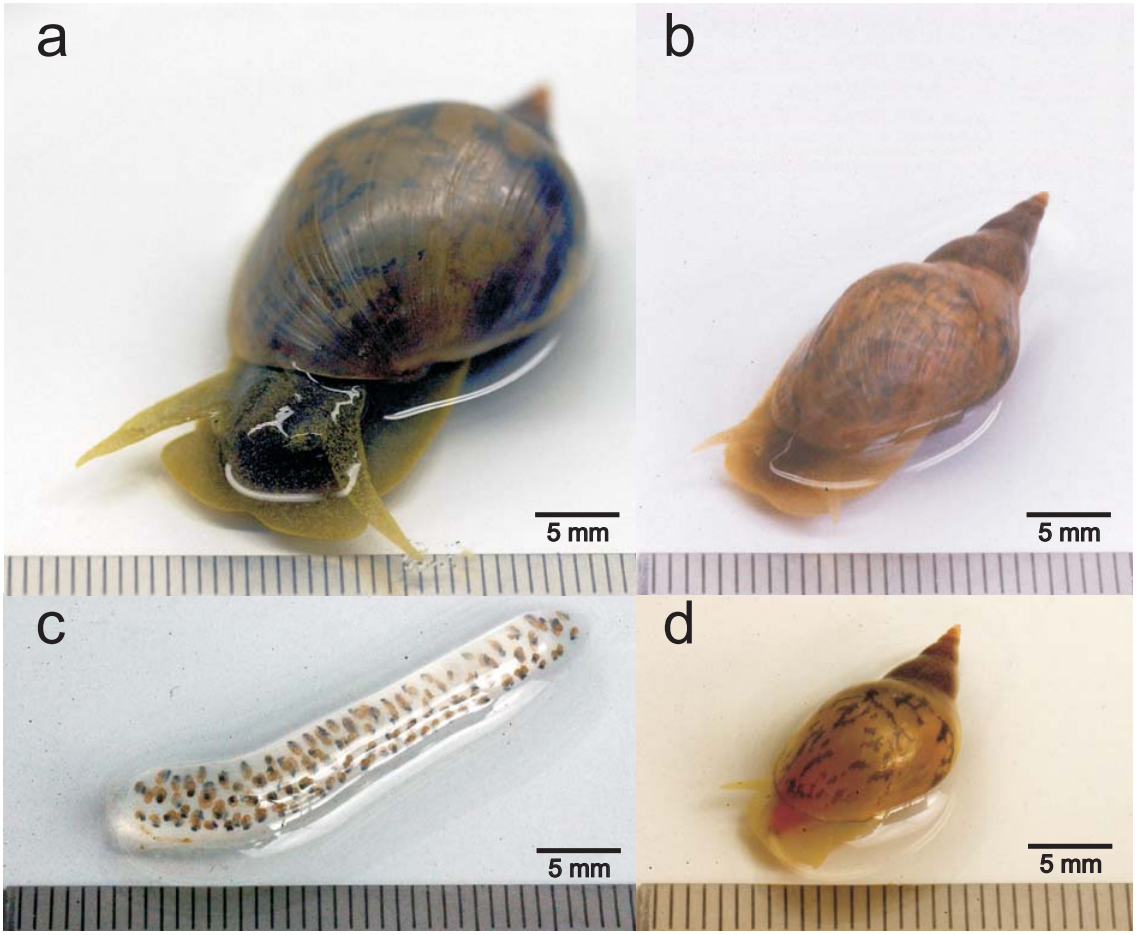

Figure 2.2: *The different developmental stages of Lymnaea stagnalis.*

a.) shows an adult snail, b.) a sub-adult animal, c.) a fully developed egg mass and d.) a juvenile snail, roughly 1.5 months old. Each dot in the egg mass in panel c.) is a fully developed small snail, the black spot being the head. Note that the one month old animals shows a healthy tiger-like coloring of its upper body portion, that gleams through the shell.

Neurons larger than 80 μm are impossible to extract without damaging the cell interior during that process. Additional neurons will render the identification of the white visceral neuron VD4 more difficult, since some newly added neuron have the same colouring that is otherwise unique in the visceral ganglion (i.e. cell cluster). For the creation of brain-conditioned medium on the other hand adult animals are suited best. This process will be described in the following subsection.

Brain Conditioned Medium

Brain conditioned medium (CM), is created from defined medium (DM), the *Lymnaea* cell culture medium (see A.2 for recipe). To obtain CM, twelve intact snail brains of sub-adult animals (see Figure 2.2b) are kept at 20°C and 70% humidity for several days in 6 ml DM in a dish. This clean, sterile 60 mm glas dish has previously been coated with a silane to prevent the proteins secreted by the brains from adhering to the substrate and can be reused multiple times. Before the incubation, the brains are washed 7 times or more in 7 different 30 mm plastic dishes each filled with 3 ml anti-biotic saline (ABS, A.2). Each cleaning step takes 20 minutes. Before and after the transfer of the brains from a dish to the next one the dish is shaken midly, as well as after 50% of the alotted time for each step. Even though, the brains can be used several times, the duration increases from 3 days, over 5 days to 7 days for the first, second and third time and subsequent CM. After taking the brains out of the new CM, the medium is transferred to polypropylene cryovials for direct freezing at -20°C or imminent use. Note that while first time CM is best suited for outgrowth, second time CM contains the most factors for excitatory synapse formation.

2.1.3 Extraction of Identified Giant Neurons

The following section outlines the schedule for a preparation day with the goal of obtaining large, identified neurons from *Lymnaea* snails. Again, besides providing a step by step recipe, the following subsection contain remarks regarding critical issues. The complete operation should be carried out at a temperature of 20°C. Since only low concentrations of antibiotics are used in this cell culture assay, sterile working conditions are self-evident.

Animal Dissection and Brain Extraction

After selecting usually 12 to 20 animals sized $16-21$ mm as stated above, the snails are cleaned with tab water and dried before taking their shells off with a pair of forceps with blunt tips. During this procedure a ligament is severed that helps the animal to retract into its housing [3]. The deshelled animals are then transferred into

[3]Even though this procedure is most likely mildly painful and disturbing to the snails, each of them survives such a treatment as shown in [Sye92]

a glass beaker filled with normal saline (NS, A.2) and 10% mouthwash solution for no more than 10 minutes: This both desinfects and reversibly anesthesizes the animals. Longer treatment leads to damage to the interior organs, including the brain. The dormant bodies are then transferred into a disection dish and pinned down, moving the animals from the insterile to the sterile environment of the laminar flow hood.

With a small cut from the middle of the body to the head (rostral to caudal), the buccal apparatus, penis and scrotum become visible which have to be pinned aside to make the snail's brain accessible. Their brain consists of several cell clusters, called ganglions, joined in two rings, one lying in the plane of the foot, the other closed around the vessels connecting buccal mass to stomach. Both the vessels and the stomach are removed with two cuts made close to the buccal apparatus and after the stomach, respectively. This unveils the buccal ganglia, which are attached to the feeding apparatus. Depending on the usage of the brains, for CM or cell extraction, the ring which was wrapped around the recently removed vessels stays either intact or is cut at the cerebral bridge respectively, transforming the second ring into a wing-shaped structure. Now the brain is still attached to the body by various nerves that run into all corners. The nerve strand running into the rostral part of the animal is kept as long as possible when cutting it: This is the handle, with which the brains are maneuvered and held. The remaining nerves are cut close to the ganglia to facilitate the following washing and enzyme treatment steps. Note that it is a common mishap to severe the buccal ganglia from rest of the brain, but with practise the ganglia can be extracted together.

After freeing a brain, it is imminently transferred into a 30 mm plastic dished filled with 3 ml ABS, that in the end contains all the extracted brains. Before continuing with the enzyme treatment, the brains are washed three times for 10 minutes in ABS dishes. Before and after the transfer of the brains from a dish to the next one the dish is shaken mildly, as well as after 50% of the alotted time for each step.

Enzyme Treatment

During the rinsing steps two additional 30 mm plastic dishes which are both filled with 3 ml DM are prepared for the enzyme treatment. Both, trypsine and its inhibitor, are removed from the $-20°C$ freezer and 6 mg of each substance are weighed and added to one of the DM dishes, yielding a final concentration of 2 mg/ml for the enzyme and and the inhibitor dish: Even though the activity of the two proteins might differ, this discrepancy is evened out by different durations of the treatments.

The following treatment is again carried out at 20°C. After the final rinsing step, the brains are transferred into the enzyme dish. The trypsin treatment lasts for 23 minutes. Then the brains are moved into the inhibitor dish for 10 minutes. Again, before and after each treatment as well as after 50% of the time, the dishes are shaken to distribute both brains and the substance evenly. During these 23

minutes the enzyme supposedly enters into the interior of the ganglions through the severed nerves to digest the membrane anchors. Prolonged treatment beyond 23 minutes endangers the integrity of the somatic membranes, which are situated furthest down into the ganglia (through the nerves), since Trypsin binding is very unspecific[4]. A prolonged inhibitor treatment results in diminuished cell adhesion, since the trypsin inhibitor molecules binding motive is complementary to the binding sites of integrins. Criteria to determine the success of the enzyme treatment are presented in the following subsection.
When the inhibitor treatment is finished, the brains are transferred into a small dissection dish filled with high-osmolarity defined medium (HODM), which is created from DM by adding a small amount of D-Glucose. With its increased osmolarity, the cells start to shrink and the cell-cell contacts come loose.

Cell Extraction

The freshly digested brains are first pinned loosely to the substrate with four needles: one is placed near the buccal ganglia, one in the long nerve that was protruding towards the rostral part of the snail as well as into the left and right cerebral ganglion. Then with the use of two #5 forceps and a pair of small dissection scissors, the connective tissue in between the remaining ganglionic ring is removed -the so-called outer sheath - that consists mainly of glia cells (see Figure 2.3b for an example brain after removal). Now the most critical and demanding manual step follows with the removal of the tissue surrounding the four central cell clusters. For this step very fine pairs of forces are used with manually sharpened tips to improve grip and to lessen stress onto the underlying somata. The movement resembles an unwrapping of the ganglion from its surrounding skin, starting on top of the cell of interest and always moving the skin away from it. After this, the pins are reset to tighten the nerves that connect the ganglia. These interconnecting nerve bundles are then crushed with the two pairs of fine forceps. Omitting this step would lead to permanent damage while extracting those neurons, whose axons project into other ganglia.
To extract and transfer the cells from the brains, a fire-polished, silane coated glass pipette of a diameter barely larger than the largest desired neuron is attached to a micrometer syringe via flexible tubing. Syringe, tubing and pipette are filled with completely HODM. Bubbles have to be removed to avoid damaging the cells, since in the case of trapped air the medium would not flow in a laminar way anymore. The pipette is then mounted onto a three-dimensional micromanipulator. By placing the manipulator close to a ganglion, the dials enable controlled movements towards the soma of interest. Turning the micrometer syringe to create an inward flow into the pipette should then easily move the cell body towards the tip. If the enzyme treatment was too short, excess force[5] will be needed to pull the cell body, which

[4]Many membrane proteins besides cell adhesion molecules have the RGD binding site and also get digested

[5]This could also a sign of bubbles in the tubing, syringe or pipette.

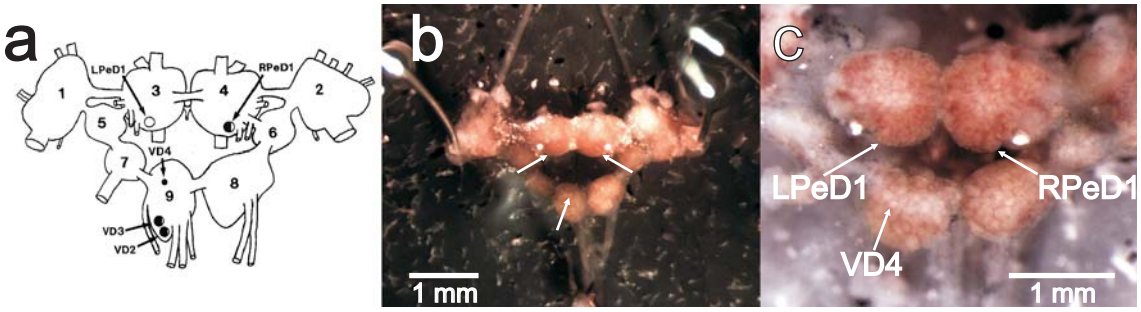

Figure 2.3: *The location of identified neurons in the Lymnaea brain.*

a.) shows a schematic of the segmented Lymnaea *brain consisting of 13 ganglia. The emphasis here is on identified giant neurons, that are known to form chemical synapses both* in vivo *and* in vitro*, as well as their exact location. The shading codes for coloring in which a fully shaded circle means milky white, and no shading means transparent orange.*
In b.) a micrograph is shown of a whole brain after enzyme treatment, pinning and removal of the outer sheath. Each ganglion here consists of roughly 10,000 cells. Only the cell bodies can be seen by looking at the surface of each ganglion.
c.) Close-up of the four central ganglia after desheating; the cell bodies now float freely, only attached to their axon hidden deep within the cell cluster.

usually damages it or leads to rupture of the axon close to the soma. If the treatment was too long on the other hand, the cell tends to fall apart even when little force is applied to it.

In a smooth extraction process, the desired cell body is sucked slowly into the pipette and subsequent fluid intake should pull both soma and axon loose from ganglion[6]. The cell should then hover in the pipette and move smoothly inside the pipette. Otherwise either the choice of pipette diameter was too small or the inside of the pipette is still rough, which can be fixed by repeatedly maneuvring floating cell debris into and out of the pipette.

Coating

Before being able to place the neurons onto the chips, these are usually coated to facilitate cell adhesion on the otherwise hydrophobic silicon dioxide surface. Three different coatings have been used during this research project: poly-L-lysine of medium molecular weight and two different fragments of beta subunits 1 and 2 of the Laminin protein. While the poly-L-lysine coating was published by Syed's and other labs for snails [Sye90, Won81], the idea to use the Laminin fragments was introduced by Ingmar Schoen during his effort to increase cell adhesion forces as well as contact area for his stimulation experiments [Sch07].

[6]If the axon does not break lose, crush the nerves in between the ganglia again

Poly-L-lysine was dissolved in Tris buffer at pH 8.4 at a concentration of 1 mg/ml. 1 ml of this solution was pipetted onto a clean chip and left up to an hour. After taking the solution off, the chip was rinsed 3 times with 1 ml of sterile, purified water (aqua ad injectabilia), then 1 ml of NS and finally once more with water. Then the chip was left to dry and then kept at least for three days at 7°C before usage. Earlier use would lead to extremely strong adhesion that would interfere with normal cell activity, as can be seen below.

Alternatively, two fragments of two different β-subunits of Laminin were tested after Schoen [Sch07] observed them to lead to strong adhesion for the fragment of the β1-subunit [Iwa87] and even outgrowth for a fragment of the β2-subunit [Tas89], as previously described for rat neurons. The lyophilized substance containing the β-subunit fragments of Laminin were dissolved in 10% acetate, yielding the working concentration of 0.5 mg/ml. To coat the active area of the chip, a 10 μl droplet of the substance was put there, left outside to dry down and used straight away.

Plating Cells & Pairing

The freshly extracted neurons were usually directly plated onto a coated chip whose cell culture chamber contained 1 ml of medium, either DM or CM, depending on the type of experiment. Alternatively there was the option of storing the neurons in a 30 mm plastic dish that was previously coated with hemolymphe, the snails' saliva and blood. The hemolymphe can be harvested from adult snails by drying them down before irritating their outer skin with a syringe needle tip. This drives the them into secreting the liquid that is subsequently taken up into a syringe. After filtering the hemolymphe a few milliliters suffice to coat half a dozen dishes.

Cells placed in hemolymphe coated plastic dishes filled with either 3 ml of DM or CM can be kept for one or two days before plating the cells onto chips. Cells treated in this manner express a larger amount of cell adhesion molecules in the case of both DM and CM and in the case of CM alone also an increased amount of synaptic factors (Syed, personal communication).

Special attention was finally taken when placing the neurons on the chip: Not only, that the neurons had to sit on the two-way contacts of the chip, but also the cells had to be placed in close proximity of one another to ensure synapse formation. A most favorable combination was the placement of the postsynaptic neurons with its axon on the chip before putting the presynaptic neuron on top of the other's axon. This procedure would lead to robust and strong chemical synapses after 16 hours in culture. Creating larger groups of neurons using this method posed a more difficult, but still solveable problem, as can be seen in the results part.

2.2 Electronic Interfacing

Now that the living side of the matter has been exhaustively discussed, the electronics side of the cell-chip contact will be introduced in the following chapter. This includes not only the semiconductor devices, but also the electronic signal conversion and amplification, the generation of stimuli well as the computer-based signal digitalisation. Before introducing the chip side of interfacing, the recording of intracellular potentials with sharp microelectrodes is presented, which was used to directly verify the results obtained from cell-chip interactions.

2.2.1 Electrophysiology

Before evoking and recording cell-derived signals with the semiconductor chips, it was always instructive to first test the viability of the investigated neurons with sharp microelectrodes. These sharp glass needles were created with a horizontal electrode puller from 6 inch borosilicate glass capillaries with an outer diameter of 1.5 mm and filaments inside. The back-filling of electrodes with a saturated potassium sulfate solution led to a final resistivity between $20 - 40$ MΩ. After contacting the cell, the pipette resistance could change beyond the compensation limit of the amplifier. During the investigation of more than two neurons, larger pipette errors were accepted due to the risk of damaging the synaptic contacts when changing pipettes. The connectors of the bridge amplifier were linked to an analog input/output (AIO) interface card for intracellular current injection and signal recording. The parameters for the currents were set in a self-written computer-based stimulation and recording program. The recorded traces were then displayed on screen for data analysis and storage.

2.2.2 Chips

Throughout this research project different types of chips have been used to investigate the chemical synapses as well as intermediate steps on the way to the interfacing of small neuronal networks. Each design as well as some technical aspects of their usage are presented in this section.

Linear Arrays with Stimulation and Recordings Sites

The most commonly used chip during the experiments was a lab-made device created by Günther Zeck and Paolo Bonifazi [Zec02, Bon02] before the beginning of this research project. The chip consists of two lines of 1 mm length with groups of two-way contacts as can be seen from Figure 2.4b. Between two stimulator pads each sized between $40 - 50$ μm in breadth and 80 μm in length, a transistor is situated, whose drain line is isolated from the stimulation lines by a thick oxide barrier to

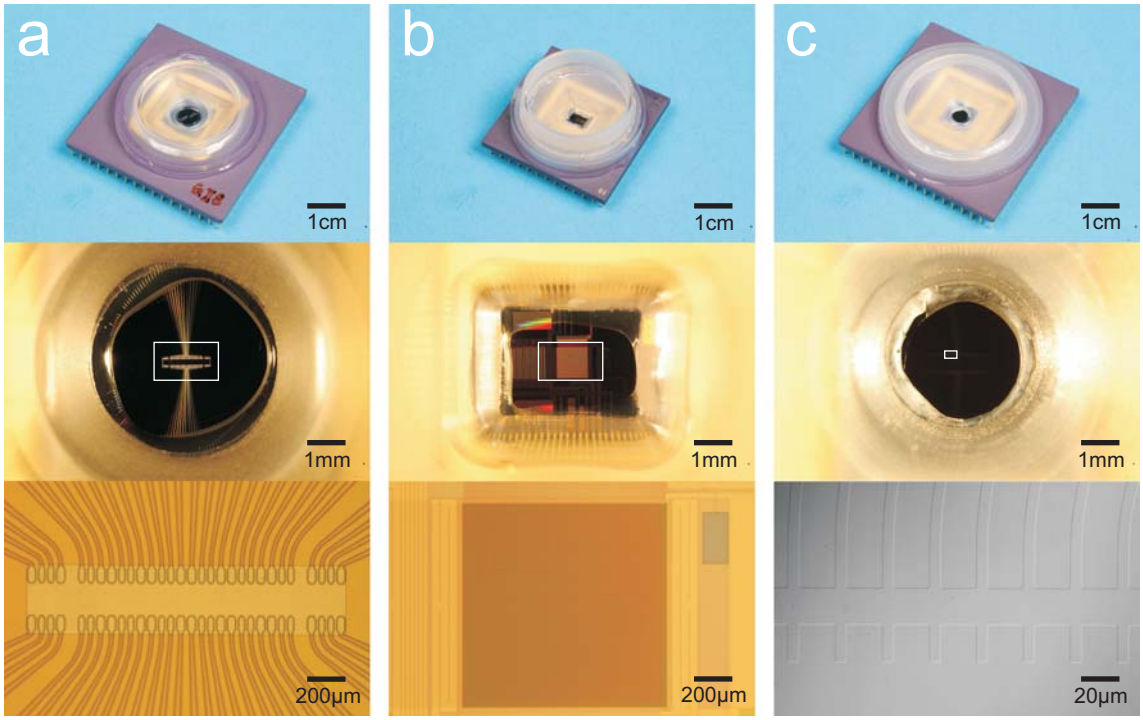

Figure 2.4: *Overview of chips with close-ups of their sensor arrays.*

This figure show the chips used during this research project, from left to right: (a) the two-way-contact chip created within the lab by Zeck and Bonifazi, (b) the planar transistor array created in cooperation with Infineon Technologies as well as (c) the high-sensitivity transistor chip created by Moritz Völker. From top to bottom one sees a side view of the whole chips, a top view of the culture chamber and a close-up of the sensor arrays.

diminish cross-talk between the stimuli and the recorded source-drain current. In this design all FETs share a common source voltage. Between source and each drain line lies a region of decreased charge carrier density, where the gates with a size of 8 μm x 3 μm are situated. In a slightly different design two stimulator pads towards the ends of each line were omitted to increase the effective gate size to 64 μm x 3 μm, lowering the total number of transistors from 62 to 58. Considering the fact, that a larger gate area reduces the noise level of a transistor - the rms noise scales with the inverse of the root of the gate area [Voe05b] - these large gates should have a noise reduction of $1/\sqrt{8}$, i.e. they show roughly 65% of the rms noise found with the smaller gates.

The insulation of the whole chip from the electrolyte is achieved by a 10 nm thick, thermally grown oxide layer with a specific capacitance of 0.8 μF/cm^2.

Like all lab-made chips, the silicon die is glued to a ceramic package with a special wax and the bond pads protected from the cell culture medium by a perspex chamber (see Figure 2.4(a)). All in all, these chips, although not optimized for low-noise measurements or opening of voltage-gated ions channels by coating with titanium oxide, are very durable: Being in cell culture for about 50 times, the oxide of these chips is still intact for recording, even though the threshold voltage - the value, at which the current through the device starts to flow - is shifted towards 3 V.

For these Electrolyte-Oxide-Semiconductor (EOS) FETs the gate potential becomes the reference for all voltages contrary to the convention for MOSFETs with source as a reference (see Figure 2.7 for an equivalence circuit of the system). The working conditions were chosen to be in the linear regime of the device with a source-drain voltage V_{SD} of 4 V and a source-gate voltage V_{SG} between $4 - 5$ V, while the bulk-gate voltage V_{BG} was set to 5 V. Note that in general $V_{BS} \neq 0$. This set of voltages led to a source-drain current I_{SD} around 50 μA for small and 250 μA for large gates (see subsection 2.2.3 and Figure 2.5 for more details on the selection of the working point).

Planar Transistor Array with 16,348 Transistors

These planar recording arrays have been planned and created in collaboration with Infineon Technologies [Eve03]. It features a field of 128x128 transistors with 1 mm side length, thus a single unit takes up roughly an area of about 7.8 μm. The chip is organized in lines and rows, which are multiplexed into 16 external 12-bit analog/digital-converters (A/D converters). After the conversion, the data is de-multiplexed by software and stored for display and analysis. The maximal duration for recording is limited by the on-board memory of the external A/D converters. At the current buffer size the whole array can be sampled at a frequency of 2 kHz for 8 seconds. By limiting the measurement to a subset of the 128 lines and rows, this total time or the sampling frequency can even be increased.

An externally created periodic signal, applied to the Ag/AgCl electrode that contacts the chip medium, of known amplitude (3 mV), calibrates the chip's digitalized output for each transistor. An internal reset cycle maintains the working conditions of each transistor such that each drain current I_D equals that of an internal current source I_D^0. The differences $I_D - I_D^0$ then reflect the changes between junction and electrolyte voltage $V_J - V_E$ picked up at the transistor's gate. After switching from calibration to working mode, these changes are amplified on chip and digitalized in the external A/D converters. After a fixed time interval the reset cycle is repeated to refresh the working conditions. The switching between reset and amplification mode results in a shift as well as a drift in the recorded transistor current. A subtraction by a numerically fitted function consisting of an exponential function and a parabola of third order, yields a trace devoid of artifacts above the noise level. The whole process is described in [Lam04].

High Sensitivity Linear Transistor Arrays

The recording of single rat neuron action potentials demanded a device with low intrinsic noise, that was created by Moritz Völker [Voe05b]. One main difference in design as compared to the former manufacturing protocol was the usage of buried channel field effect transistors as compared to inversion channel devices. Their advantage is that the charge carrier distribution is shifted away from the silicon silicon-dioxide interface, where a main source of noise intrinsic to the device lies. There are multiple mechanisms that can lead to a higher noise level like the introduction of dangling silicon bonds by mechanical deformation, insufficient oxidation or the introduction of alien atoms into the oxide layer. All these result in electronic interface states, that wash out the energetic levels in the band gap and thus make the processes of random creation and recombination of electron-hole pairs more likely at room temperature. A strict policy of design and manufacturing rules could help to reduce the rms noise to a level far below 100 μV, sufficient to detect single mammalian action potentials [Voe05b].

Only chips with the largest gates sized 22 μm x 24 μm were used for the experiments described in the results section. As stated by Völker in his thesis, the rms noise in the relevant frequency range can be as low as 20 μV for these devices [Voe05b]. For good adhesion conditions the measurements with these transistors are not limited by the noise intrinsic to the device any more but by thermal noise of the cleft resistivity [Voe06]. Therefore these field-effect transistors are best suited to investigate even small electrical events between synaptically connected neurons like for example post synaptic potentials.

The working conditions were chosen to be in the linear regime of the device with a source-drain voltage V_{SD} of 0.5 V and a source-gate voltage V_{SG} between $0.3 - 0.5$ V, yielding a source-drain current I_{SD} around 20 μA, while the bulk-source voltage V_{BS} was set to 0 V.

2.2.3 Electronics

This subsection is mainly concerned with the lab-made transistors created by Günther Zeck and Paolo Bonifazi [Zec02, Bon02]. Even though the chips had been created before the beginning of this project, an amplifier consisting of a unit to convert and amplify the drain currents as well as to multiplex externally created voltage pulses to be applied to the stimulator pads had to be designed first. Due to spatial as well as practical restrictions the designed amplifier was limited to recording from up to 16 different transistors simultaneously out of 62 available ones, while two voltage pulses could be independently applied to any of the 64 stimulation spots. The amplifier box itself was running on battery power to eliminate noise from power converters. Of the following subsections, the first one will deal with the aspects of stimulation, while the second will be concerned with the details of recording electrical signals with these chips.

Stimulus Creation and Application

Two external function generators were connected to the input channels of the in-lab created amplifier. With the self-written software both the parameters and waveforms for the function generator as well as the stimulation spots, were selected. The function generators were programmed and triggered from computer by using a general purpose interface bus (GPIB) card, while a digital output card switched all spots into exclusively one of the three states: closed, open to pulse 1 or open to pulse 2.

Two different kinds of pulses were used: square and ramp pulses. In general, square pulses were used in bursts of $4-8$ pulses with amplitudes around 2 V and frequencies around 1 kHz. Ramp pulses on the other hand, were applied in bursts of up to 20 pulses with amplitudes of 5 V and frequencies up to 10 kHz. Note that for capacitive stimulation the important attribute is dV_{St}/dt (see section 2.4). In the case of square pulses, this value can only be determined experimentally for the combined system of function generator and chip resulting in a rise time of 1 μs which corresponds to a value of 1000 V / ms. For ramp shaped pulses the steepness can be computed directly and ranges from $0.1 - 100$ V / ms.

To directly open voltage-sensitive ion channels with ramp shaped pulses the steepness range is limited: On these chips, with a silicon dioxide thickness of 10 nm, the first Ohmic currents start to show in when the stimulus voltage V_{St} across the oxide exceeds +5 V. On the other hand, the time scale on which the gating of ion channels happens is in the milliseconds range. Therefore the physical and physiological limits result in a maximal steepness of 5 V / ms for the stimulus induced gating of ion channels.

When exceeding that range, the effect of electroporation will most likely contribute to a change in membrane potential. Wallrapp investigated the membrane current after the application of single ramp pulses of increasing steepness and found them

to qualify for one of three different regimes [Wal06]: opening ion channels, causing transient or causing permanent electroporation. Transient electroporation increases the resting membrane potential by a few millivolts as compared to the value before the stimulus. As compared to permanent electroporation, this effect vanishes after up to 1 s.

The creation of prolonged neuronal activity for several seconds, as demanded for investigations on inhibitory chemical synapses (see section 3.3), cannot be achieved with single pulses. Using one pulse to create just a single action potential would result in permanent damage to the neuron. The experience with square pulses showed, that a scaffold of multiple, weaker pulses resulted in cellular activity without damage persisting longer than a few seconds [Fro95, Zec01]. Therefore the question, whether even better results could be obtained using ramp shaped pulses, was addressed (see section 3.1.2).

The rationale to find a set of suitable pulse parameters to satisfy minimal invasive action in the case of electroporation, differed for the two pulse shapes: For ramp-shaped pulses, the pulse frequency was increased at a fixed amplitude of around 4.5 V, just below the threshold of oxide breakdown. After observing a change in membrane potential, the number of pulses was increased to get temporal summation of single effects, which would eventually add up to an intracellular voltage near the threshold of cell spiking. Sometimes the fast decay of intracellular potential demanded an additional increase in ramp frequency (decrease in pulse duration) in order to get temporal summation.

When determining the set of parameters for square pulses, the amplitude was increased starting from 1.5 V at a fixed frequency of 800 Hz (which equals a duration of 1.2 ms) until the intracellular potential began to change. Then the number of pulses was set to 6-8. If this burst were not able to elicit a single action potential after repeating it for 4-5 times in a row with a break of roughly a second in between, the amplitude was increased by 0.1 V while the number of pulses was decreased again. Like this, in both cases it was possible to find pulse trains, that could be used to drive the neuron into periodic activity when repeated every 100-200 ms.

Transistor Working Conditions and Readout

The design of the amplifier restricted the number of simultaneously recorded transistors to 8 per line for a total number of 16. The multiplexing scheme was devised in such a manner, that the 8 channels per line could always be chosen to amplify signals from 8 neighbouring transistors, while for each channel the to be recorded transistor could be selected individually. For the purpose of monitoring the activity of small neuronal networks this limitation proved to be negligible.

The amplifier channels themselves created two different outputs for each transistor: One for the net source-drain current I_{SD}, one for the changes in current dI_{SD}. Technically this was done by high-pass filtering I_{SD} with a cutoff frequency close to

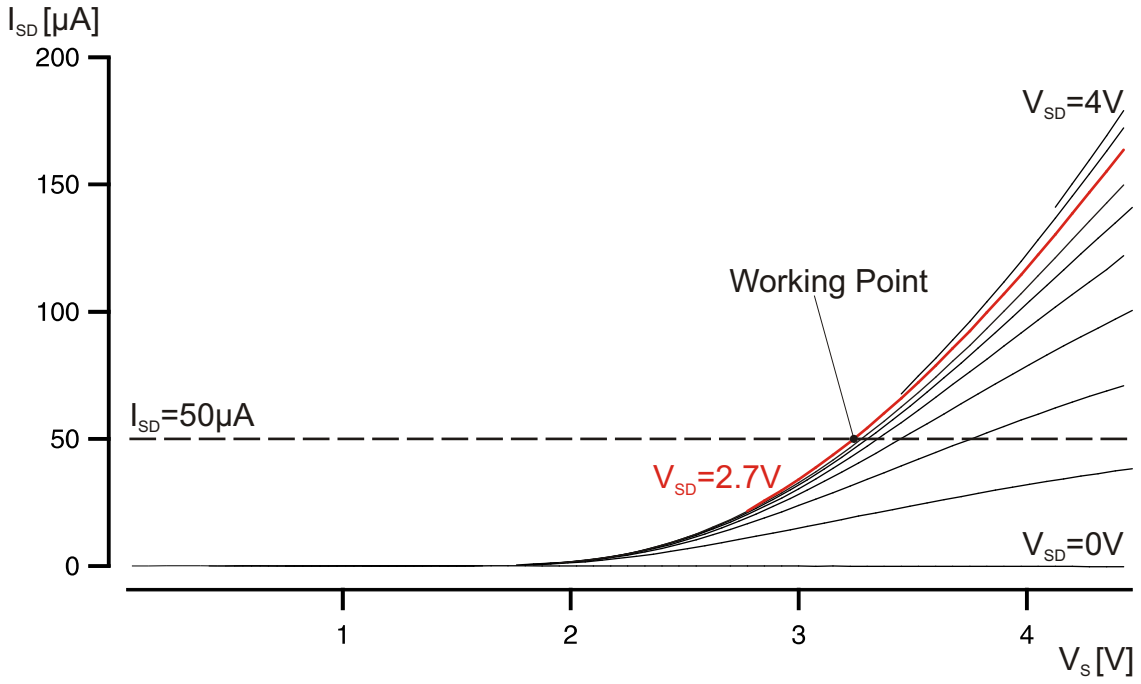

Figure 2.5: *Typical I_{SD}-V_{SD}-characteristic field for two-way contact chips.*

The figure shows a group of I_{SD}-V_S-characteristics for different constant source-drain voltages V_{SD} ranging from $0 - 4$ V. The line $I_{SD} = 50$ μA defines the working points when intersected with the characteristics, as shown for the curve $V_{SD} = 2$ V, which is highlighted in red. Note that for all characteristics $V_B = V_S$.

1 Hz before amplifying the remaining signal. All 32 outputs were connected to an analog input interface card for digitalization, display on screen, data analysis, and storage. See Völker [Voe05a] on details regarding the electronic design.

A digital output card transferred the operating voltages - source, drain and bulk - to the amplifier for two different purposes: to record the I-V-characteristics for the selected transistors and to set the working point. A self-written program created a user-interface for the selection of the transistors, the recording of the characteristics, the setting of the working point, as well as the visualizing the changes in drain currents dI_{SD}. The principle of finding the maximal transconductance dI_{SD}/dVS for a constant current of around 50 μA aided in the selection of the working point from the field of I_{SD}-V_S-characteristics illustrated in Figure 2.5. In this example a source, drain and bulk voltage of $V_{SG} = 3.3$ V, $V_{SD} = 2.7$ V and $V_{BG} = 3.3$ V, respectively, yielded a drain current of 50 μA for small gates and 250 μA for large ones. To minimize damage to the gate oxide during large stimulus amplitudes, the bulk voltage V_{BG} was usually set to the fixed value of 5V. This larger bulk voltage V_{BG} lowers the source-drain current I_{SD}, compensated for by a larger voltage difference between source and drain, in this case $V_{SD} = 3.2$ V.

Measurement of Transconductance dI_{SD}/dV_{SG} for Gate Voltage Computation

To actually convert the changes in source-drain current into a voltage that was applied to the gate, which is the quantity of interest in this application, the transconductance dI_{SD}/dV_{SG} at the given working point of the transistor needs to be determined. The main assumption for both available methods to obtain its value is that the source-drain current I_{SD} varies as a function of the gate voltage V_{SG} in a linear fashion. Therefore during the selection of working point, the analysis of the characteristics of each transistor has to guarantee the assumption of linearity.

There are two ways of measuring the transconductance: either by directly computing the slope in an I_{SD} vs V_S plot or by applying an external alternating voltage to the bath electrolyte. The first method assumes for small changes $dV_G = dV_S$, since $V_G \approx V_E = 0$V (see Figure 2.7 for a schematic of measurement situation) [7]. The second methods relies on a negligible filtering of the alternating voltage for the given stimulus frequency. Within the given error margins these two methods result in the same value.
One major issue with computing the transconductance from the characteristic itself is, that during its measurement $V_B = V_S$, while in the working point V_B is fixed at 5 V. It is known, that a change in V_B not only results in a different source-drain current I_{SD} but also in a different value of transconductance due to a change in threshold voltage[Sze98].

[7] $V_S = \phi_S - \phi_{Ground} = \phi_S - \phi_E \approx \phi_S - \phi_G$

Therefore the choice was made to measure the transconductance by directly modulating the gate voltage. The modulation took place by applying a periodic square pulse of known amplitude at a frequency of 266 Hz to the Ag^+/AgCl-electrode. The maximal change of the measured source-drain current $|dI_{SD}|$ during a single period was associated with the applied voltage. Like this, a mapping between 25 applied pulses of increasing amplitude between -10 mV to $+10$ mV to the measured changes in source-drain current yielded through a linear fit both, the transconductance as well as the q-factor for the fit. Therefore each computation of the transconductance checked whether the assumption of linearity was fulfilled for the whole range of applied voltages. Additionally the plot of the transconductance would reveal potential inhomogeneities between negative and positive changes[8].

This method of determining the transconductance was carried out right before the measurement of cell signals, to minimize errors due to changing working points, changes in source-drain current due to warming of the device, etc. Unfortunately the bath modulation of the gate potential could create errors in the applied amplitude for strongly adhered neurons, which would show in a non-rectangular shape of the square pulse during the measurement of the transconductance[9]. In this case a reduction of the stimulus frequency would help to reduce the error in the voltage profile in the junction.

[8] Although they never occurred within the limits of the measurements' error

[9] A Fourier analysis of the recorded current signal could determine the time constant of the filter consisting of cell membrane and junction resistance

2.3 Cell-Substrate Distance Measurement

One of the important parameters that influence the size of the recorded signals as well as the magnitude of the stimulus amplitude in the junction is the distance between the cell and the substrate it adheres to. To measure this distance, a method to determine the width of the cleft between the lower membrane and the oxide has been created by Lambacher [Lam02]. The principle is shown in Figure 2.6: Panel (a) shows a cell adhered to a silicon substrate that is covered with an oxide layer of four different heights. Light with a wavelength of 546 nm interferes with its reflection at the silicon dioxide-silicon interface forming a standing wave. The maximal amplitude of the interfering light therefore depends on the optical distance to the silicon surface. After staining the cell membrane with the fluorescent dye $DiIC_{18}$ according to an involved protocol described in Appendix C, the dye molecules absorb photons from the standing light wave. The intensity of the emitted light detected in the range between $545 - 565$ nm is limited by the maximal amplitudes of the excitation wave. Thus the measured intensity codes for the distance between the dye molecules and the silicon surface.

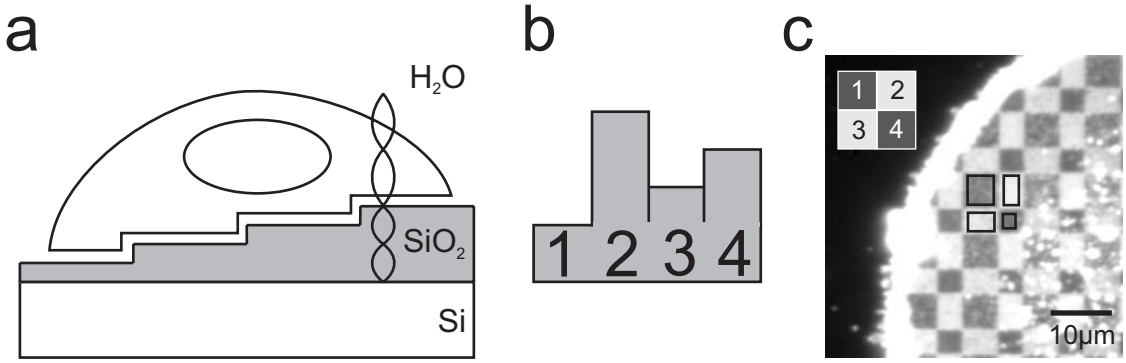

Figure 2.6: *Fluorescence Interference Contrast (FLIC) microscopy*

(a) Schematic of a cell on a FLIC chip, a silicon wafer piece with steps of different heights made from silicon dioxide. The membrane that is stained with the fluorescent dye $DiIC_{18}$ is illuminated with monochromatic light that interferes with its reflection from the silicon surface (indicated by a wave train with two periods). Oxide steps and cell-substrate distance are not drawn to scale.
(b) shows a cartoon of the height profile of the different silicon dioxide steps.
(c) a segment of a stained cell's adhesion membrane: the investigated segments are highlighted with black boxes. Note that the oxide steps have a thickness between $10 - 160$ nm; the distance between cell and oxide is 37.2 ± 0.2 nm in the example shown in (c).

Surprisingly the distance between cell and the surface it is attached to remains mostly constant along the adhesion profile. The different intensities detected for the

four different heights of the silicon dioxide steps can therefore be used to create an intensity profile. The heights of the oxide steps were selected to result in extremely low or high values of fluorescence. A theoretical intensity profile can be computed from the dye's dipole characteristics, it's orientation in the membrane, the refractory indices of silicon, silicon-dioxide and water as well as the numerical aperture of the microscope's objective. The theoretical curve allows for one parameter in its fit, which is in this case the distance between oxide and lower membrane. An iterative fit of the four intensities to the theoretical curve yields the cell-substrate distance with a certain minimal accuracy. The main error sources for this fit are the variations of the intensity in a selected quadrant that can result from for example staining of inner membranes of the cell like the nucleus or the endoplasmatic reticulum. In the given example in figure 2.6(c), the outer rim of the cell as well as parts in its center shine brighter then their surroundings. Thus selecting a homogeneously fluorescing area for evaluation of the local intensity at a given height can lead to a significant reduction in the computed error. Even though in some cases the choice seems arbitrary to the neutral observer, other selections will usually lead to large errors or no fit at all. In this example, a snail neuron adhered to silicon dioxide coated with poly-L-lysine after 16 hours in culture in the presence of brain-conditioned medium (CM), the fitted distance yields a value of 37.2 ± 0.2 nm. Since the intensities for the same oxide heights differ only slightly for the given staining, this value is assumed to be constant along the adhesion profile of this particular neuron.

2.4 One-Compartment Model

The voltage profiles created with stimuli applied to the capacitors underneath a neuron as well as the signals recorded by the field-effect transistors can be understood in the context of the theoretical models developed within the department [Fro05]. When considering a neuron with large adhesion area that is probed with a point-like transistor at the center of its adhesion profile, the point-contact model describes this situation well [Wei97]. In this model all needed electrical compartments are replaced by single resistors, capacitances and voltage and current sources. Still, for computational reasons as well as the convention in electrophysiological literature, it is convenient to express quantities in area specific values. Figure 2.7 shows an overview of the electrical components necessary to sufficiently describe the cell-chip interaction for snail neurons. The schematic can be divided into three logical units: glass electrode, transistor and stimulator pad.

2.4.1 Explanation of the Model

Analysis of the Intracellular Node

The glass electrode serves two purposes: stimulation of cell activity via an injected current I_{inj} which results in a change in intracellular potential and monitoring of the intracellular voltage V_M by recording the pipette voltage V_{pip}. During current injection, the pipette's measured voltage V_{pip} does not only record the membrane voltage V_M, but also the potential change due to the ohmic current along the pipette with a resistance R_{pip}:

$$V_{pip} = V_M + R_{pip} I_{inj} \tag{2.1}$$

To obtain the membrane voltage, one can either physically compensate for R_{pip} with electrical components in the recording device or computationally after recording.

The current injection not only affects the membrane voltage V_M, but also leads to changes in the currents across the membrane. Each ionic current has its own specific conductance g_i and a non-zero reversal voltage V_i^0, depicted by a voltage source, that results from the difference in ionic concentration between the intra- and extracellular compartment. In this model the membrane is divided into two halves: The upper, free membrane with area A_{FM} as well as the lower, junction membrane with area A_{JM}. Both halves have the same specific capacitance of the cell's membrane $c_M = C_M/A_M = C_{JM}/A_{JM}$. Along both membranes capacitive currents flow during the injection of a pipette current $i_{inj} = I_{inj}/(A_{FM} + A_{JM})$. Using Kirchhoff's law for the intracellular node with $g_{i,FM} = G_{i,FM}/A_{FM}$, $g_{i,JM} = G_{i,JM}/A_{JM}$ and $\beta = A_{JM}/A_{FM}$, we obtain:

$$i_{inj} = \frac{1}{1+\beta}\left[\sum_i g_{i,FM}(V_M - V_E - V^0_{i,FM}) + c_M(\frac{dV_M}{dt} - \frac{dV_E}{dt})\right] + \frac{\beta}{1+\beta}\left[\sum_i g_{i,JM}(V_M - V_J - V^0_{i,JM}) + c_M(\frac{dV_M}{dt} - \frac{dV_J}{dt})\right] \quad (2.2)$$

The free membrane voltage $V_{FM} = V_M - V_E$ is usually associated with the term membrane potential, the observable for intracellular recording methods, while in this configuration the junction voltage V_J can only be probed by extracellular recording with field-effect transistors.

Analysis of the Junction Node

When considering the cell-chip interface, the voltage changes in the junction become important, as can be seen from the following equation for the current along the junction node with $g_J = G_J/A_{JM}$:

$$g_J V_J = c_{St}(\frac{dV_{St}}{dt} - \frac{dV_J}{dt}) + c_M(\frac{dV_M}{dt} - \frac{dV_J}{dt}) + \sum_i g_{i,JM}(V_M - V_J - V^0_{i,JM}) \quad (2.3)$$

By comparison of the more general area contact model with the point contact [Fro03], one finds for a circular junction of radius a_J with $A_{JM} = \pi a^2_{JM}$ a relation between the junction conductivity g_J, the width of the junction d_J and $r_J = \rho_J/d_J$, with ρ_J being the specific resistivity of the junction:

$$g_J = \eta\frac{1}{r_J A_{JM}} = \eta\frac{d_J}{\pi\rho_J a^2_J} \quad (2.4)$$

The constant η which is derived from averaging the contribution of the covered area A_{JM} of radius a_J to the junction potential ranges in from $4\pi - 8\pi$, depending on the weights involved in averaging. Thus both, the reduction of the cell-substrate distance as well as the increase of the adhesion radius decreases g_J, yielding larger junction potentials.

2.4.2 Consequences for Stimulation

As far as chip stimulation is concerned, the voltage V_{St} applied to the stimulator pad underneath the neuron with a specific capacitance $c_{St} = c_{Oxide}$, leads to a capacitive current along the junction with its specific conductivity g_J. These capacitive currents can also affect the current across the adhesion membrane through a transient change in V_J in two ways: First, a different junction membrane voltage V_{JM}, results in a new net current flowing across the lower part of the cell. Second, the new V_{JM} might also lead to a different conductivity $g_{i,JM}$ for any given ionic species due to gating of voltage-sensitive ion channels in the adhesion membrane.

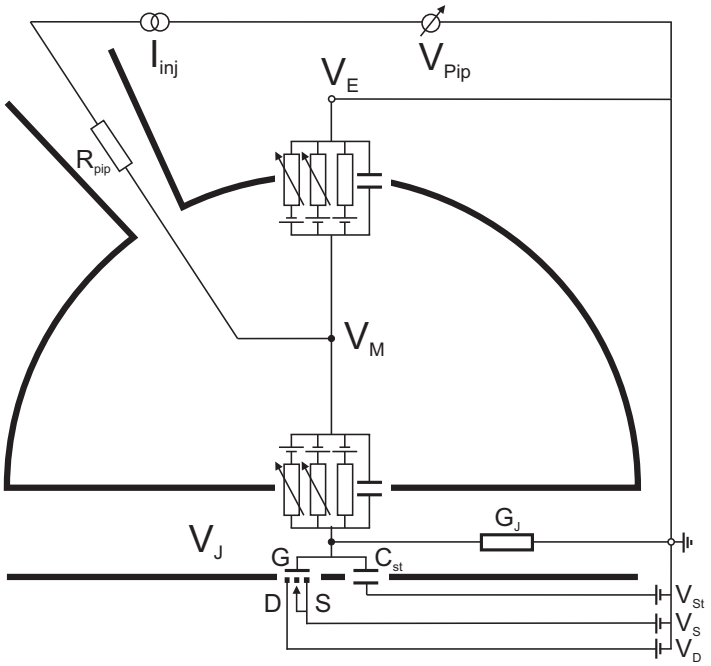

Figure 2.7: *Schematic of a neuron on semiconductor chip contacted by a glass pipette.*
The cell with intracellular voltage V_M, which the pipette can monitor the intracellular potential by recording the voltage V_{pip}, is divided into two halves: The upper part, the free membrane with its area A_{FM}, that has direct contact to the bulk electrolyte voltage V_E, which is again connected to ground. The lower part, the adhesion membrane with its area A_{JM}, is electrically separated from the electrolyte through the junction via an area specific conductivity $g_J = G_J/A_{JM}$, that enables the build-up of a transient difference between bulk and junction voltage V_E and V_J, respectively. At the chip level, the source and drain voltages V_S and V_D define the current that runs through the field effect transistor between source S and Drain D, while the junction voltage V_J at the gate G modulates this current, the observable I_{SD} of transistor recording.
Two ways exist to change V_J: Either by injecting a current I_{inj} into the cell through the pipette with the resistance R_{pip} or by applying a voltage pulse V_{St} at the stimulator with the area specific capacitance $c_{St} = c_{Oxide}$. The first way leads to a difference in membrane voltage V_M, which then diminishes or increases the current across the adhesion membrane. Additionally, a capacitive current due to differences in the conductivities between the free and adhered membrane would affect V_J.
The chip stimulation directly changes V_J through a capacitive current that runs while the stimulation spot is charged. This transient change dV_J then affects the voltage-sensitive ionic conductivities in the adhesion membrane and thus the intracellular potential.
The cell, junction and chip devices are not drawn to scale. The thick line between cell and chip stands for the field oxide of 150 nm thickness. Cell size is 100 μm, cell-chip distance 50 nm or less, gate width 10 μm, stimulator width 40 μm.

Electroporation

Another, less desired effect of the stimulation pulse happens, when the electrical field across the junction membrane exceeds a certain threshold value of 400 V/m [Jos00] during the stimulation pulse. Electroporation - the formation of small pores in the membrane - might happen [Wal06]. Its effect would be the increase of the leak conductivity across the lower membrane, regardless of the sign of the change in the junction voltage V_J. Since the leak's reversal voltage V^0_{leak} equals that of the bulk electrolyte[10], electroporation will reduce the voltage difference between the intra- and extracellular space $V_M - V_J$: The cell depolarizes, which increases the likeliness of action potentials.

Even though this form of stimulation seems blunt compared to the physiological mechanism of opening ion channels, it usually is a result of one of the following: the preference of easy handling, a poor understanding of the parameters involved in the stimulation process, or the desire for the least demand on the technical and/or biological side.

Opening Ion Channels

To actually affect voltage-sensitive ion channels, a change in junction membrane potential dV_{JM} has to be at least on the same time scale as the gating of ion channels happens, on the order of milliseconds. Additionally, V_{JM} has to be increased by several millivolts, better tens of millivolts to lead to a cell-intrinsic amplification of the chip stimulus. A successful stimulus therefore has to fulfill both requirements.

Unfortunately the success of such a stimulus depends not only on the design of the electronic device, which affects mainly V_J through a well-designed V_{St} (describe above in Section 2.2.3), but also on the parameters that contribute to the junction resistivity r_J (see Equation 2.4): the cell-substrate distance d_J as well as the radius of the adhesion area a_J and further the specific conductivity in the cleft ρ_J, which in most cases equals the specific conductivity of the electrolyte [Gle06].

In the case of snail neurons several factors affect the junction conductivity in a positive manner as compared to mammalian neurons: The increase in adhesion area by a factor of ~ 10, but also a 50% decrease in specific conductivity of the extracellular medium due to halved salt concentrations. Therefore snail neurons are well suited for tests on the opening of ion channels via capacitive stimulation.

Using a pure stimulation chip coated with titanium oxide, which has a 30 times larger dielectric constant ϵ than silicon, Schoen [Sch07] could use capacitive stimulation to create activity in snail neurons by pure opening of voltage-gated ion channels. Schoen found for stimuli that resulted in both, positive or negative changes in junction potential, a range of parameters suitable to evoke neuronal activity. Analysis of

[10] a leak will always lead to complete equilibration of the differences in the ionic concentrations across the membrane

the stimuli as well as simultaneous intracellular recordings led to a model explaining the effect on ion channels due to the capacitive currents that charge the cell's free and adhered membrane during the stimulus. In this model, positive changes in junction potential V_J result in an increase in sodium conductivity in the free membrane, since the decrease in junction membrane potential V_{JM} during the stimulation has to be balanced by the membrane potential of the remaining membrane V_M. Negative changes in junction potential V_J, on the other, led to an increase in sodium conductivity in the adhesion membrane, since the stimulus directly increased V_{JM} through lowering V_J.

2.4.3 Consequences for Transistor Recording

When it comes to transistor recording, the transistor's gate probes the junction voltage V_J. Any of the above-mentioned mechanism, capacitive currents due to stimulation or recharging of the cell's membrane as well as the change in the conductivity across the adhesion membrane will lead to a different junction voltage V_J. The concomitant change in the electrical field emanating from the junction will affect the conductivity of the source-drain channel and lead to a difference in the source-drain current, the observable of the transistor.

Again, like mentioned in the previous subsection, the size of the junction voltage V_J depends largely on the junction conductivity G_J, which is lower for snail neurons as compared to mammalian neurons, thus increasing expected cell signals.

Additional Sources Affecting the Recorded V_J

Several other mechanisms besides the change in the junction voltage V_J might result in a different conductivity of the source-drain channel though. Intrinsic to the device are changes in the electronic structure due to the transient electrical fields of a stimulation pulse, leading to artifacts in simultaneous transistor recordings. On the junction side, local changes in the concentration of ionic species, especially the potassium concentration, lead to a different surface potential, which was observed by Brittinger [Bri05]. This effect might become important when investigating long-term neuronal activity.

Although in principle it is possible to model the different ionic conductivities, the carrying out of this task for real neurons poses a serious challenge: One not only needs to know the parameters for a single ion channel, but for all different populations of ion channels for the cations Na^+, K^+, Ca^{2+}, H^+ as well as the anion Cl^-. Zeitler extracted all available data on ionic conductances from literature for *Lymnaea* and created a simulation for a typical snail action potential [Zei04], showing good agreement especially with the time scale, which failed to match for a simple Hodgkin-Huxley model[11] [Mer05]: Snail action potentials are ten times slower due

[11] A result presented in the doctoral thesis of Merz

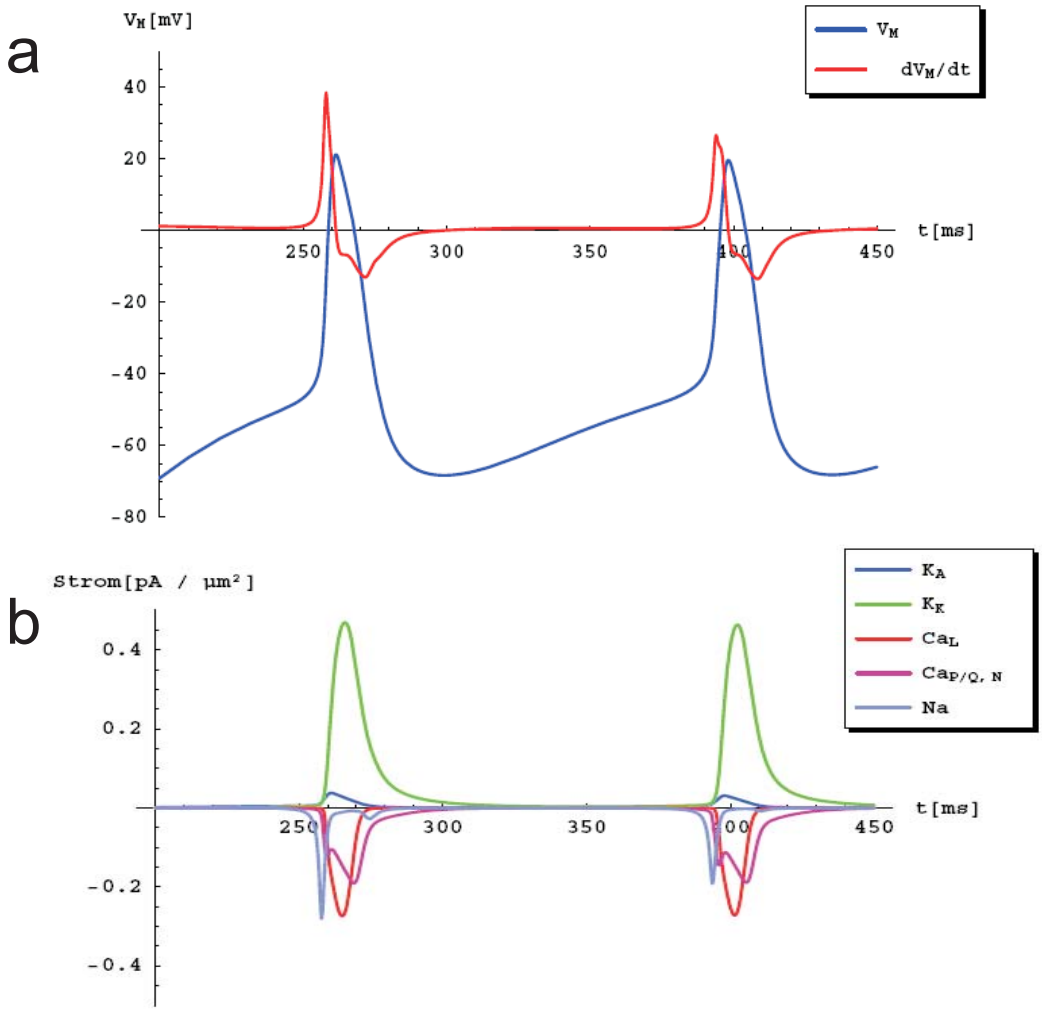

Figure 2.8: *Simulation of membrane voltage and current density of a Lymnaea neuron. Simulation results of two snail action potentials as conceived and computed by Zeitler[Zei04] (reproduced with permission). (a) shows the action potential (blue) and its time derivative (red). (b) shows the membrane current density for the different ion channel populations used in the simulation. Two potassium (dark blue, green), one sodium (light blue) and three different calcium channel classes (red, purple) were used in this model.*

to a large, sustained Ca^{2+} influx, the so called Ca^{2+} shoulder of the action potential, which is balanced by an efflux of K^+ ions. In Zeitler's simulation - the result is reproduced in Figure 2.8 - the current density for K^+ transiently shoots up to $0.5\text{pA}/\mu m^2$ during the peak of the action potential with an average efflux of the total K^+ current of $0.2\ \text{pA}/\mu m^2$ for about 50 ms. It seems safe to assume, that the K^+-current balances mostly Ca^{2+} influx - two potassium ions for one calcium. These results from the simulation become important when discussing transistor recordings of sustained single neuron activity.

All work and no play
That's the way it is, ain't it?
There's a rhythm deep inside of you
And you must get reacquainted

When was the last time you danced?

- Gnarl Barkley, *The Last Time* (2006)

Chapter 3

Results & Discussion

Let's dance -
Put on your red shoes and dance the blues
Let's dance -
To the song
They're playin' on the radio

- David Bowie, *Let's Dance!* (1983)

The collected data appears in context-derived order, meaning, that even the outline reflects the evolution of the project, in a few cases the appearance of presented data in the text does not reflect the chronological order of events.

3.1 Single Cell Observations

Before looking at networks of neurons, the basic mechanisms of the single cell interactions will be presented. It it is a long-established fact that it is possible to record strong neuronal electrical signals like action potentials [Fro91] as well as to stimulate single action potentials [Fro95] as was shown for leech neurons. None the less questions like 'is every cell capable of being recorded [Mer05]' or 'what is the exact mechanism of stimulation [Wal06]' demand a closer look in the light of the most recent observations within the department.
In the following section devoted to the signals recorded by field effect transistors first the parameters that affect the magnitude of the extracellular amplitudes will be investigated followed by some observations during the optimization of cell coupling. In the stimulation section, different pulse forms as well as their putative mechanisms to evoke neuronal activity will be described and discussed.

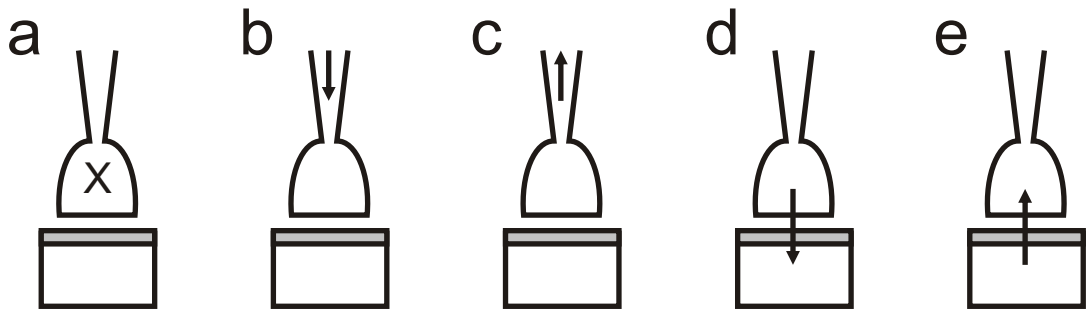

Figure 3.1: *Introduction to pictograms.*

(a) A capital letter X inside the cell abbreviates the name of the investigated large identified neuron: L for LPeD1, V for VD4 and R for RPeD1. (b) An arrow pointing away from the neuron's center stands for intracellular recording, while in (c) the arrow that points towards the cell body codes for stimulation via current injection through the pipette. (d) denotes extracellular recording with field-effect transistors while (e) shows the chip stimulation with a voltage pulse applied to a capacitor underneath the neuron. A shape underneath the arrow might indicate a special waveform that was used for the stimulus (not shown).

Ahead of the detailed discussion, Figure 3.1 presents the pictograms that will be used throughout this chapter to discuss the different aspects of cell-chip interactions of identified giant neurons (a): intracellular recording (b) and stimulation (c), as well as chip recording (d) and stimulation (e).

3.1.1 Single Cell Recording

The opportunity to investigate not only cells from a single organism, but also individual, identified neurons, that exist only once per animal brain opens the door

to unravel some aspects of cell coupling that could not be addressed before. Is it possible, to fully understand the recording from a single, real neuron? Would two identical cell on a transistor results in two exact same signals? How does the environment affect the coupling of those two identical neurons?
In the following subsection first the general shape and magnitude of the transistor signal will be discussed. As a consequence of the large observed signals, the measurement of cell-substrate distance on poly-L-lysine, one major parameter, that affect the magnitude of the transistor coupling, will be presented. That strong adhesion conditions, that lead to large transistor signals, might also have negative effects on cell physiology, is discussed in the paragraphs on 'Oscillations': The neuron's excitability is diminished periodically, which will be discussed through the comparison of intra- and extracellular recordings. The latter changes both in baseline as well as in shape, and both effects can be directly linked to the reduced excitability observed intracellularly. The results on Single Cell Recording are rounded off by the presentation of recordings on the 2-dimensional transistor array, that resolve the question, what parameters affect the cell's capability to be recorded extracellularly. Finally, a summary of the observations rounds off this subsection.

Magnitude and Shape of Transistor Signals of Single Identified Neurons

The three groups of recorded traces in Figure 3.2 show typical intra- and extracellular responses of RPeD1 neurons stimulated by current injection, as an example for all snails neurons investigated in this research project. The intracellular recordings are shown in red in Figure 3.2(b)-(d), the extracellular traces in black. All cells have been cultured on poly-L-lysine coated chips, in panel (b) and (c) in defined medium (DM), in panel (d) in brain-conditioned medium (CM).
Looking at the intracellular recordings, the first observation is that apart from minor differences shape and amplitude of the action potential resemble one another for all three neurons. When looking at the cells cultured in DM, the traces of the extracellular recordings show a similarity between the shapes of recordings in (b) and (c). The amplitudes differ on the other hand from transistor to transistor.
The shape for the extracellular recording in (d) differs not only in amplitude, but also in shape significantly from the other transistor traces. While in DM (b and c) a positive peak during the rising phase of the action potential is followed by a negative valley with its minimum during the repolarisation phase, in CM a minor peak during the rising phase is followed by a positive hump afterwards. Not only the absence of the negative part of the signal in CM meets the eye, but also the much smaller amplitude of the signal as observed by the relatively large noise level when compared to the cell's signal. At last only one transistor picks up a signal from the neuron RPeD1 in the case of CM, while the cells in DM couple to several ones.
The fact, that all three cells show similar action potential shapes and amplitudes confirms the advantage of comparability of experiments with identified giant neurons, even though each cell originates from a different snail. Even though no N

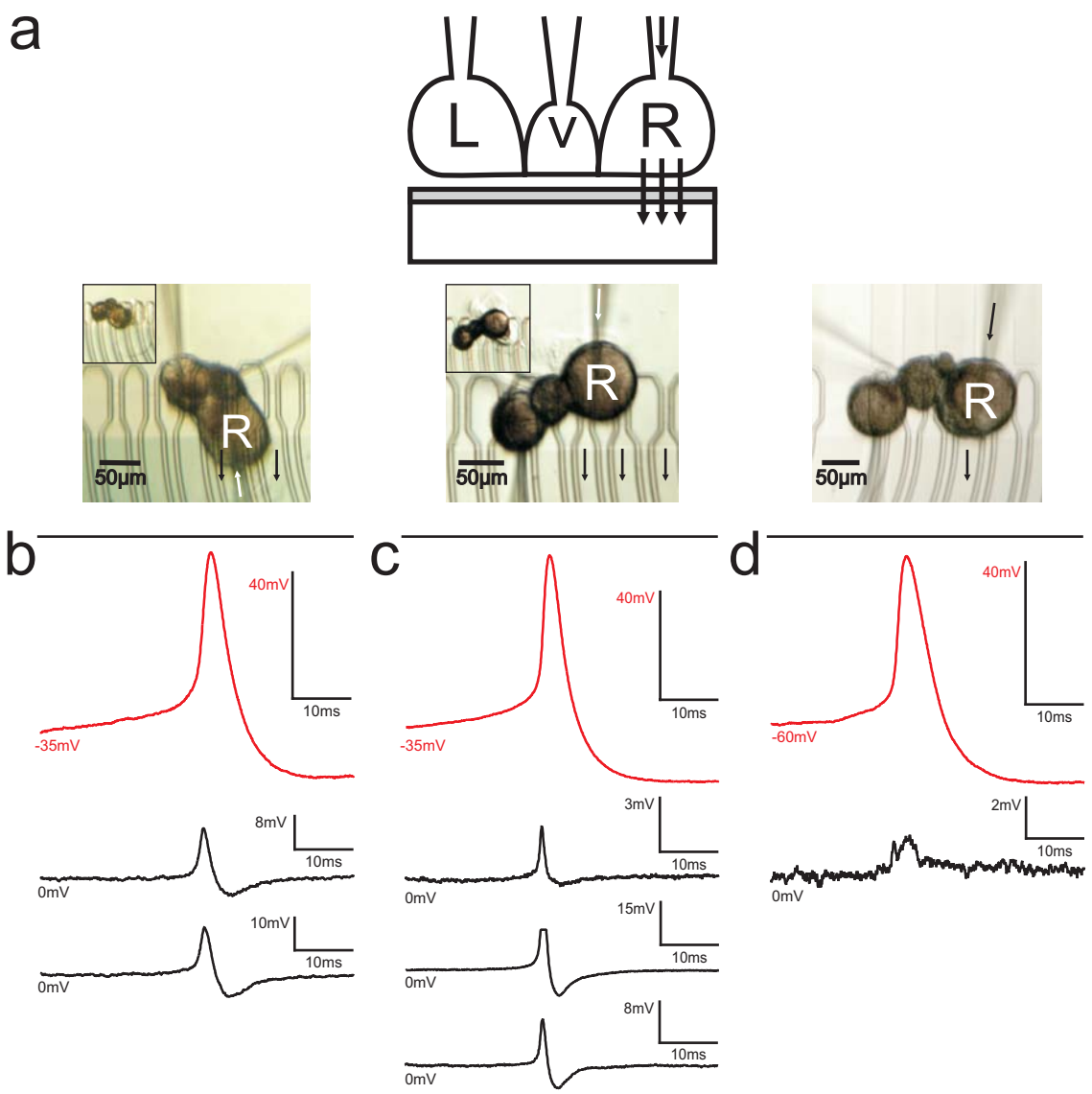

Figure 3.2: *Example for differences in amplitudes and shapes of transistor responses.*

(a) shows a schematic of the experiment, the extracellular recording of neuronal activity with field-effect transistors. The three micrographs show the placement of the neurons for the three different recordings shown below. Black or white arrows indicate the signal flow. The insets indicate the adhesion area of the investigated neuron RPeD1.
(b)-(d) All graphs have the same layout: on top the intracellular recording in red, in black the other recordings made extracellularly with transistors in the order from left to right of the arrows shown in the corresponding micrograph in (a). The black bars indicate the duration of the current injection.

will be put to the number of likewise observations made as presented in Figure 3.2, considering that hundreds of identified neurons have been extracted and measured for this research project, the traces chosen here represent the observations made on a large number for each neuron LPeD1, RPeD1 and VD4 cultured on poly-L-lysine coated chips. The analysis of the transistor signals for three RPeD1 neurons therefore has implications on all cells recorded with the same adhesion conditions, regardless of them being identified giant snail neurons.

When looking at the transistor signals in more detail, the shape of the extracellular recordings can be interpreted in terms of the equations presented in section 2.4 about the point contact model. The first peak for all three signals coincides with the rising phase of the action potential, a sure indication for a contribution from the sodium current. The sign is positive, meaning that a net positive charge remains in the cleft between cell and chip when compared to the bulk electrolyte. Considering the fact, that the sodium current is inward bound with respect to the intracellular compartment, a sodium influx decreases the density of positive charge carriers in the extracellular space. Therefore the sodium current density across the adhesion membrane has to be smaller than across the free membrane due to the sign of the sodium peak.

The interpretation of the late phase of the action potential is not so easily made, since two currents contribute during that phase of the action potential, potassium and calcium (see Figure 2.8). A high calcium current density would show in a shoulder and an extended repolarisation phase of the action potential. Assuming that the main contribution to the signal comes from the increased potassium current needed to return the neuron to resting membrane potential. Along the same line of discussion as for the sodium current, this would mean in the case of DM, that the outbound potassium current density would be larger across the free membrane as compared to the adhesion membrane.

In the case of CM on the other hand, the extracellular signal ends before the neuron's membrane potential has returned to its resting value. This indicates a major contribution of the calcium current to the second, more prolonged peak, which would also have a higher current density in the free part of the membrane. Unfortunately the small signal-noise ratio hides the repolarising potassium current within the device's noise. Only a nonzero running average value for the late phase of the action potential can hint at its presence.

These interpretations have two common messages: First, neurons cultured in CM on poly-L-Lysine show completely different signals as compared to neurons cultured in DM, even though the shape and amplitude of the action potential remains the same. Second, signals on poly-L-lysine coated chips show large contributions from the current across the free membrane, especially in the case of neurons cultured in DM. Two published papers support this view: Brittinger [Bri05] showed, that an increased potassium or calcium current in the cleft would result in a change in surface potential after a significant increase in ionic concentration. At least for the

potassium ions needed to repolarise the neuron this effect would show, as will be seen below. The other publication by Rink [Rin94], hints at the tendency of polycathionic molecules like poly-L-lysine to block negatively charged or electrically neutral ion channels when applied in micromolar concentrations. Santini et al [San97] observed an increase in conductivity and permeability for cultures adhered to poly-L-lysine as compared to uncoated plastic substrates for the cell line K562. Whether these effect take place in the case of snail neurons adhered to poly-L-lysine substrates, cannot be judged on the analysis of the transistor signal alone. Several unknown factors contribute to the signal besides the channel densities in the free membrane, namely those contributing to the junction's conductivity: the area of the adhesion membrane, the distance between membrane and chip as well as the conductivity of the electrolyte in the cleft (see Equation 2.4). When comparing the measurement on poly-L-lysine in DM and CM, the difference in signal amplitude might have some contribution from the difference in the area of the adhesion membrane, which shows in the insets in the micrographs in 3.2(a) as well as in the fact that only one transistor records a signal from RPeD1 in CM as compared to two or three transistors in the other case. Even though the evaluation of RPeD1's ion channel current densities would have gone beyond the scope of this thesis research project, an attempt to determine the junction parameters was made as shown in the following paragraphs.

Diminished cell-substrate distance on poly-L-Lysine in DM

The method of fluorescence interference contract (FLIC) microscopy that was developed in this department (see Subsection 2.3), allows to determine the distance between cell and silicon-oxide substrate grown on a silicon wafer. After staining the membrane with the fluorescent dye $DiIC_{18}$, the following typical images could be observed as shown in Figure 3.3[1]. In the following, the distances obtained from the numerical fit will be taken to show differences in the adhesion profile of single neurons as well as differences between neurons subjected to various adhesion conditions. Even though the accuracy of the values might be contested, the computed differences reflect the fluorescent light intensities, which can be verified with the eye.

Figure 3.3 shows two neurons stained with the fluorescent dye $DiIC_{18}$ after having been 16 hours in culture on a freshly coated poly-L-lysine substrate in different kind of adhesion conditions. In the case of panel (b), prior to the placement of the neurons on the chip, brain-conditioned medium (CM) was left in the chip's chamber and after half an hour replaced by defined medium (DM). The staining shows that the membrane of the nerve cell in panel (b) spreads itself along the surface surrounding its soma, increasing the contact area to a radius up to twice its soma's diameter. The adhesion on the other hand is anisotropic: Not only the area is covered in a non-radial fashion, but also the cell-substrate distance calculated in

[1]For the exact staining protocol see Appendix C

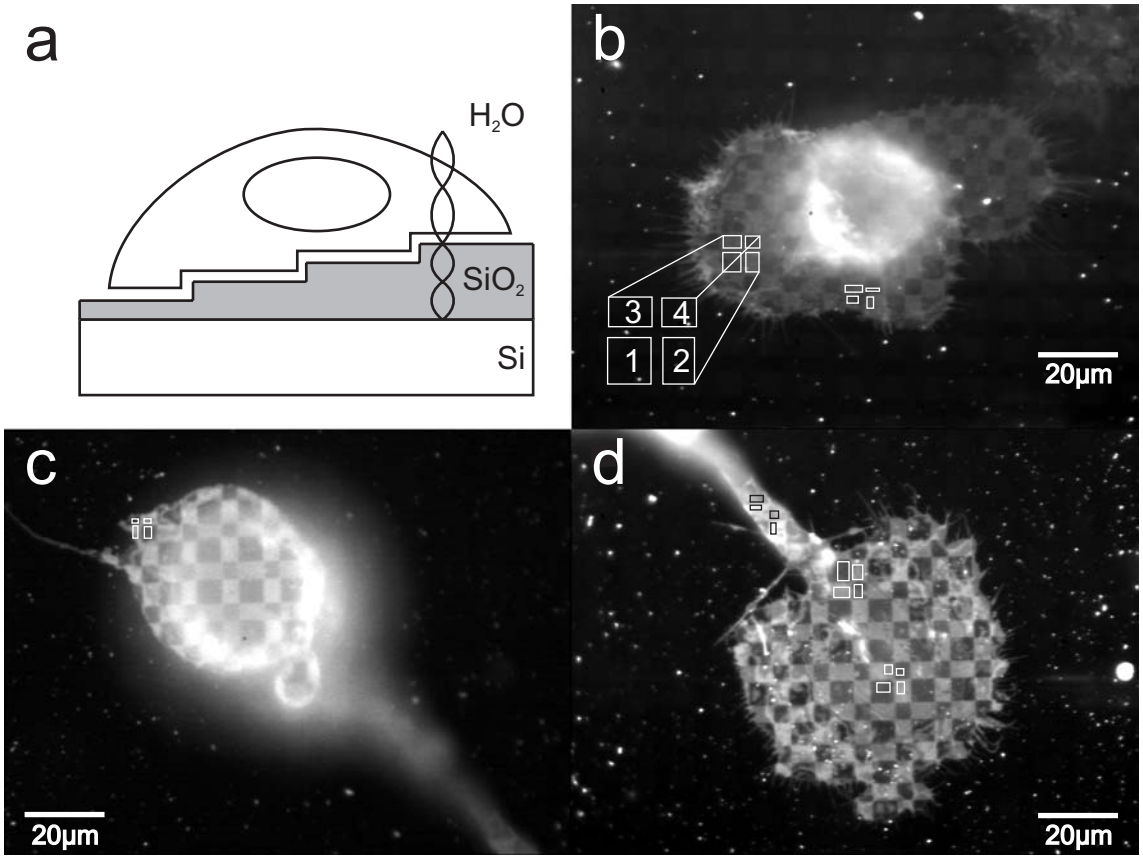

Figure 3.3: *Two Examples for Cell-substrate Distances on Poly-L-Lysine.*

(a) Schematic of the fluorescence interference contrast microscopy (FLIC) principle showing a cell in electrolyte (H_2O), silicon dioxide layers (SiO_2) of four defined thicknesses, the silicon substrate and two periods of a standing light wave. The dimensions are not to scale, cells are $100\mu m$ sized, the oxide thicknesses increase equally ranging from $10nm$ to $160nm$, the cell substrate distance measures less than $50nm$ (see below) and the excitation wavelength used is in the visible spectrum at $546nm$.
(b), (c) and (d) show fluorescence images of the emitted light from the adhesion membrane using the dye $DiIC_{18}$. (b) shows soma (bright) and additional adhered membrane of a typical neuron. The step height distribution is indicated by the white squares labeled 1 ($10nm$) through 4 ($160nm$). Another example is the soma of a nerve cell in (c), while its strongly adhered axon is shown in (d). The different groups of four white squares shown in (b)-(d) indicate different spots of investigation, yielding the fitted distances: (b) $41 \pm 12nm$ (left), $25 \pm 2nm$ (right); (c) $13 \pm 5nm$, (d) $27 \pm 3nm$ (upper left), $18 \pm 2nm$ (middle) and $26 \pm 4nm$ (lower right).

two different spots results in a size of 41 ± 12 nm on the left and 25 ± 2 nm on the lower side of the micrograph.

On a chip that only contained DM the neuron's soma (c) and axon (d) formed two areas of strong adhesion. The brightness of the central part of the neuron makes the evaluation of the distance difficult. None the less near the edge a distance of 13 ± 5 nm could be found. The axon on the other hand is more homogeneously illuminated, yielding distances of 27 ± 3 nm, 18 ± 2 nm and 26 ± 4 nm.

When comparing those two adhesion conditions, it seems more likely in the case of pure DM on a chip freshly coated with poly-L-lysine for cells to form a membrane-chip distance below 30 nm as compared to a substrate pre-conditioned with CM. The literature values, which were measured by Zeck [Zec03] for *Lymnaea* neurons after 3 days in vitro on poly-L-lysine in presence of 2 additional whole brains per ml of medium for co-conditioning, give averages around 50 nm, with the lowest value of 42 ± 2 nm.

A first conclusion is, that the distance values obtained by Zeck for his given conditions do not reflect the situation for measuring after 16 hours in vitro in DM. The distances found here on fresh poly-L-lysine with DM are at least 10 nm smaller than the smallest value reported by Zeck. The situation with CM is ambiguous: It is assumed, that CM contains a soluble fraction that readily adheres to the substrate after 30 minutes of incubation [Won81][2]. Even though this might be the case, strong adhesion can also take place as can be seen from 3.3(b). Therefore we conclude, that the distance found on poly-L-lysine regardless of the presence of CM varies between $20 - 30$ nm. The low number of conducted experiments disallows speculations about the source of these variations. Additional attempts to determine the specific conductivity of the electrolyte in the cleft - a distance of 20nm and below could lead to a significant decrease (Gleixner, personal communication) - could not be evaluated due to the inhomogeneous adhesion profile of the investigated, large neurons ($d > 50$ μm, data not shown).

Single Cell Oscillations

Besides a healthy neuron coupling to the transistor underneath its adhesion area, another requirement is the prolonged activity over several seconds for the investigation of chemical synapses, especially inhibitory ones. One of the major issues in extending the work on excitatory to inhibitory synapses was to overcome the problem for poly-L-lysine covered chips described below.

Figure 3.4 shows two examples of neurons recorded simultaneously for the testing of synaptic activity (trace for third neuron not shown) after 16 hours in culture on poly-L-lysine coated chips in the presence of DM. As can be seen from panel (a) and (b) the activity of the neurons stops even though the injecting current persists.

[2]Data was obtained from snail *Helisoma*, which is phylogenetically close to *Lymnaea*

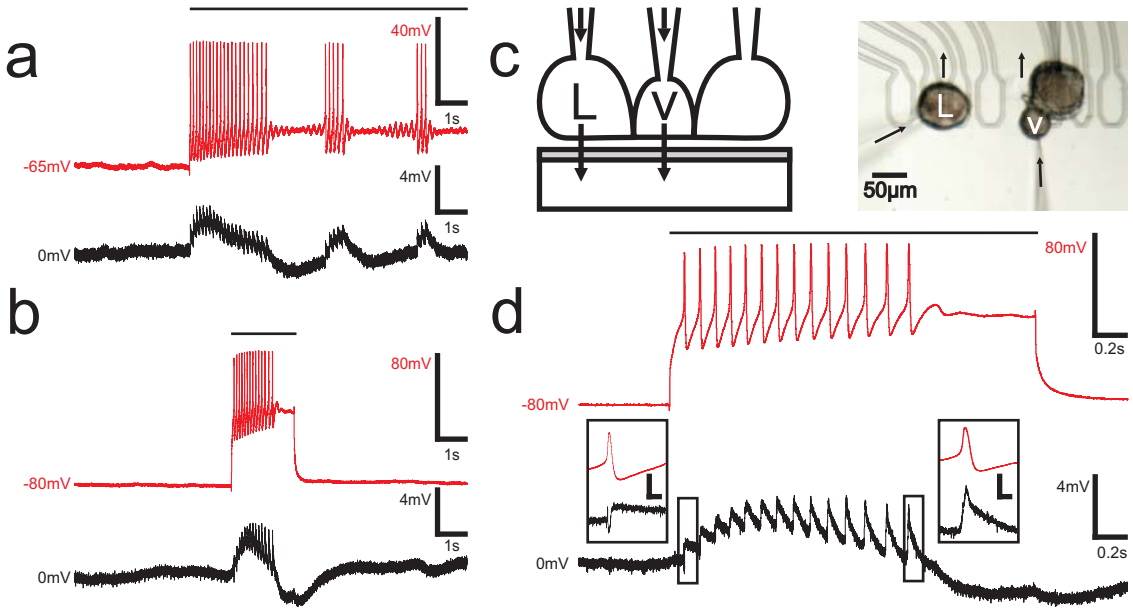

Figure 3.4: *Single cell oscillations.*

(a) and (b) show two examples for cells, whose continuous activity diminishes during current injection. Intracellular measurements are drawn in red, extracellular ones in black. The black bar indicates the duration of current injection. In (a) LPeD1 stops its activity for about 2s before picking up again, while in (b) VD4 mutes although the stimulating current persists.
(c) shows the schematic of the experiment as well as a micrograph of the investigated neurons. (d) show the same measurement as in (b), but in more detail along with two close-ups of the first and last action potential. insets: electrophysiology 40 mV, transistor 2 mV / time scale 20 ms.

In the case of the neuron LPeD1 in panel (a), the activity picks up again after a resting period of about 2 s. This happens twice during this measurement.

Panel (d) shows more details of VD4's recording in panel (b). The transistor trace shows, that during the activity of VD4, the recorded junction potential increases before the activity diminishes. The similar effect can be seen in panel (a) for LPeD1. For VD4, the change in the recorded potential goes up to 4 mV, before the cell activity diminishes. Additionally, during the time course of the activity, the shape of the extracellularly recorded junction potential changes from a small transient of 2 mV size followed by a plateau potential of 1.5 mV height on the left inset to a 3 mV peak followed by a downward slope with a gradient of 2 mV over 100 ms.

The interruption of continuous activity was a phenomenon frequently observed while working with groups of neurons on poly-L-lysine (PLL) coated chips in the presence of DM (N $>$ 50). On the other hand, the interruption of activity was a lesser issue when working on the same substrate but in the presence of brain-conditioned medium (data not shown).

Potassium Efflux into the Junction changes Potassium Reversal Voltage

The recorded transistor potentials, along with the knowledge about the diminished cell-substrate distance on PLL/DM lead to the working hypothesis, that a activity-dependent effect takes place in the junction, which reduces the excitability of the neuron. This notion was supported by the observations made by Brittinger ([Bri05], Figure 5), that changes in the extracellular concentration of K^+ or Ca^{2+} lead to a shift in the surface potential of the silicon oxide. Potassium - K^+ - which is found in a concentration of 1.7 mM in the cell culture medium (see Appendix A.2) and which enters the junction through potassium ion channels in the adhesion membrane during an action potential, would be a candidate for such an effect for two reasons. One the one hand, its increase in extracellular concentration would lead to a positive change in surface potential, while on the other hand it would reduce the excitability of the neuron due to its effect on the potassium reversal voltage in the junction $V^0_{K^+,JM}$. A decreasing potassium current would lead to a diminished repolarising current during the late phase of the action potential and would prevent sodium and calcium channels to change their states from inactivated to closed[3]. Taking the extracellular voltage change during the activity of VD4 of 4 mV as a key value for the increase in potassium concentration, this would correspond with Figure 5 of [Bri05] to a concentration change of from 2 mM to at least 3 mM. Since $\ln c_J(K^+)$ enters into the calculation of the reversal voltage $V^0_{K^+,JM}$ of potassium in the junction using the Nernst equation, a increase of 50% in concentration leads to decrease of the reversal potential by 27 mV $*ln(2.55\text{ mM}/1.7\text{ mM}) = 11$ mV, an increase of 100% in concentration shifts the reversal potential by 27 mV $*ln(3.4\text{ mM}/1.7\text{ mM}) = 19$ mV.

[3] About the model of voltage gated ion channels with states like open, inactivated or closed see [Hil01]

Therefore the reversal potential for potassium is changed from a putative −80 mV to a value between −70 to −60 mV: the intracellular voltage cannot go lower than this value. Therefore the sodium channels in the adhesion region, needed to create action potentials, become very sensitive to the potassium efflux during activity.

When looking at the typical potassium current density for a snail neuron (see 2.4 for a simulation of the ionic conductances), one can check whether the neuron actually emits a number of potassium ions needed to create such a change in concentration as observed by the transistor. A straightforward calculation assuming an adhesion radius of 80 μm, a conservative cleft width of 50 nm and a number of roughly $3 * 10^{10}$ potassium ions entering the junction during a single action potential, leads to a concentration change by 1 mM. Considering an equilibrium situation between efflux from the neuron and diffusion from the junction into the bulk during activity, a steady state value of the potassium concentration close to the concentration change found by the extracellular recording can be imagined. Unfortunately, a more thorough analysis of the extracellularly recorded potential change is limited by the temporal resolution of the amplification circuit of the transistor current, which has an intrinsic cutoff frequency such that effects with a lifetime beyond 1 s will be diminished in amplitude. Therefore the steady-state situation cannot be evaluated properly with this amplifier [4].

Diminishing Contribution from Adhesion Membrane shows in Transistor Coupling

The two insets in figure 3.4 show the junction voltage recorded by the transistor during the first and last action potential in this volley. Apart from the offset in junction voltage, which was extensively discussed above, also the shape of the coupling changed during those few action potentials. The difference is especially obvious when looking at the insets in panel (d).

In the left inset, the transistor coupling at the beginning of the activity coincides with the rising phase of the action potential. The recorded signal can be described consisting of three parts: in the beginning the junction potential rises sharply, then a negative flank follows, rounded off by a second positive extremum at the end. In the right inset, a positive flank rises simultaneously with the intracellular potential of the neuron. Its peak coincides with peak of the action potential. The recorded signal remains positive throughout the action potential.

With the knowledge of the different currents that contribute to the signal as presented in Section 2.4, both signals can be interpreted completely in the context of sodium and potassium currents. In the case of the first action potential, the fast voltage change is characteristic for a capacitive current running along the membrane, the rise indicates that it runs from the free part of the membrane into the

[4] During the design, no temporal signal persisting more than 250 ms was expected considering synaptic transmission as the limiting time scale

junction. The second part due to its negative sign indicates a removal of positive charges from the junction, as would be the case for sodium ions entering the neuron through the adhesion membrane. The sign of the third part, now again positive like in the case of a current of positively charged ions from the cell into the junction, supports the idea of the potassium current, which ultimately leads to a change in surface potential at the gate oxide as discussed above.

In the case of the right inset, when comparing the timing and the shape of the transistor record with the result of Zeitler's simulation of ionic currents for snail neurons during an action potential in Figure 2.8, the similarity with the K_K potassium current becomes obvious. Therefore it is tempting to draw two conclusions: First, in the right inset the recorded signal actually shows the potassium current through the adhesion membrane, which fits both in sign and shape. Second, the absence of the negative sodium peak in the right inset as compared to the first phase in the left inset, would undermine the previously discussed increase in junction potential due to the continuous efflux of potassium. Since this current increases the the junction potential ϕ_J as well as the voltage across the junction membrane V_{JM}, it would locally inhibit the voltage-dependent transition of sodium channels from the inactivated into the closed state, thus leading to a decreasing contribution of the sodium current to the recorded transistor signal.

Even though three different recorded characteristics of the transistor trace - the first and last recorded action potential as well as the lasting increase in surface potential - seem to indicate towards the interplay of sodium and potassium channels in the adhesion membrane, the evidence is circumstantial: Only the offline analysis of the signal by comparison with a theoretical model of snail activity as well as a titration curve of the dependency of the surface potential on the extracellular potassium concentration could give this indirect insight. Only a direct measurement of the sodium and potassium current through a patch-clamp recording would verify the evidence.

To separate the influence of the junction from that of the coating, the observation in Section 3.3, that inhibitory synapses form more reliably on surfaces coated with the fragments of the β-subunits of Laminin might help, since Schoen found cell-substrate distances in the same range as presented above for poly-L-lysine [Sch07]. Along with the results found in literature, that poly-L-lysine not only has an increasing effect on the conductivity and permeability of cells adhered to a poly-L-lysine substrate[San97], but also can also block specifically negatively charged ion channels [Rin94], a negative effect of poly-L-lysine on the excitability of neurons in cell culture becomes obvious. Unfortunately, the Laminin coating became available only at a late stage of the research project. Otherwise comparisons between the signals recorded on Laminin versus poly-L-lysine would have helped to isolate the exact mechanism of the cell-coating interaction.

Recordings of Cell Activity in Adhesion Region with a Transistor Array

Considering the fact that a necessary prerequisite for the creation of large groups of synaptically connected neurons was the high survivability of the extracted neurons, the question whether all neurons are able to couple finally gets addressable. At the same time that the new cell culture technique was in the process of being established within the department, the planar field-effect transistor arrays built in cooperation with the company Infineon Technologies [Eve03] made high-resolution recordings of large groups of neurons feasible, regardless of their placement.

Figure 3.5 illustrates a representative measurement: a group of three A-cluster neurons interconnected with electrical synapses is contacted intracellularly. The activation of the neuron marked 'I' leads to a group activity shown in panel (b). Due to the fact, that before plating the cells in DM the substrate was freshly coated with poly-L-lysine, large contact areas were formed as can be seen from the intracellular staining of the cell cluster with Lucifer yellow (inset of panel (a)). The most important contribution for this research project is the simultaneous recording of several transistors during single cell activity in panel (c): the transistor underneath the adhered membrane of each neuron registers its activity as shown during the peak of the action potential marked in panel (b).

As a conclusion, recording signals extracellularly is not a matter of the cell's capability to couple to a transistor. Its viability and the fact, whether its adhesion membrane covers the field-effect transistor, determines the appearance of a signal during activity. The degenerate case of balancing currents due to equally distributed ion channels across the membrane is not fulfilled for a healthy neuron, since the axon-hillock contains a high density of sodium channels [Bru91]. Synaptic partners on top have specialized zones of high conductivity for all ions in the synaptic area. Therefore the only imaginable cases where no signal is observed is that that of a damaged neuron or of insufficient adhesion in the gate area - either the area is not covered at all or the cell-substrate distance is too large. The latter was most likely the case during the study conducted by Merz [Mer05], and could probably have been fixed by increasing the width of the troughs and channels.

Summary - Single Cell Recording

In detail, in the section on observations of single cells, it has been shown, that the activity of snail neurons gives a reliable signal with amplitudes around $0.5 - 2.5$ mV in the presence of brain-derived proteins, but much larger, varying amplitudes up to 30 mV in the case of neurons grown on fresh poly-L-lysine coated substrates. None the less, measurements on a two-dimensional sensor array proved the possibility of detection of neuronal activity, across the whole contact area of each healthy neuron in culture. Measurements of the cell-substrate distance on the other hand showed, that in the case of strong adhesion on poly-L-lysine coated silicon-dioxide surfaces the junction can be as narrow as 20 nm, which partially could explain the large

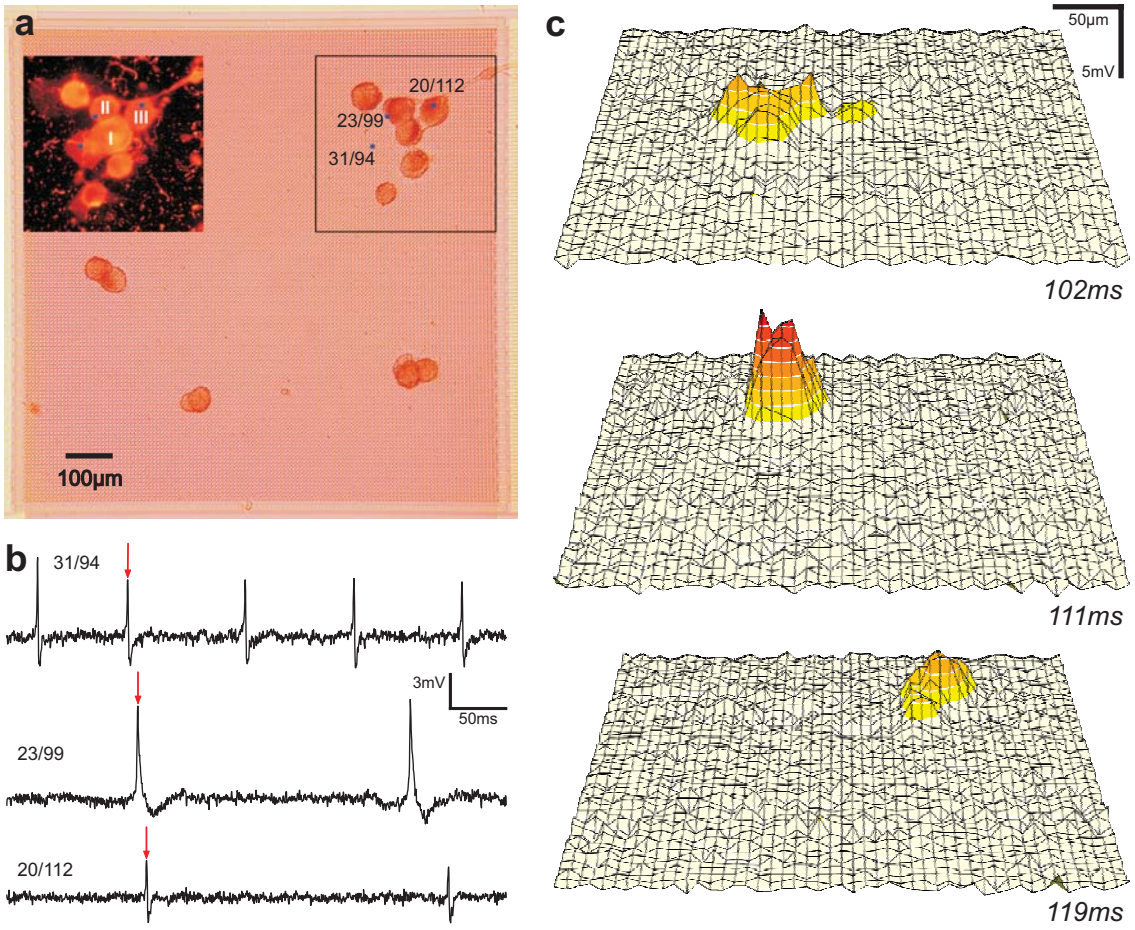

Figure 3.5: *Recording of neuronal activity with a 2D sensor array.*

(a) top view on a 1 *mm* $*$ 1 *mm planar transistor array with 16.384 transistors. On the array several groups of A-cluster neurons from* Lymnaea stagnalis *formed clusters interconnected via electrical synapses. The black box frames the recorded sector (shown in c), while the blue spots mark the investigated transistors in (b), which are labeled in a row/column fashion. Inset: Lucifer yellow staining of the group within the framed area, I-III indicate the order of the extracellular recordings in (b).*
(b) Time traces of the indicated spots from (a). The two coordinates code for the transistor's row and column. The red arrows indicate the time, at which the activity of the sector framed in (a) is shown in (c). Current injection via an intracellular electrode drives the activity of the neuron recorded in the top trace.
(c) Local activity for three given time points indicated in (b). Each extracellular voltage landscape shows the potential distribution during the peak of the action potential of each of the three interconnected A-cluster neurons.

observed signals. This close contact in itself, has consequences on the physiology of the neurons: neuronal activity over a period of seconds under these adhesion conditions could underlie a cyclic activity pattern of several action potentials followed by prolonged resting phases. It could be shown, that the cellular activity in itself has effects on the potential recorded by the transistors in the junction: using results of a previously made simulation, the shape of the recorded signal during the phases of the action potential showed, that an efflux of potassium ions largely contributed to the junction potential. It was concluded using premade titration curves, that the potassium concentration in the junction increased during the cellular activity leading to a significant change in the potassium reversal potential across the adhesion membrane. This new reversal potential, that results in an increase in the resting membrane potential, would prevent an increased fraction of voltage-sensitive sodium channels to return to an excitable state, thus providing a model for the oscillatory behavior observed. Whether this large observed potassium current, that shows in the extracellularly recorded potential, is the sole reason for this limit-cycle activity or just an effect of interactions between the poly-L-lysine coating of the surface and the adhesion membrane, could not be investigated.

3.1.2 Single Cell Stimulation

Ever since the first successful capacitive stimulation of neurons [Fro95], square pulses were the pulse shape of choice due to their high steepness values dV_{St}/dt. The higher the steepness, the larger the extracellular voltage V_J created in the junction between chip and lower cell membrane (see Section 2.4, Equation 2.3). Even though a large dV_{St}/dt is a prerequisite to get any response from the neuron, the duration for a sustained dV_{St}/dt is also important: For square pulses the duration of the current that leads to the charging of the capacitor is very short being less than a microsecond - the exact evaluation of the rise time for such a pulse reveals a measurement problem intrinsic to the chip: The capacitive current not only charges the stimulator pad situated at the junction, but also the silicon-silicon oxide interface along the whole stimulator line. An effect of this charged stimulation line for combined recording-stimulation chips, results in recording artifacts in transistors close to the charged capacitor, since the electrical field is not limited to the gate region alone, but also builds-up vis-a-vis the drain lines.

Ramp shaped pulses on the other hand have the advantage that their well defined amplitude and duration help to determine their dV_{St}/dt computationally as well through simultaneous transistor recording. Applying these pulses results in a constant junction potential for the duration of several milliseconds, the time frame in which voltage-sensitive ion channels start reacting to changes in the junction membrane potential V_{JM}. Although the two-way contact chips used in this study (see Section 2.2.2) are not coated with a high K material like titanium or hafnium oxide, the for snails favorable parameters affecting the junction conductivity G_J, especially the extremely close distance between cell and chip found in 3.1.1, increase the likeliness of opening voltage-gated ion channels in the adhesion membrane even on silicon dioxide.

In the next paragraphs, stimulation with ramp-shaped pulses will be introduced: after an introductory experiment, an analysis of the different parameters that affect the steepness of ramps - amplitude and duration - as well as the effect of membrane potential on the cell's response to the stimuli will be presented. The ensuing discussion will be divided between effects of the stimuli on the intra- and extracellular potential. The second part of the stimulation results will evolve around the comparison between ramp and square pulses with respect to their suitability for electroporation. Again, a paragraph summarizing the results on stimulation concludes this section.

Physiological Opening of Ion Channels via Ramp Stimulation

With the cooperation of Ingmar Schoen, a first try at the capacitive opening of ion channels of snail neurons on silicon dioxide coated chips with two-way contacts was made, as can be seen in Figure 3.6. This and the following experiments regarding ramp stimulation were conceived by Ingmar Schoen and carried out in his presence.

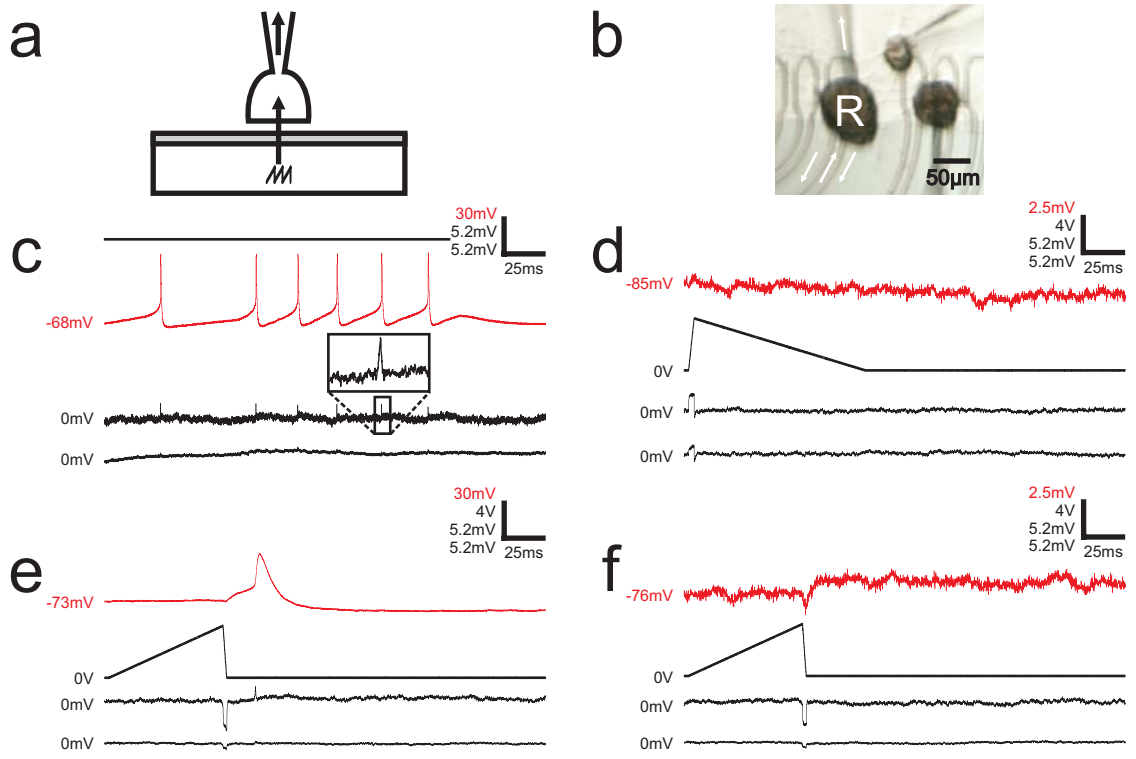

Figure 3.6: *Introduction to Stimulation with Ramp Pulses.*
(a) Schematic: A ramp pulse applied to a stimulator pad while monitoring membrane potential with an intracellular sharp electrode.

(b) Micrograph of the investigated neuron.
(c) Intra- (top, red) and extracellular recording of this cell's activity caused by pipette stimulation to demonstrate cell coupling to the transistor to the right of the stimulator pad (middle trace), while the transistor to the left of it registers almost nothing (bottom trace).
(d) A ramp pulse with large positive slope (2nd trace from above) applied to the stimulator pad indicated in (b) does not elicit any response intracellularly (top, red) while both transistor recordings (bottom traces) register the extracellular voltage change.
(e) A ramp stimulus with large negative slope (second trace) applied to the chip causes an action potential (top trace, red) and is recorded by the transistor to the right of the stimulator (third trace). The adjacent transistor (fourth trace) records only a fraction of the junction potential.
(f) The sub-threshold response of the cell to the same stimulus as in (e). The transistors pick up the stimulus-derived change in junction potential, but nothing from the neuron. Scaling: (c) inset: 2 *mV/*20 *ms.*

Introduction to Stimulation with Ramp Pulses The intact and active neuron shown in the micrograph in panel (a) couples to the transistors next to it (panel c), when stimulated intracellularly by the micropipette. When applying voltage ramps to the stimulator pad underneath the cell (micrograph, panel b), a rising edge ramp, that results in a constant large increase in junction potential for a few milliseconds followed by a constant small decrease during the remainder of the pulse, does not evoke any intracellular voltage change, even though the transistors pick up a locally different extracellular voltage change during the fast rising phase. Only when using a falling edge pulse, which results in a constant large decrease in junction potential for a few milliseconds followed by a constant small increase during the remainder of the pulse, as shown in panel (e) and (f), an action potential can be evoked and an intracellular change in membrane potential be observed, respectively. Note that in (e) the coupling of the cell activity is similar to that recorded during micropipette stimulation in panel (c). It can also be seen, that even though the stimulus amplitudes are similar, the extracellular responses to the pulses vary in amplitude between the different panels, getting smaller from (e) over (f) to (d) (which reflects the temporal order of the events).

Considering the model underlying the opening of ion channels presented in Section 2.4.2, the falling edge pulse affects the ion channels in the junction membrane. Schoen could evoke action potentials with smaller values of pulse steepness using falling edge as compared to rising edge pulses [Sch07]. The decrease in the junction potential seen when comparing panels (e), (f) and (d), reflects on the other hand a worsening of the adhesion conditions during the time course of the experiment. Therefore a preference to stimulate neurons with falling over rising edge pulses on silicon dioxide cannot be unambiguously concluded from this experiment. None the less, in principle even with a material of lower ϵ like silicon dioxide, large neurons can be stimulated capacitively in the case of strong adhesion conditions. This is even more surprising, since the extracellular voltage applied to the stimulator affects only a part of the adhesion membrane fully, as can be seen from the recording of the adjacent transistor (lowest trace in panels c-f).

Limitation in Stimulus Amplitude on Silicon Dioxide After the first promising results a more thorough analysis was necessary to determine the influence of the different parameters. In Figure 3.7 the effect of increasing stimulus amplitudes were tested on a different chip and neuron (see micrograph in panel a). Stimuli around 5 V were applied to the stimulator pad underneath the cell and the intra- and extracellular potentials were recorded with a micropipette and two transistors, respectively. The set of measurements presented here represent several stimuli of increasing amplitude applied to the investigated neuron. Looking at the first set in panel (b), the intracellular potential decreases slightly during the falling phase of the stimulus. Both transistors record a decrease in junction potential. In panels (c), the stimulus amplitude is increased by 0.5 V as compared to the previous panel.

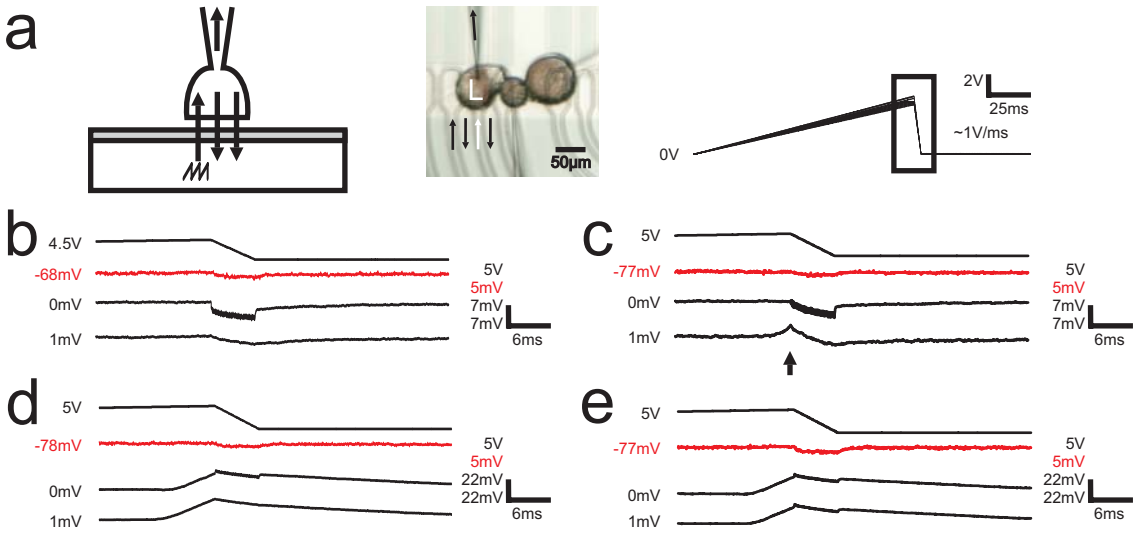

Figure 3.7: *Ramp analysis: increasing amplitudes.*

(a) shows a schematic of the experiment (left), a micrograph of the cells and chip (middle) and the set of voltage ramps used to stimulate the neuron (right). In the schematic and micrograph inbound black arrows depict chip stimulation, outbound arrows transistor or pipette recording. The box around the stimuli highlights the time interval for figures (b)-(e). From (b)-(e) stimuli (top trace) of increasing amplitude and the transistor responses (third and fourth trace) were recorded along with the intracellular potential (second trace, in red). Note that in (c) the transistor further away from the stimulation spot records a potential change prior to the stimulus onset (arrow). In (e) the same stimulus was used as in (d), but was applied at the spot indicated by the white arrow in (a).

When the voltage applied to the stimulator pad increases to a value beyond 5 V, the source-drain current recorded with the second transistor increases before the falling phase of the pulse begins. When increasing the stimulus amplitude even further, as shown in panel (d), both transistors record changes in the current prior to the beginning of the falling phase. For comparison, panel (e) shows the transistor and cell responses, when using a stimulator next to both transistor drain lines.

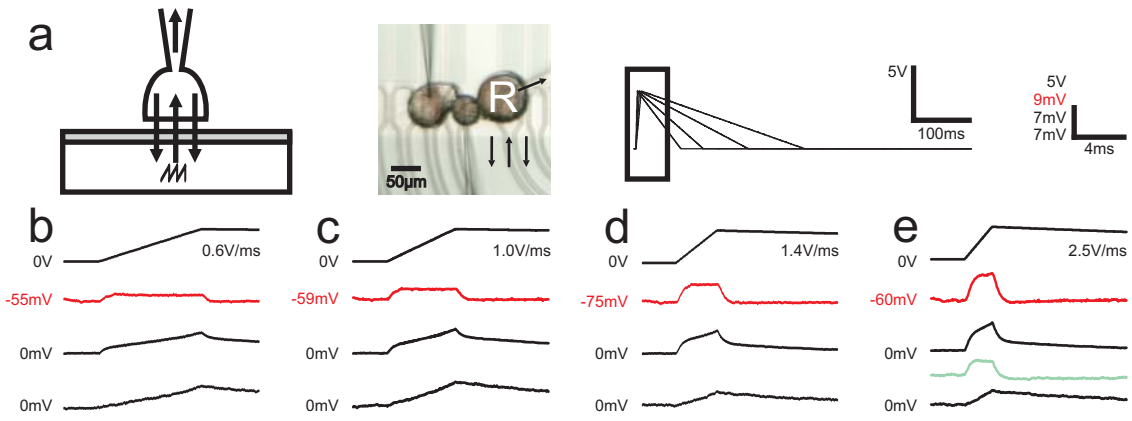

Figure 3.8: *Ramp analysis: effect of increasing rising ramp pulses' steepness on transistor, junction and neuron.*
(a) shows a schematic of the experiment (left), a micrograph of the cells and chip (middle) and the set of voltage ramps used to stimulate the neuron (right). The frame around the stimuli indicates the time frame for figures (b)-(e).
From (b)-(e) stimuli (top trace) of increasing steepness of the rising phase create intra- (2nd trace, red) and extracellular responses (third and fourth trace). The green trace in panel (e) is derived from subtracting the two transistor traces from one another and is scaled like the first transistor trace. Note that all graphs (b)-(e) share the same scaling.

Effects of Increasing Stimulus Steepness on Intracellular Response After having applied voltages larger than +5 V which most likely resulted in damage to the thin oxide, the next experiments were carried out on the other large neuron of the group. Figure 3.8 (b)-(e) shows how an increase in steepness of the applied pulse affects the intracellular voltage change in a proportional manner. The transistors record an increasing junction potential during the whole rising phase of the pulse, which decreases slowly after the stimulus has ended.

Dependency of the Intracellular Response on the Membrane Voltage In a third experiment we tried to determine which ionic current mainly contributes to the potential changes observed during the capacitive stimulation. For this we repeatedly stimulated the cell with the same pulse while changing its intracellular potential

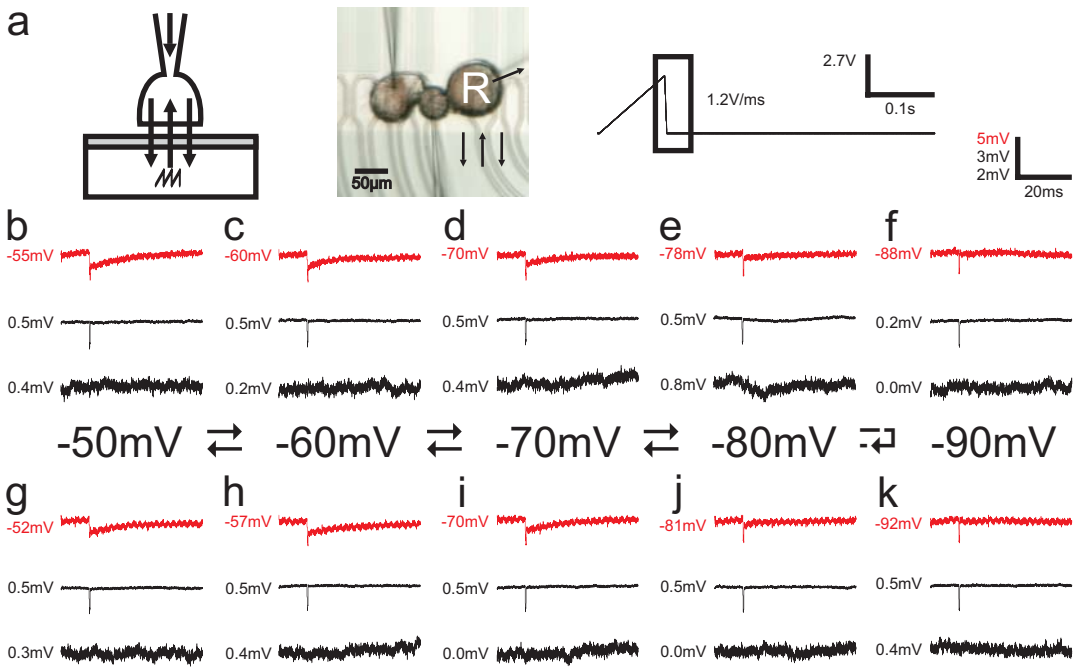

Figure 3.9: *Effects of membrane potential on the intracellular voltage change during falling ramp stimulation.*

(a) shows a schematic of the experiment (left), a micrograph of the cells and chip (middle) and the voltage ramp used to stimulate the neuron (right) while its intracellular potential is under external control. In the schematic and micrograph the inbound arrows depict chip stimulation and pipette current injection, outbound arrows transistor recordings. The frame around the stimuli indicates the time frame for figures (b)-(k).
From (b)-(f) the cell's response to the same stimulus (not shown) at decreasing membrane potential is recorded (middle trace) along with the two adjacent transistors (top and bottom trace). From (k)-(g) the membrane potential increases again. Note, that there is a significant decrease in the noise level as well as an increase stimulus artifacts of the transistor in the top trace due to the larger gate area. Note that alls graphs (b)-(k) share the same scale bar.

through the impaled micropipette. Figure 3.9 shows the intra- and extracellular potentials during a series in which the membrane potential is first lowered (b-f) and then subsequently raised (k-g). The main observations are that the change in membrane potential during the pulse disappears between −80 mV and −90 mV and the constantly increases up to −50 mV. A more positive intracellular membrane potential was not possible with a sharp electrode, since it would lead to spiking of the neuron, which can only be suppressed in a whole-cell patch-clamp configuration.

Discussion of Intracellular Response during Ramp Stimulation The three different experiments first of all confirm, that the stimulation with ramp pulses affects the intracellular potential proportional to the steepness of the applied pulse (Figure 3.8). But already the first experiment shows, that a falling ramp pulse did not lead to an increase in intracellular potential Figure 3.7 as expected from theory. The extracellular recording on the other hand shows a decrease in junction potential, therefore a failure in the process of the stimulus application can be ruled out. This discrepancy for falling phase pulses between intracellular response and the model introduced by Schoen in [Sch07] might be explained by the dependency of the stimulus response on the membrane voltage, which is shown in Figure 3.9, even though a different neuron was investigated: The only ionic conductivity in the cell with a reversal potential between −80 and −90 mV is that of potassium. Thus, even though a falling ramp stimulus increases the junction membrane voltage V_{JM}, the decrease in membrane potential results from a potassium driven net current across the junction membrane. Whether voltage-sensitive potassium conductances are involved cannot be deduced from these experiments. All in all, this observation is in agreement with those made in the context of transistor recording on poly-L-lysine leading to oscillations in the excitability of neurons.

Discussion of Transistor Response during Ramp Pulse Stimulation In an experiment, that would perfectly reflect the underlying theory, the transistor would record a constant junction potential during the linear change in stimulus voltage flanked by a charging and uncharging curve during the change in sign in the slope of the stimulus with the time constant of the low-pass filtering junction. The first experiment (Figure 3.7 shows, that exceeding the voltage limits of 5 V, parasitic currents start to flow within the chip, which disturb the detection of the changes in junction potential at the transistor's gate. That this effect persists even after the stimulus drops below 5 V as seen in panel (d), indicates drastic effects taking place, like the onset of Ohmic currents across the silicon-silicon oxide barrier, which should happen only beyond 5 V. But in this case, these effects not only take place when a threshold voltage is exceeded. In Figure 3.8, for rising ramp pulses, the effect, which is additive, happens during the whole pulse. By subtracting a neutral transistor trace from the trace belonging to a transistor in the junction of the investigated neuron, a signal shape as expected from theory could be computed. A source for

this effect could not be isolated. The fact, that the artifact begins even for a small applied stimulation voltage, indicates, that the source might not be intrinsic to the chip but resulting form the stimulus creation. The function generator used to create this pulse accepts only a limited number of data points for an arbitrary waveform. Since the ramp pulses were optimized to minimize the steepness of the repolarization phase of the pulse, the steeper phase becomes ragged for large amplitudes as can be seen in the first transistor traces of Figure 3.7. Whether this explains all artifacts, remains to be tested.

In conclusion, even though it is in principle possible to evoke a single action potential through capacitive stimulation of snail neurons well-adhered on chips covered with silicon-dioxide, it is a very unlikely event: Large amplitudes close to the electrical breakdown of the oxide are needed to create small intracellular effects driven by the potassium current - probably due to damage to the voltage-sensitive sodium channels when the cells are plated on substrates with a fresh poly-L-lysine coating. The large applied voltages interfere with the extracellular measurement of neighbouring field-effect transistors, which is most likely a chip design problem. Whether soma-soma paired neurons lack the channel distribution for a direct stimulation of the adhesion membrane or the intracellular recording interferes with its physiology in such a way, that stimulated oscillations cannot be observed, the capacitive stimulation of single neurons did not seem practicable with the given setup. Since the main focus of this study was on working with groups of neurons on chip, another approach to evoke single cell activity was pursued as described in the upcoming section.

Electroporation: Ramp Pulses versus Square Pulses

Since ramp-shaped pulses could not open voltage-gated ion channels directly through a prolonged change in membrane potential during the stimulus, a test of their suitability for electroporation lay at hand. The following experiment tried to address the question, whether ramp-shaped pulses could result in a less invasive form of electroporation.

Figure 3.10 shows both, ramp (panels a-c) and square (panels d-f) pulse shaped stimuli used to evoke trains of action potentials from the presynaptic neuron VD4. As can be seen in panels (b) and (e), a train of pulses evokes something similar to the action potentials found by intracellular stimulation, even though the shape, amplitude and duration might vary as compared to intracellular stimulation. The extracellular recordings reveal that neither neuron is coupling to the transistor next to the stimulation spot, but the critical time period in which most extracellular signals are recorded, might have been obscured by the stimulus artifacts of the pulse train. In panel (c) a series of several pulse trains evokes something similar to periodic activity. Unfortunately this kind of stimulus leads to irreversible damage to the investigated neuron as can be seen from the second micrograph as well as the second intracellular recording in the lower trace of panel (a). When using square

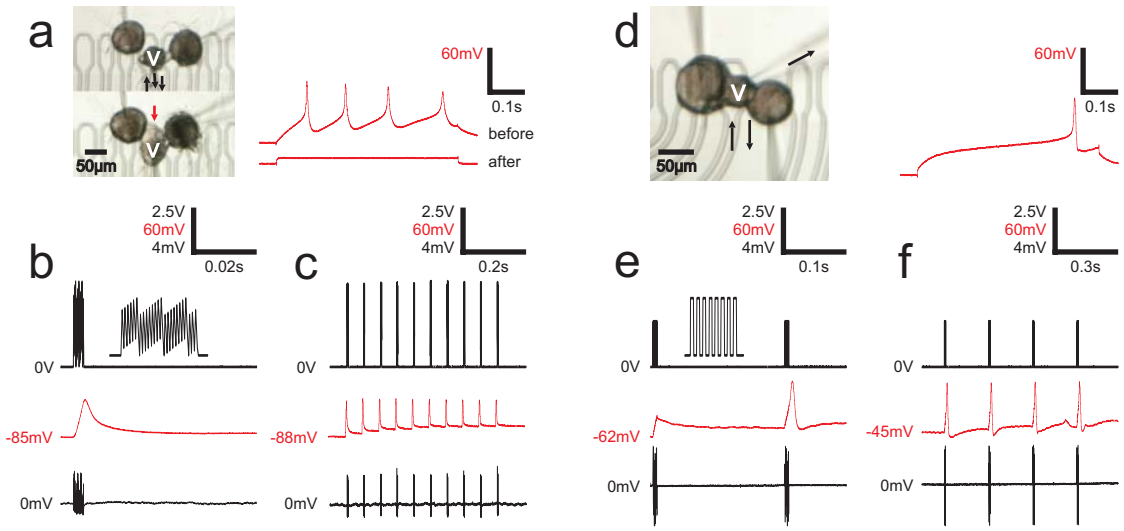

Figure 3.10: *Suitability for electroporation of ramp vs. square pulses.*

(a) shows two micrographs (left) with the investigated cell, one prior and one after stimulation. The black arrows indicate signal flow, the red arrow points out the change in cell shape after the stimulation. The plots show the cell's intracellular response to pipette stimulation before (top) and after stimulation (bottom). (d) shows on the left a micrograph of the cell with the stimulation spot, transistor and recording pipette indicated by arrows and on the right the cell's viability.
(b) and (e) show intracellular responses (middle, in red) to the chip stimulus (top and inset) along with a measurement of the junction potential by transistor (bottom trace). (c) and (f) show multiple action potential evoked by repeated stimulation with the pulses shown in the inset in (b) and (e), respectively.

pulse trains on the other hand, a steady train of action potentials can be observed in panel (f). The chip stimulated action potential (e) matches the intracellularly evoked spike (d) in shape and amplitude, when comparing them after the onset of the rising phase.

The measurements in panel (d)-(f) sum the experience of numerous experiment with square shaped pulses: Stimulation of this kind does not affect the integrity of the cell as in the case of ramp-shaped pulse trains. Early investigations of square shaped stimuli with amplitudes of around 5 V similar to those used for the ramps here - see Section 2.2.3 for details of the pulses - had the same damaging effect on neurons. As a consequence, the protocol to obtain a minimal invasive stimulus had been changed to the one described above.

While trying to copy this least-invasive approach to ramp-shaped pulses, the problem arose to get any intracellular voltage change for ramps with a rise time around 0.1 s or smaller. Therefore a large, constant amplitude was chosen, then the stimulus frequency increased until an effect for single pulses could be observed. In several cases the decay of intracellular voltage change before the next pulse demanded an increase of frequency beyond the least-invasive limit. This resulted in frequencies above 10 kHz, as can be seen from the aliasing effect in the stimulus trace, that was sampled at 25 kHz. A pulse to evoke prolonged activity then resulted in permanent damage to the cell, sometimes, like in the case shown above, after a single run.

Wallrapp investigated single pulses of increasing steepness dV_{St}/dt as well as their effect on the adhesion membrane after a healing period of 1 s. When it comes to a series of multiple stimuli - named a 'burst' - as in the case shown above, the results suggest, that not only the steepness is important, but also how long the electrical field exceeds the critical field strength of 400 V/m. A hypothetical ramp pulse with same steepness, but half the rise time, e.g., would then be better suited to evoke action potentials out of three reasons: First, since the pulse is shorter, its effect does not have enough time to decay before the next stimulus follows. Second, the duration that damage is done to the membrane is halved, leading to smaller pores that heal faster. Third, when considering the doubled amplitude of the hypothetical pulse with half the rise time, the driving force for the pore during the time of the transient pulse is larger as compared to the longer pulse, resulting in a larger net increase of membrane potential, although the steepness values match. Therefore the optimal pulse for minimal invasive electroporation is a square pulse, due to the shortest technically available rise time.

Summarizing the observations on the two types of pulses presented here, the following conclusions can be made: When trying to get capacitive stimulation of neurons, it is necessary to maintain the largest possible dV_{St}/dt over a period of several milliseconds, the time constant of the gating of voltage-sensitive sodium channels, to significantly increase their conductivity. Ramp-shaped pulses fulfill these requirements best. For electroporation, on the other hand, a large dV_{St}/dt has to be present to rupture the membrane. A large V_{St} increases the depolarization per pulse, but for

healing purposes it is necessary, that the electrical field in the stimulated membrane region is maintained only over a minimal period of time. Square shaped pulses fulfill both requirements best. Therefore both pulses are best suited for their designated purpose: the direct opening of ion channels should preferably be done with ramps, electroporation with square pulses. Thus, in the following chapters, all experiments with groups of neurons used square pulses to drive neurons into activity.

Summary - Single Cell Stimulation

Recent results in this lab indicate, that non-invasive stimulation of neurons in a reliable manner, could best be achieved using ramp shaped pulses combined with oxides that have a large dielectric constant ϵ of $25 - 40$ depending on the oxides' material, thickness and composition. Therefore attempts have been made, to reproduce the opening of voltage-gated ion channels even on silicon-dioxide, with a relatively low ϵ of 3.5. First experiments showed, that it is possible to evoke neuronal activity by opening sodium channels in the adhesion membrane. A more thorough analysis of the limits of stimulation with ramps lead to the conclusion, that only in rare cases the change in junction potential emanating from the stimulator pad sufficed to drive the neuron into activity. Again, an inhibiting effect of the poly-L-lysine coating, that would explain the negative response of the neurons to stimulation of the adhesion region, could not be ruled out.

Due to the inability to reproduce the stimulation successes with ramp shaped pulses using physiologically relevant parameters, the focus returned to the long established method of stimulating neurons with square pulses. These pulses presumably damage the adhesion membrane through electrostatic forces when exceeding an electrical field strength of 400 V/m, a process called electroporation. Therefore it is important, when considering the demand of prolonged cellular activity for the investigation of inhibitory synapses, that the stimulation happens in a minimal invasive manner. A comparison of ramp and square pulses for their suitability to evoke cell activity through electroporation showed that square-shaped stimuli are suited best for the purpose of least-intrusive electroporation with multiple subsequent pulses.

3.2 Pairs Connected via an Excitatory Chemical Synapse

The simplest neuronal circuit imaginable is a group of two cells interconnected by a chemical synapse. This system should be - as compared to two neurons connected via electrical synapses - unidirectional and trainable. A chemical synapse can come in different flavors: Excitatory, inhibitory or a mix of both. In *Lymnaea stagnalis*, three identified giant neurons form all these kinds of synapses in between one another [Smi01, Woo02]. VD4 is the presynaptic neuron in all cases, LPeD1 the postsynaptic neuron for the excitatory synapse and RPeD1 for the inhibitory. Additionally, the use of defined medium (DM) or conditioned medium (CM) determines, whether the synapse VD4-LPeD1 becomes inhibitory or excitatory, respectively [Woo99]. Figure 3.11 summarizes all three combinations investigated in this section.

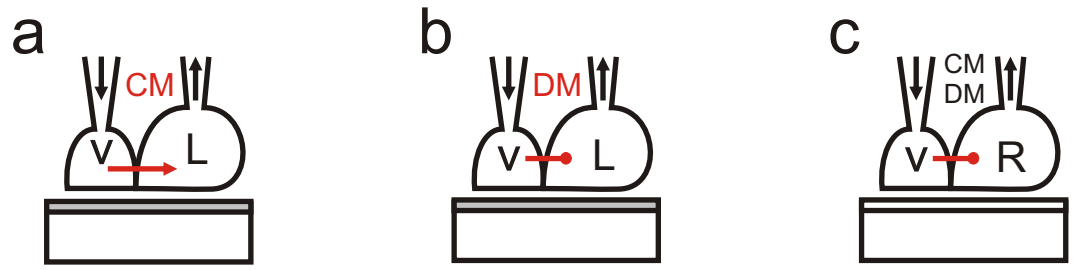

Figure 3.11: *Overview of chemical synapses formed in Lymnaea cell culture.*

(a) VD4, the presynaptic neurons, forms in vivo as in vitro a chemical synapse with LPeD1. Using brain-conditioned medium (CM) for the incubation overnight, excitatory synapses, depicted by an pointy arrow, like in vivo form.
(b) When VD4 and LPeD1 are cultured in defined medium (DM), which is devoid of snail-derived growth factors, a preliminary inhibitory synapse, depicted by a blunt arrow, form [Woo99].
(c) VD4 can also make synaptic contact to RPeD1. Regardless of the present medium, the synapse remains inhibitory like in vivo, which shows during prolonged activity of VD4. The presence of CM might add a transient excitatory part in RPeD1's response to VD4 activity, which shows only during the first few action potentials after a longer resting phase of VD4 (see [Woo02] for more details).

When it comes to the comparison of excitatory and inhibitory synapses, it is not only important to take a look at the sign of the postsynaptic potentials: These can both be e.g. depolarizing, depending on the reversal potential of the postsynaptic current as well as the membrane potential of the postsynaptic neuron. A better test for synaptic sign is the postsynaptic activity as a function of presynaptic action potentials. Even though the postsynaptic neurons of an inhibitory synapse might fire

an odd action potential or two at the beginning of presynaptic spiking, the inhibition shows best through the decrease of postsynaptic firing frequency down to quiescence during and after presynaptic activation. For excitatory synapses, only an increase in postsynaptic activity can be observed during simultaneous presynaptic action potentials. With this in mind, the following results will be easier to understand.
The subsection on excitatory synaptic contacts is divided into three parts: The first part will introduce the synaptic physiology in the presence of the anti-biotic Ampicillin, which had not been previously used in *Lymnaea* cell culture. The result subsection will then be continued with the presentation of a signal transmission from chip through the synaptically coupled neurons back to the chip, a so-called loop. The second part consists of a learning effect evoked and recorded by chip. In the final section, issues with the recording of single postsynaptic potentials in soma-soma configuration will be discussed. This subsection again will be concluded by a short summary of the presented data along with the results of its discussion.

3.2.1 The Excitatory Loop VD4-LPeD1

The easiest imaginable experiment consists a group of two neurons interconnected via an excitatory synapse: Activating the first neuron will eventually result in the activity of the second one due to temporal summation of the excitatory postsynaptic potentials in the receiving cell.

Synaptic Physiology

Figure 3.12(b) shows this temporal summation, panel (c) shows a single excitatory postsynaptic potential. These cells were cultivated in defined medium that differed from the medium published by Syed [Sye90, Rid91] in the anti-biotic agent that was used. Since our animal culture was contaminated with bacteria resisting Gentamicin, we introduced Ampicillin into the medium [see Appendix 2 for details] as sole anti-biotic. This figure proofs that the cell culture is not negatively affected by the changed medium and also brain-conditioned medium created from defined medium with Ampicillin was potent enough to create excitatory synapses[5].

The Excitatory Loop VD4-LPeD1

The key experiment is shown in Figure 3.13: panel (b) shows the stimulation from chip of the presynaptic neuron with three groups of dual voltage ramps. These pulses elicit several action potentials which are both recorded intra- and extracellularly. On the postsynaptic side shown in panel (c) the second postsynaptic response drives the neuron into spiking, which is recorded from the transistor (see inset). Thus a signal

[5] otherwise a premature inhibitory synapse as in pure defined medium would have formed

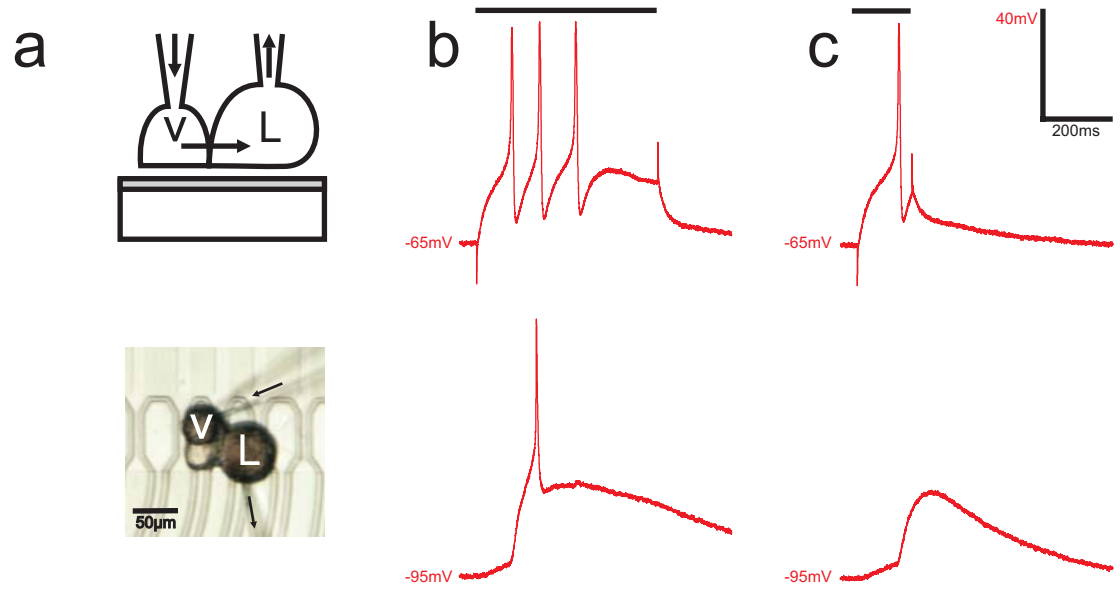

Figure 3.12: *Synapse formation in CM containing the anti-biotic Ampicillin.*

(a) Schematic of the presented experiment (top) and micrograph of the investigated neurons (bottom).
(b) presynaptic intracellular voltage (top) and postsynaptic action potential (bottom) recorded from synaptic couple after 16 hours in brain-conditioned medium with Ampicillin as anti-biotic reagent (Ampi-CM) instead of Gentamicin. The black bar marks the duration of the pipette stimulation in the presynaptic neuron.
(c) A single post-synaptic potential recorded from the same couple.

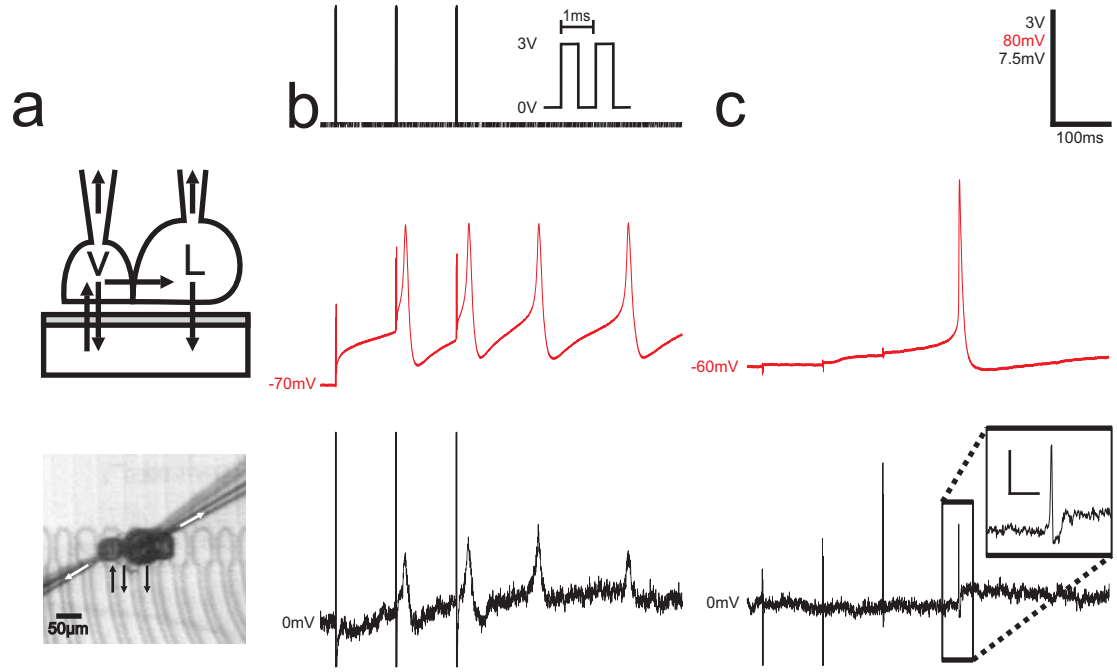

Figure 3.13: *An excitatory synapse monitored while activated by chip.*

(a) shows schematic of the conducted experiment (top) as well as a micrograph of the investigated neurons (bottom).
(b) presynaptic side: top shows chip stimulation (inset: stimulus shape and number with amplitude of $3V$ *and single pulse length of* 1 *ms). The middle and lower trace show the intra- and extracellular recording.*
(c) postsynaptic response recorded intra- (middle trace) and extracellularly (bottom trace). Inset shows the close-up of the transistor recording during the post-synaptic action potential. Inset: 2 *mV*$/10$ *ms.*

flow from chip across the cell-cell contact back into the chip, a so-called Loop is established.

Even though micropipettes were used to monitor the cells' intracellular potential, they would have not been necessary: that the responses of the presynaptic neuron VD4 and the postsynaptic LPeD1 are recorded from different, but neighboring transistors. Both cells' extracellular signals are also distinguishable in their shape and amplitude. None the less for a proof of principle experiment the intracellular recording was indispensable.

This experiment has been carried out in cooperation with Naweed Syed from Calgary. Similar experiments have been repeated at a later stage of the thesis within the lab (data not shown due to redundancy, $N > 10$). In conclusion, a complete chip-synapse loop with single neurons has been proven in cell culture [Kau04].

3.2.2 Potentiation via Chip Stimulation

A especially nice feature of this synaptic couple is the fact that it exhibits a simple form of learning - potentiation - which can last up to hours. The layout of the experiment is simple. After evoking a postsynaptic potential from the couple, a train of six to eight action potentials leads to a loading of the presynaptic terminal. This loading of the synapse can persist for several hours [Syed, personal communication]. With another single action potential the synapse can then be unloaded, yielding an increase in a single postsynaptic potential by up to 250%.

Figure 3.14 shows results from the experiment described above: In panel (a), the postsynaptic response triggered by chip stimulation of the presynaptic neuron VD4 is insufficient to evoke an action potential in LPeD1. Then the presynaptic cell is stimulated from chip in such a way, that the VD4 is driven into spiking (panel b). Finally, panel (c) shows the postsynaptic action potential as a result of the potentiation of the synapse between VD4-LPeD1.

The experiment could therefore be interpreted in the language of computer science, that it is possible to store and read out single bits of information in an individual synapse for intermediate periods of time: The excitatory synapse VD4-LPeD1 can be seen as a building block for a neuronal storage unit.

Again, this kind of experiment could be repeated multiple times ($N > 10$).

3.2.3 Investigation of Single Postsynaptic Potentials with Transistors

Considering the fact, that single postsynaptic potentials in the neuron LPeD1 from *Lymnaea stagnalis* can be as large as 20 mV, with potentiation up to 30 mV (see Figure 3.15b), the question arises, whether it is possible to see a corresponding extracellular signal. As a rule of thumb, the signal would be proportional to the

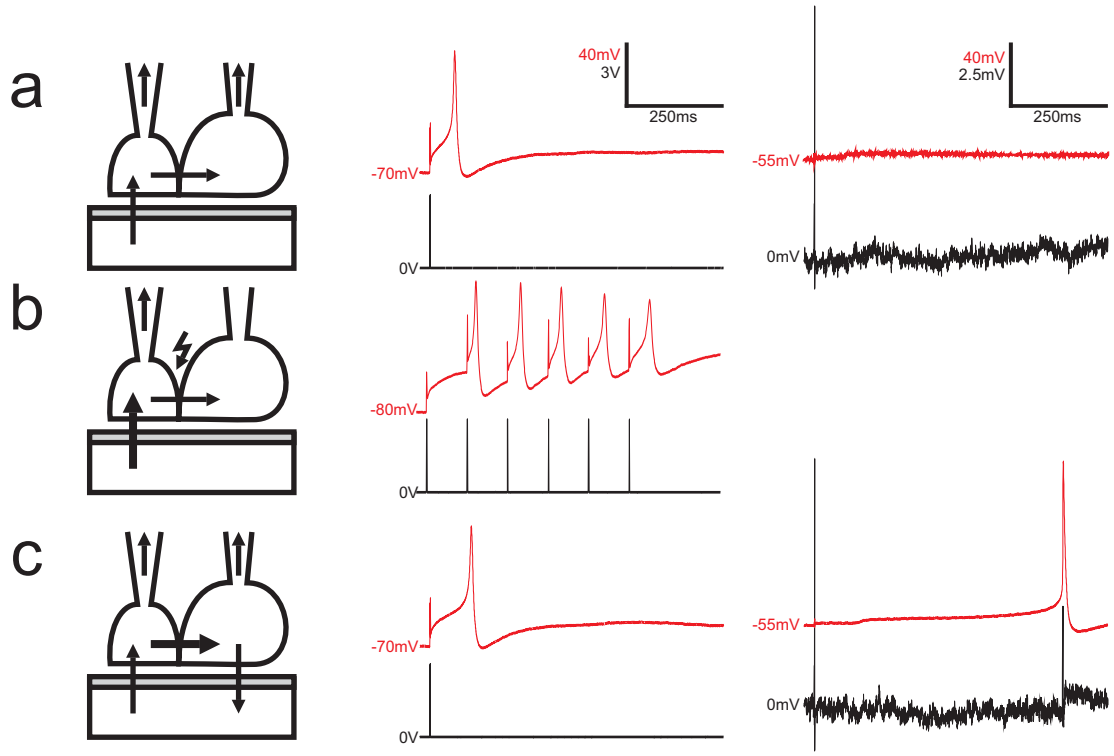

Figure 3.14: *Neuronal network stores information written and read out by chip.*

(a) On the left one sees the schematic prior to potentiation: The presynaptic neuron is stimulated from chip (middle traces: intracellular recording on top) while the postsynaptic response is insufficient to elicit a postsynaptic action potential (traces on the right: intracellular recording on top).
(b) The potentiation takes place via massive activation of the synapse.
(c) After the potentiation the synaptic response is strong enough to cause an action potential in the postsynaptic neuron, which is also recorded extracellularly.

change in membrane voltage dV_M/dt. Taking the numbers of $dV_M = 20$ mV and $dt = 20$ ms we find $dV/dt = 1$ V/s. Compared with the coupling of a neuron during an action potential we have $dV/dt = 100$ mV/1 ms= 100 V/s. As a regular signal is around 5 mV during an action potential (see Figure 3.13c for example), we will get 1/100 of 5 mV, i.e. 50 μV. A "signal" like this would be lost in the noise of the transistors of the two-way contacts used for the previous stimulation-transistor coupling experiments, as can be seen from the transistor recording in panel (b).

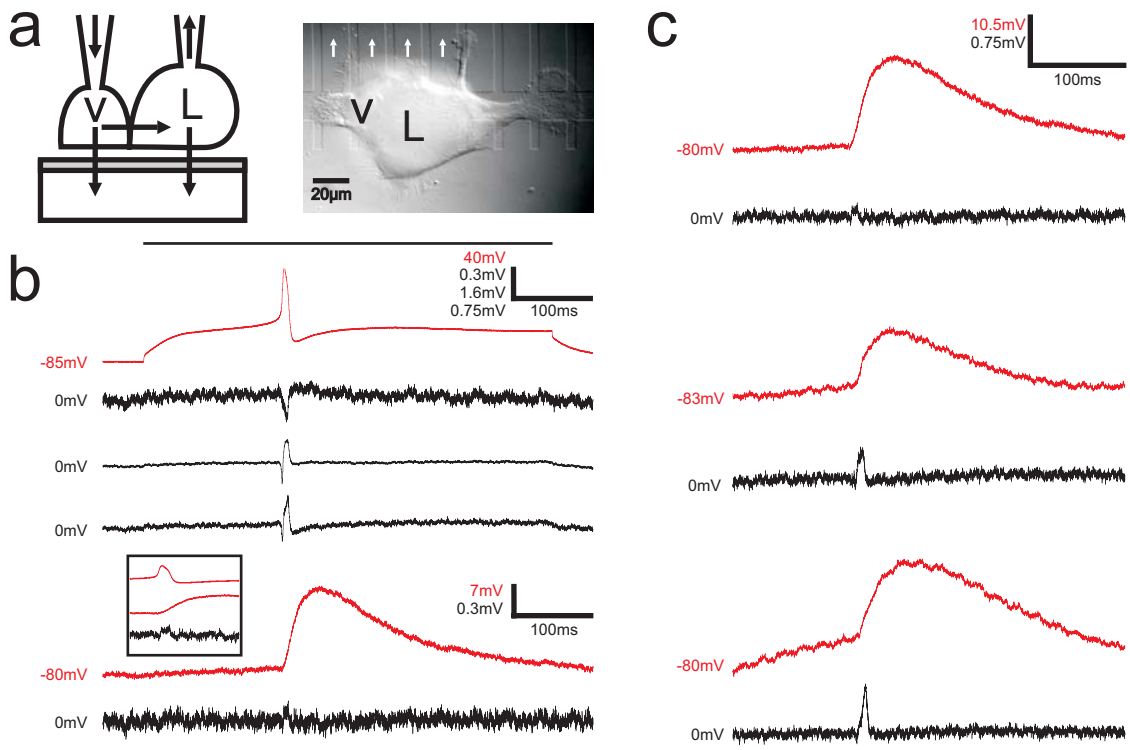

Figure 3.15: *Issues with high-resolution recording of synaptic contact.*

(a) Schematic of the conducted experiment (left) and micrograph of the investigated neurons (right).
(b) intracellular recording of the presynaptic (top trace) and postsynaptic (fifth trace) neuron along with extracellular recordings in the order left to right with respect to the white arrows in (a). Inset shows presynaptic membrane potential (top), recording of transistor underneath the postsynaptic cell (bottom) and its membrane potential (middle).
(c) Comparison of three postsynaptic potentials recorded intracellularly (top traces) and three corresponding transistor recordings (lower traces). The measurements represent a dataset of roughly thirty measurements recorded during a few minutes, earliest at the top.

Figure 3.15a shows a synaptically connected soma-soma pair of VD4-LPeD1 on a high-sensitivity transistor array created by Moritz Völker, with whom the experiment was carried out. These transistor arrays have a remarkable signal-noise ratio

resulting in a peak-peak noise amplitude of less than 20 μV making the detection of purely capacitive currents along the postsynaptic membrane possible (see calculation above). Panel (b) shows a typical experiment with the presynaptic signal showing up in several adjacent transistors (second until fourth trace, different scaling), while under the postsynaptic neuron (sixth trace) only a small signal close to the noise level can be observed in the transistor, that shows the largest response during a postsynaptic action potential (not shown). The inset shows the temporal order of events, where the peak of the transistor signal coincides both with the rising phase of action and the postsynaptic potential.

Since the recorded transistor trace is close to the noise level of the device, an averaging of several consecutive, but similar experiments could yield a clearer shape and amplitude of the recorded event. Therefore during the period of a few minutes, thirty data sets were collected. Three recordings of the postsynaptic intra- and extracellular voltage during an early, intermediate and late stage of the experiment are shown in panel (c). Interestingly, although the peak amplitude of the postsynaptic potential basically remains constant, the amplitude of the signal recorded with the transistor underneath LPeD1 triples in size. Additionally, the outline changes from a roughly rectangular to a triangular shape. All in all, this observation makes it clear, that averaging these thirty traces would not be an allowed operation on this data set. Therefore it cannot be unambiguously concluded, that a pure postsynaptic response was recorded.

In this case, it is even more likely, that the electrical signal emanating from the activated presynaptic neuron propagates along the adhesion membrane of the soma-soma pair and is recorded from the transistor underneath the postsynaptic cell. A pharmacological testing by blocking synaptic vesicles could have provided a tool to separate the contribution of the presynaptic action potential from the postsynaptic event. A new approach to rule such a case out would be an experiment with a chemical synapse between outgrown neurons. Both features were not available during the time of the experiment. Therefore the question, whether field-effect transistors can probe single excitatory postsynaptic potentials remains unanswered.

3.2.4 Summary - Excitatory Synapses

An introduction to the synaptic connectivity between presynaptic neuron VD4 and postsynaptic cell LPeD1 showed, that single postsynaptic potentials around several tens of millivolts are common for this synapse. When evoking several presynaptic action potentials, these can add up temporally to elicit a postsynaptic action potential, the extracellularly detectable 'marker' for synaptic transmission.

In a straightforward approach, a group of two to three presynaptic action potentials evoked by chip stimulation temporally added up to a response that was recorded

with a transistor in the junction underneath the postsynaptic neuron. Comparison of intra- and extracellular recordings showed, that signal successfully has been transmitted from chip through the chemical synaptic contact back to the chip.

Like most known neuronal connections, the synapse between VD4 and LPeD1 shows plasticity: its synaptic strength can be increased by 150-250%, in a process previously coined Potentiation. When comparing the postsynaptic responses after and before training, one can deduce from the presence or absence of a transistor signal, whether the synapse has undergone potentiation or not. When rephrasing the finding in terms of binary logic, the potentiation protocol stores a single bit of information in the simple neuronal network formed by two synaptically connected neurons.

Due to the large postsynaptic potentials recorded in LPeD1, the question, whether transistors could detect these postsynaptic potentials, arose. The recording of the postsynaptic current was investigated with low-noise transistor arrays. Unfortunately, the shared adhesion area of soma-soma paired neurons, although it augments the junction potential changes, results in interference of presynaptic action potentials in transistors underneath the postsynaptic neuron during the recording of postsynaptic potentials. Thus, this approach to record postsynaptic activity has to be thoroughly revised before starting a new attempt at recording postsynaptic potentials.

3.3 Pairs Connected via an Inhibitory Chemical Synapse

After showing that the activity of excitatory synapses can be evoked and modified by chip stimulation while being monitored extracellularly, the natural extension of these results would be to inhibitory synapses. The challenge on chip and cells here is even larger for the reason that inhibition, the decrease of postsynaptic activity, requires persistent spiking of the postsynaptic neuron for the duration of seconds - something which has not been achieved with capacitive stimulation before. Before addressing the question of stimulating prolonged activity by chip, observation like the oscillations described for single neurons (see section 3.1.1), demand a proof of the cell's capability to sustain prolonged spiking in our cell-culture conditions.
In the subsequent subsection, first the nature of inhibitory synapses found on three different substrates will be described in general terms with the example of the inhibitory synapse found between VD4-LPeD1 in the absence of brain-derived growth factors. Again, for this pair it will be shown, that a signal can be transmitted through the neuronal network back to the chip, now as a function of absence of postsynaptic signals due to presynaptic activity. The subsection afterwards will deal with the inhibitory synapse between VD4-RPeD1 along the same lines as in the previous subsection. After the loop experiment, an additional results introduces the issues with double stimulation of both, pre- and postsynaptic neuron by chip. Again, the section will be rounded off by a short summary on the observations made herein.

3.3.1 The Inhibitory Loop VD4-LPeD1

Since the work on excitatory chemical synapses was done in collaboration with an expert in the field of *Lymnaea* cell culture, a rigorous proof of our own capability to extract and maintain snail neurons would be the synapse formation in defined medium: Without the external growth and nutritional factors that are added to the conditioned medium during the co-culturing, only fit cells would survive and form premature inhibitory synapses in defined medium as found in the literature [Mun00].

Synaptic Physiology

As Figure 3.16 shows, this task of synapse formation was achieved not only on poly-L-lysine coated chips, but also on chips that used fragments of two different β subunits of Laminin (panel b). On all three substrates, post-synaptic potentials in LPeD1 can be observed as shown in panel (c). The depolarizing postsynaptic potential on the other hand does not indicate the sign of the synapse. To prove their inhibitory nature using micropipettes, different approaches can be pursued, which are independent of the coating used: in (d, left panel), the postsynaptic neuron was

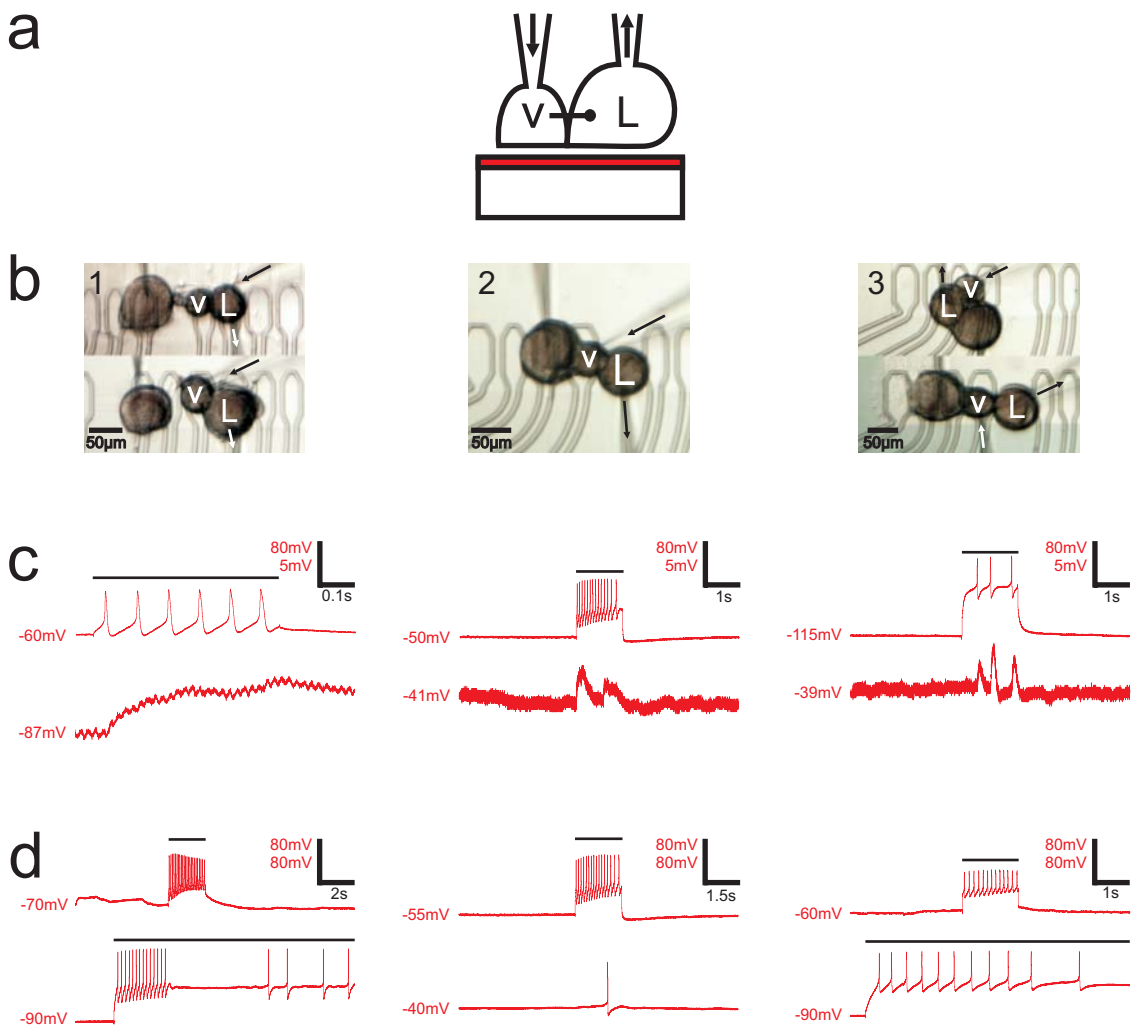

Figure 3.16: *Electrophysiology of inhibitory synapses cultured on three different substrates.*

(a) contains schematic of the conducted experiment.
(b) the micrographs of the different coatings tested: (1) Poly-L-Lysine, (2) fragment of the β1-subunit of Laminin, (3) fragment of the β2-subunit of Laminin. In both panels the arrows indicate signal flow. (1) and (3) contains two micrographs, one for (c) and one for (d).
(c) shows the presynaptic action potentials (top) and inhibitory post-synaptic potentials recorded with micropipettes in the order of (1)-(3) as shown in (b).
(d) shows the inhibition of the activated post-synaptic neuron due to presynaptic activity in different forms: instantaneous, lasting quiescence (left), evocation of a single post synaptic action potential with subsequent quiescence (middle), diminishing firing frequency as a result of inhibition (right). Note that these effects are not substrate dependent: They can be observed on all substrates (data not shown).

driven into spiking and its activity is subdued by the presynaptic burst and slowly picks up seconds after the inhibition. In (d, middle panel), the presynaptic burst merely causes usually no more than a single action potential in the postsynaptic neuron LPeD1, much less than expected for an excitatory synapse as to be seen below (see Figure 3.23(a) for a comparison). Finally, inhibitory synaptic transmission can be observed as a reduction of firing frequency, which also returns to normal after a few seconds (not recorded).

It is surprising to see, that fragment that was introduced by Schoen to achieve large adhesion areas after several minutes in cell culture does not prevent synapse formation, as is the case of poly-L-lysine, if plating cells on freshly coated chips. This was a major issue in determining optimal cell culture conditions for inhibitory synapse formation. For excitatory synapse formation on the other hand, the adhesion conditions found on a fresh poly-L-lysine coating were most likely rescued by the additional factors that brain-conditioned medium contains as compared to defined medium.

The Inhibitory Loop VD4-LPeD1

Therefore it is not surprising to see, that the inhibitory loop experiment of activating the presynaptic neuron from chip and recording the effect on the postsynaptic side extracellularly could not only be created on poly-L-lysine coated chips, but also for the two different fragments of Laminin (see Figure 3.17). Panel (c) shows postsynaptic potential changes as a response to the capacitively stimulated neuron VD4. The panels in (d) depict the inhibitory nature of the interconnected cells: for poly-L-lysine and the fragment of the β1-subunit (left and middle) the activity is interrupted for one second, for the fragment of the β2-subunit a sole postsynaptic action potential is elicited while the remaining potential change stays below the threshold of activity.

All in all, this proves, that the in-lab cell culture of *Lymnaea* neurons is not only able to create viable premature inhibitory synapses on chip as seen in literature, but also to interface them by chip. None the less the problem of dual stimulation remains. The investigations in the previous section will try to shed some more light on that issue.

3.3.2 The Inhibitory Loop VD4-RPeD1

Especially when considering the fact, that the creation of a larger cellular network is the goal of this thesis research, the inhibitory synapse VD4-LPeD1 in defined medium will not be sufficient to create a network with synapses of both signs: On the

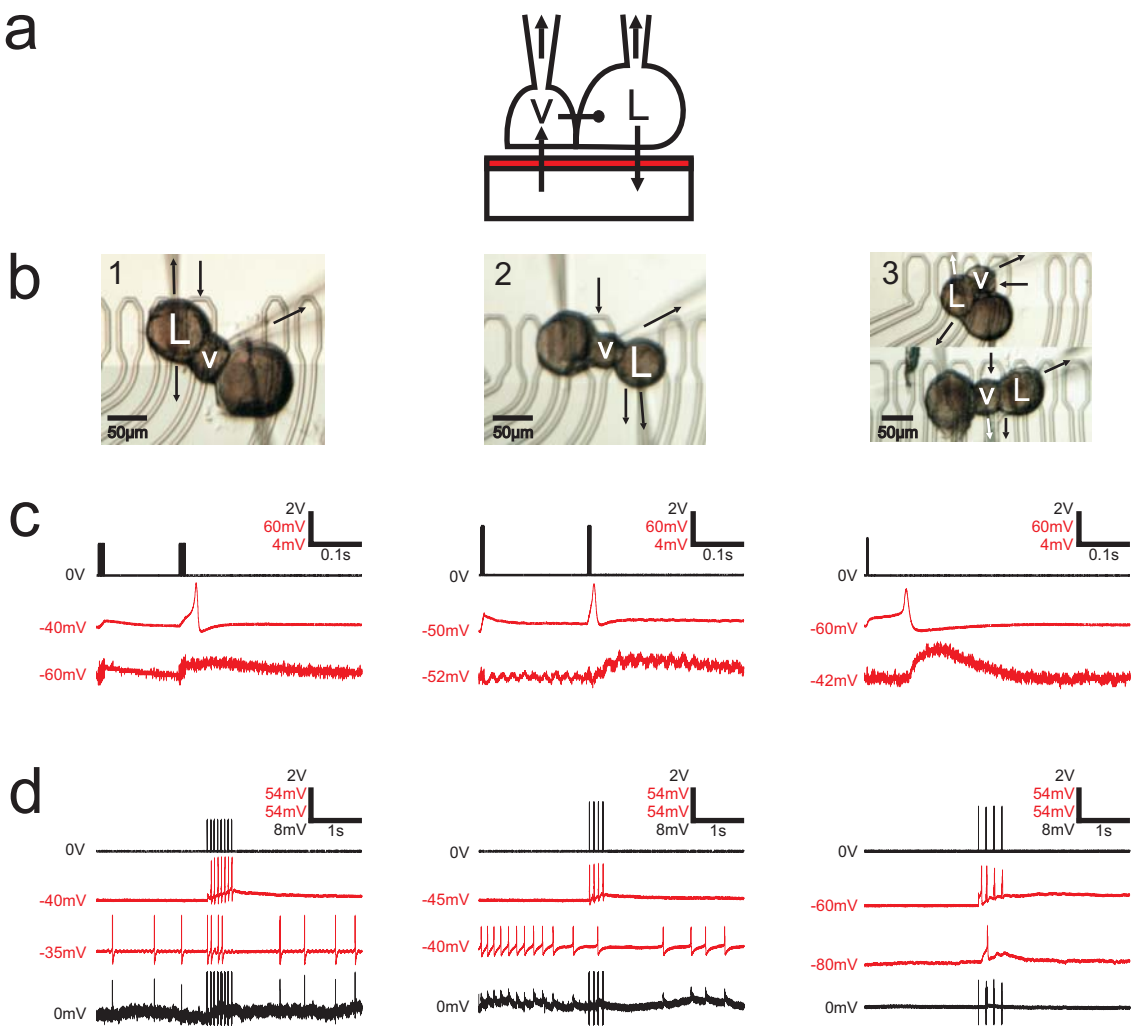

Figure 3.17: *Activation and recording of inhibitory synaptic activity by chip.*

(a) shows schematic of the conducted experiment, while in (b) (1)-(3) show micrographs of the used substrates in the order poly-L-lysine, fragment of $\beta 1$ subunit of Laminin and fragment of $\beta 2$ subunit of Laminin. (3) contains two micrographs, one for (c) and one for (d). The arrows indicate signal flow.
(c) shows intracellular recordings of single inhibitory post-synaptic potentials (bottom trace) elicited by chip stimulation (top trace) of the presynaptic neuron (middle trace) for the different substrates depicted in (b). (d) shows the inhibition of postsynaptic events through chip-stimulated (top trace) activity of the presynaptic neuron (second trace). The inhibition of the postsynaptic neuron is recorded both intra- (third trace) and extracellularly (bottom trace).

one hand, excitatory and inhibitory synaptic pairs require different cell culture conditions (CM vs DM, respectively), on the other hand, a double synapse VD4-LPeD1-VD4 will not form in cell culture [personal communication with Syed]. Another approach to create a larger network would then be to connect the existing excitatory synapse LPeD1-VD4 to another neuron, namely RPeD1. The synapse VD4-RPeD1 is found to be bidirectionally inhibitory in vivo and vitro [Sye90, Woo02]. For our purpose we focus on a two-layered feed forward network, therefore we disregard the synapse RPeD1-VD4, where RPeD1 inhibits VD4.

Synaptic Physiology

The physiology of the VD4-RPeD1 inhibitory synapse again yields postsynaptic potentials as can seen from Figure 3.18(b) and (c): both panels show pre- and postsynaptic intracellular voltages recorded during activity of VD4 on two different substrates, poly-L-lysine and the fragment of the β1-subunit of Laminin. As expected for inhibitory responses, their reversal potential is close but below the threshold of spontaneous activity as can be seen from panel (c). The remaining panels (d) and (e) depict the reduction of activity or its absence, respectively, due to the inhibition of RPeD1 by VD4.

The Inhibitory Loop VD4-RPeD1

With the use of intracellular stimulation of the postsynaptic neuron, this synapse VD4-RPeD1 can also be activated and read-out by chip, in a so-called inhibitory loop (see Figure 3.19). One experiment was carried out on poly-L-lysine, the other on the β1-subunit fragment (panel a): in (b) and (c) the synaptic activity is recorded intracellularly, in (d) and (e) the frequency of action potentials in the postsynaptic cell RPeD1 is reduced and picks up again shortly after the presynaptic activity ceases. Note that, the periodic stimulation of the presynaptic neuron is done in such a way, that the first pulse not necessarily causes an action potential. Considering a sequence of 5-8 pulses, this guarantees, that the neuron will survive a longer series of stimulation trains. In the case of the VD4 neurons depicted in panel (e), the change in intracellular potential before and after driving the periodic activity indicates a larger amount of damage than desired. None the less, the simple loop experiment could be carried out as well for the inhibitory synaptic couple VD4-RPeD1, making an attempt at interfacing groups of three neurons feasible.

3.3.3 Double Stimulation VD4 and RPeD1

Before moving on to groups of three neurons, the issue of double stimulation needs to be addressed once more. Figure 3.20 shows again the group of neurons depicted in Figure 3.18(e). In panel 3.20(b) the electrophysiology measurement has been

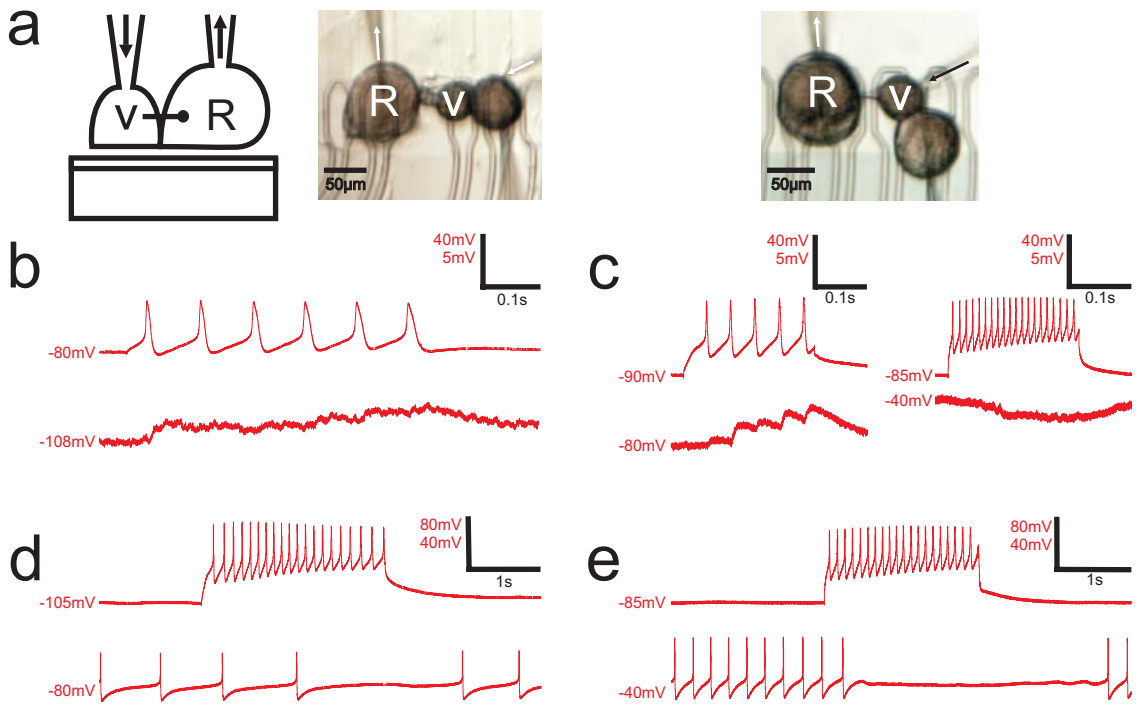

Figure 3.18: *Physiology of synapse between VD4 and RPeD1.*

(a) show a schematic of the conducted experiment along with two micrographs of the used substrates poly-L-lysine (left) and a fragment of the β1-subunit of Laminin. The arrows indicate the current flow.
(b) shows the presynaptic activity (top trace) elicited by current injection (not shown) along with inhibitory post-synaptic potentials (bottom trace) both recorded intracellularly.
(c) has the same layout as (b): on the left the potentials were recorded at a lower resting potential of the post-synaptic neuron than on the right. One can clearly see the reversal of synaptic response.
(d) and (e) show the inhibition of the post-synaptic neuron (bottom) during presynaptic activity (top) by quiescence.

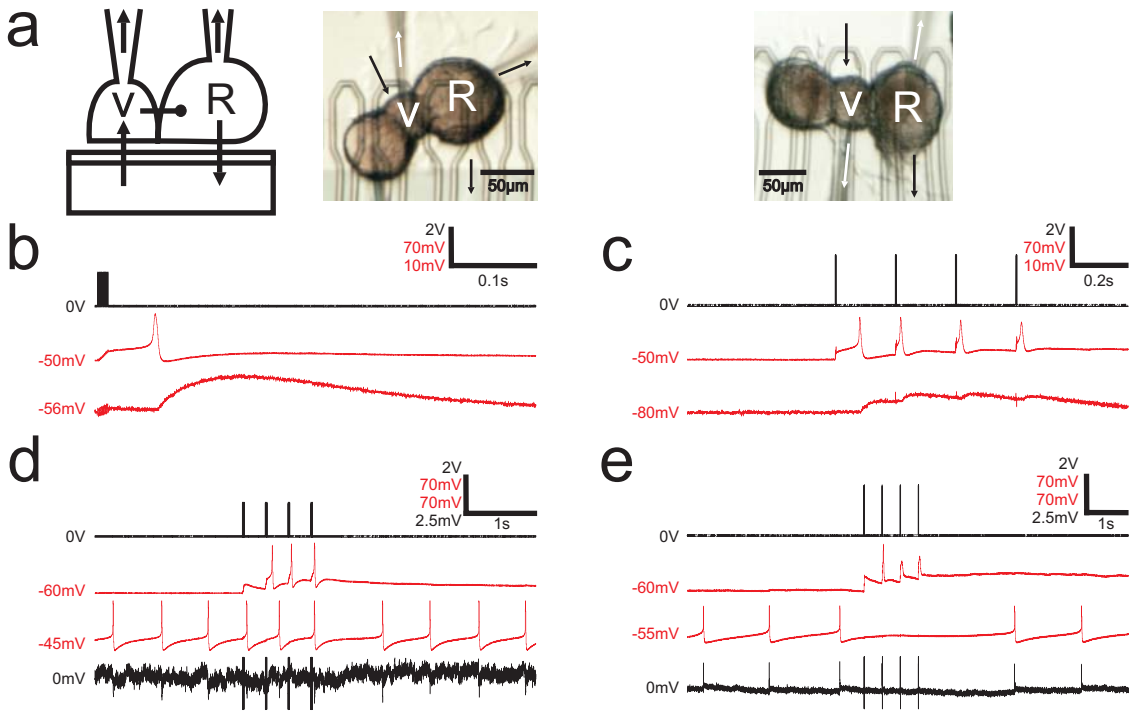

Figure 3.19: *Inhibitory synapse between VD4 and RPeD1 activated and recorded by chip.*

(a) show a schematic of the conducted experiment along with two micrographs of the used substrates poly-L-lysine (left) and a fragment of the β1-subunit of Laminin. The arrows indicate the current flow.
(b) and (c) show for the different substrates described in (a) the presynaptic activity (middle trace) elicited by chip stimulation (top trace) along with inhibitory post-synaptic potentials (bottom trace) both recorded intracellularly.
(d) and (e) show intra- (third trace) and extracellular (bottom trace) recordings of the inhibition of the post-synaptic neuron during chip-stimulated (top trace) presynaptic activity (second trace) by diminishing frequency (d) or quiescence (e).

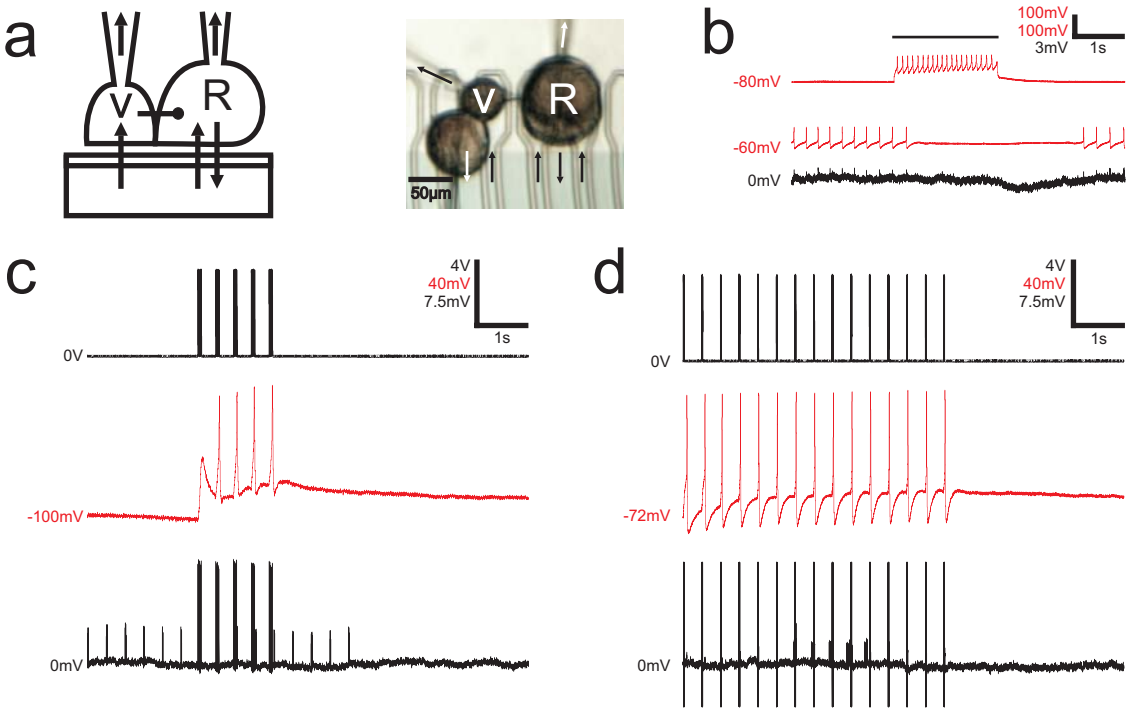

Figure 3.20: *Issues with simultaneous stimulation of pre- and postsynaptic neurons.*

(a) show a schematic of the conducted experiment along with a micrograph of the investigated neurons. The arrows indicate the current flow, postsynaptic RPeD1 in white, presynaptic VD4 in black.
(b) shows the presynaptic activity (top trace) elicited by current injection (black bar) along with a spiking postsynaptic neuron which is turned quiescent for two seconds (middle trace) - both traces are recorded intracellularly. The bottom trace shows the transistor recording underneath RPeD1.
(c) and (d) show VD4 and RPeD1, respectively: stimulation from chip (top), intracellular (middle) and extracellular recording. Note that the activity in RPeD1 does not diminish during stimulation of VD4.

amended by an extracellular recording of RPeD1's activity. The recordings of the double stimulation experiment are shown in panel (c) and (d) for VD4 and RPeD1, respectively. The top traces show the stimuli fed into the capacitors underneath each neuron. Note that this experiment used ramp, not square pulses to elicit the action potentials. In the middle the intracellular recordings are shown, underneath the extracellular recordings of the transistors indicated in the micrograph (panel a). Two observations are critical for this experiment: For one, it is not possible to inhibit the postsynaptic neuron RPeD1, even though, the stimulation of VD4 elicits a series of action potentials. This is not surprising considering the fact, that the synaptic response has to counterbalance a large, undefined current through the membrane underneath postsynaptic neuron, that has been created to drive RPeD1 into firing. Especially in this experiment it is obvious, that the extracellular stimulation of neurons has to be fine-tuned to remain in a current range associated with physiological cell activity. The other observation introduces a general measurement problem, that the transistors underneath both neurons pick up stimulus artifacts, that in the case of periodic stimulation obscure the change in junction potential created during cell activity. This is not a mere signal to noise ratio problem, but more fundamental, due to the capacitive nature of the stimulation and the geometrical design of this chip. Solely decreasing the amplitude of the stimulus will not remove the problem of the close timing between the stimulating pulse and the concomitant action potential. Maybe the fine-tuning of purely capacitive pulses that are applied to stimulator pads covered with a material with a high dielectric constant to physiologically open the voltage-gated channels in the adhesion membrane could solve this issue. Due to the absence of two-way contact chips of this kind during the thesis research period, this issue could not be settled. Therefore all remaining experiments were carried out while driving the postsynaptic neurons into activity by intracellular current injection. This solution is not as invasive as it might seem, since the postsynaptic neurons usually have an intracellular potential close to firing threshold [Kyr89]. Only the intracellular contact with micropipettes interferes with the intracellular potassium concentration in such a manner, that the reversal potential is shifted into a more negative potential region, thus making all contacted neurons more stable or in other words less excitable. When considering pairs of neurons, the physiology could be optimized by recontacting the neurons, risking the integrity of the synapse and of the cell-chip contact. For groups of three neurons, this approach is not feasible anymore, since the yield of well-placed neurons interconnected by chemical synapses is low as can be seen from the following chapter.

3.3.4 Summary - Inhibitory Synapses

When working with the parts for the excitatory synapse between VD4 and LPeD1, the literature also shows, that it is possible to form premature inhibitory synapses when culturing the cells in medium devoid of brain derived proteins. Imagined as

a test to the robustness of the *Lymnaea* cell culture in this department, this kind of investigation turned out to be more a test of the whole cell-chip coupling: Even though synapses could be formed on poly-L-lysine coated substrates, the yield of synaptically coupled neurons, that would be available to both, extracellular recording as well as prolonged activity necessary to detect inhibitory synapses, turned out to be an almost impossible venture: On the one hand, the desire for large extracellular signals interfered with the ability of the neurons to form proper synaptic cell-cell contacts on the other hand. Again, poly-L-lysine, due to its large adhesion forces exerted by the coating as well as a putative remnant toxicity at micromolar concentrations of molecules that go into solution, turned out to be the culprit. This observation sparks the idea, that the mobility of neurons observed by previous researchers [Jen01, Zec01] might partially be attributed to the properties of poly-L-lysine, which would drive the neurons away from the hazardous environment towards their healthier cellular partners.
Why the published papers in the field that use poly-L-lysine do not mention issues with the coating might be seen as an indicator for the fact, that the differences between cell culture on pure glass surfaces and on semiconductor chips might rescue the first approach: The glass cover slips, that are glued into 30 mm plastic dishes which can be filled with up to 3 ml of medium, are only used once, while the chips, stocked with chambers that only take up 1 ml of medium, are taken several times into culture. Since in case of the chips, the poly-L-lysine solution is in contact with both, the silicon oxide as well as the plastic chamber. In late experiments, the coating of the silicon chip was done with small droplets of poly-L-lysine, which improved the yield of healthy synapses further, making experiments with three interconnected neurons coupled to the chip possible[6]. Additionally, the time between coating and usage differs in the case of published literature and the research presented here: the glass cover slips are not used for cell culture prior to three days after coating, for the chips the demand to get large extracellular signals favored earlier usage.

None the less, first experiments with two different substrates derived from binding motives of the adhesion molecule Laminin, showed promising results: on both substrates several inhibitory chemical synapses formed, even though only a small number of preparations used chips coated with these molecules. After passing the electrophysiological testing for intact synaptic contacts, the extension of the experiment to chip stimulation and transistor recording turned out to be the much easier task: On all three substrates signals could be send from the chip to the presynaptic neuron, silencing their postsynaptic partner.

Going towards groups of three neurons, the issue, that both LPeD1 and VD4 form synapses with only a single partner neuron, posed a natural limit on the scalability of the neuronal network working with these neurons alone. Therefore another identified neuron RPeD1, which is known to also form inhibitory chemical synapses with VD4, was introduced into cell culture. Again, both on poly-L-lysine as well as a fragment

[6]Personal observation, data not shown

of Laminin, the activity of VD4 diminished the firing of RPeD1 or even turned the neuron quiet for a few seconds. Extending these results to stimulation of VD4 and recording of the activity of RPeD1 posed no problem.

When thinking of a synaptic environment fully controlled by chip devoid of intracellular electrodes, the testing of inhibitory synapses poses the intrinsic problem of postsynaptic activity prior to the presynaptic activation. Therefore an attempt was made to extend the stimulation via electroporation towards two neurons simultaneously. While in principle it is not difficult to evoke single action potentials from both neurons, a synchronized activity that gets muted or diminished by synaptic inhibition, again exposes two contradictory principles at work: the stimulation via electroporation, with its goal to reliably drive the postsynaptic neuron into activity, versus the synaptic inhibition that is designed to balance activating currents in a physiological range of a few nA and smaller. To suppress activity caused by electroporation with a single inhibitory chemical synapse therefore turns out to be an ill-posed problem.

3.4 Cell Triples with Two Chemical Synapses

The final chapter of the results part presents a complete experiment with a group of three neurons stimulated and recorded from chip. In general, several types of interconnected groups of cells can be imagined: in the case of *Lymnaea* neuronal cell culture unfortunately the only two-layered structure with three neurons consists of one presynaptic neuron and two postsynaptic partner cells given the published knowledge in snail physiology. Figure 3.21 illustrates the the three stages of such a successful experiment.

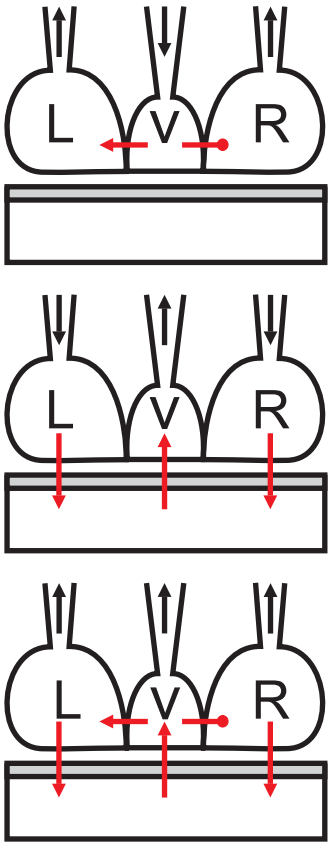

Figure 3.21: *Schematic of the Double Loop Experiment.*

Schematic of the conducted experiment with groups of three cells. First, the synapses are tested (top), then the coupling to the chip's transistor array (middle), last the stimulation of the presynaptic neuron from chip, while the activity of the post-synaptic cells is recorded intracellularly with micropipettes and extracellularly by the field-effect transistors (bottom).

First, the group of neurons is tested for chemical synapses by recording intracellular potential changes and subsequently by determining the changes in postsynaptic activity - increasing activity for excitatory synapses, decreases for inhibitory ones.

Then follows a verification of the cells' interaction with the components of the chip: for the postsynaptic neurons by extracellular recording, for the presynaptic neuron by ramp stimulation. If each neuron is connected to both its partner cell and the chip structures appropriately, then in the final stage the synaptic transmission is triggered by chip stimulation and recorded on the postsynaptic sides by transistors. This it the outline for the experiment in theory. When looking at the practical side of recording and stimulation, the following observations were made.

3.4.1 An Excitatory-Inhibitory Double Loop LPeD1-VD4-RPeD1

The partners that are used in the realisation of the synaptic triples, LPeD1, VD4 and RPeD1 were introduced along with their interconnectivity in the previous chapters 3.2 and 3.3: in brain-conditioned medium we find an excitatory synapse between VD4 and LPeD1 as well as a mixed excitatory-inhibitory synapse between VD4 and RPeD1 [Woo99, Woo02]. A mixed synapse shows in the fact, that even though usually the activity of the postsynaptic cell is reduced, sometimes single action potentials can be elicited through synaptic transmission (see section 3.3.1, Figure 3.16(f) for an example in the case of the inhibitory synapse VD4-LPeD1 in DM).
In the final stage for this set of experiments, it would have been desirable to proof the nature of the synaptic transmission solely by using chip stimulation and recording. Unfortunately, the issues with double stimulation of both the presynaptic neuron VD4 and postsynaptic cell RPeD1 could not be resolved with the available technology (see Subsection 3.3.3 for a detailed discussion). Therefore the necessary spontaneous activity for detection of synaptic inhibition resulted from intracellular stimulation.

In Figure 3.22(b) and (c) show the postsynaptic potentials in the neurons LPeD1 to the left and RPeD1 to the right of the central cell, respectively, after an intracellularly evoked activity of VD4. These potential changes alone, which are in both cases depolarizations, do not clarify the sign of the underlying synaptic transmission. Only the Figure 3.23(b) clarifies the excitatory nature of the connection from VD4 to LPeD1 and the inhibition of RPeD1's activity through VD4.

After verifying the synaptic connectivity, according to the schematic in the first Figure 3.21, the second step would be the testing of the coupling of the postsynaptic neurons to the transistors, also shown for both neurons in Figure 3.23(b). During the synaptically evoked firing of LPeD1 and during the intracellularly driven periodic activity of RPeD1 both transistors underneath the neurons record each action potential extracellularly. In the case of LPeD1 these signals remain small, but discernible from the noise level. As can be seen from the transistor signal, in the case of LPeD1, the activity increases. For RPeD1 it diminishes before it picks up again after several seconds of quiescence. These two observations prove again the excitatory or respectively inhibitory nature of the connection between VD4 and its

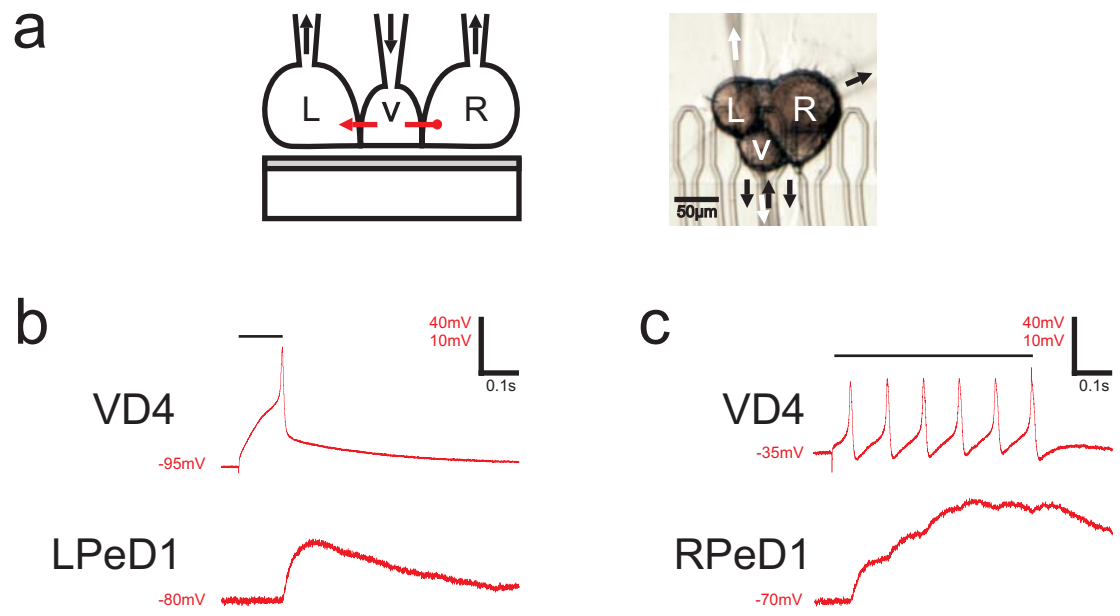

Figure 3.22: *Physiology of investigated neurons.*

(a) shows a schematic of the first conducted experiment. The arrows indicate the signal flow.
(b)-(c) Intracellular recordings of presynaptic activity (top trace) and postsynaptic potentials (bottom trace) for LPeD1 (b) and RPeD1 (c). The bars denote the duration of presynaptic current injection.

two partner neurons with extracellular recordings alone. This observation concludes the first half of stage two, the testing of the detection of postsynaptic activity with transistors on the chip.

In the second part of stage two, seen in Figure 3.23(c), chip stimulation successfully activates the presynaptic neuron VD4 and its synapses to the postsynaptic neurons. In this case only intracellular measurements confirm the synaptic responses in LPeD1 and RPeD1. Note, that a hyperpolarizing current in the postsynaptic neurons (not shown) prevents them from firing.

Equally important, the stimulus creates no crosstalk to the postsynaptic cells, since their intracellular potential changes happen only after the first action potential of VD4 and not during the stimulus application to VD4.

Thus, the two experiments in this Figure show that both prerequisites for a loop experiments, intact synapses as well as full chip control with stimulation and recording have been fulfilled.

For the final stage of the experiment - the proof of a complete double loop - the same stimulus pattern used in in Figure 3.23(c) drives in Figure 3.24(b) both postsynaptic cells LPeD1 and RPeD1 into activity after releasing the cells from the hyperpolarizing current that had been applied in the previous stage. The stimulus leads again to presynaptic action potentials in VD4. Now, the potential changes in the postsynaptic neurons sum up to create postsynaptic action potentials. The resulting activity of neuron RPeD1 is not contradictory considering the excitatory-inhibitory nature of the VD4-RPeD1 synapse in CM mentioned above.

In the final panel 3.24(c) for this set of experiments, RPeD1 is driven into continuous firing through injection a small positive current. During the activity of VD4, both intra- and extracellular recordings of RPeD1 show a short increase in frequency followed by a break of half a second before the activity picks up again. On the other hand the postsynaptic cell LPeD1[7] shows action potentials only during the stimulated firing of its presynaptic partner as can be verified by aligning the stimulation artifacts in the extracellular recording with the voltage applied to the capacitor underneath VD4.

3.4.2 Summary - Triples with two Chemical Synapses

In conclusion, a successful set of experiments consisting of all three stages depicted in Figure 3.21 has been presented. It proves, that it is possible to stimulate and record activity from larger groups of neurons which are interconnected by chemical synapses. On the other hand it also hints at the complexity in analyzing extracellular recordings when having groups larger than two cells. For example, without all three intracellular references, the extracellular recording of the transistor underneath LPeD1 can not be unambiguously identified to belong to the postsynaptic neuron

[7]The spikes showing during the activity of RPeD1 are an indication for the electrical synapse between LPeD1 and RPeD1, an inappropriate connection supposedly not found *in vivo*.

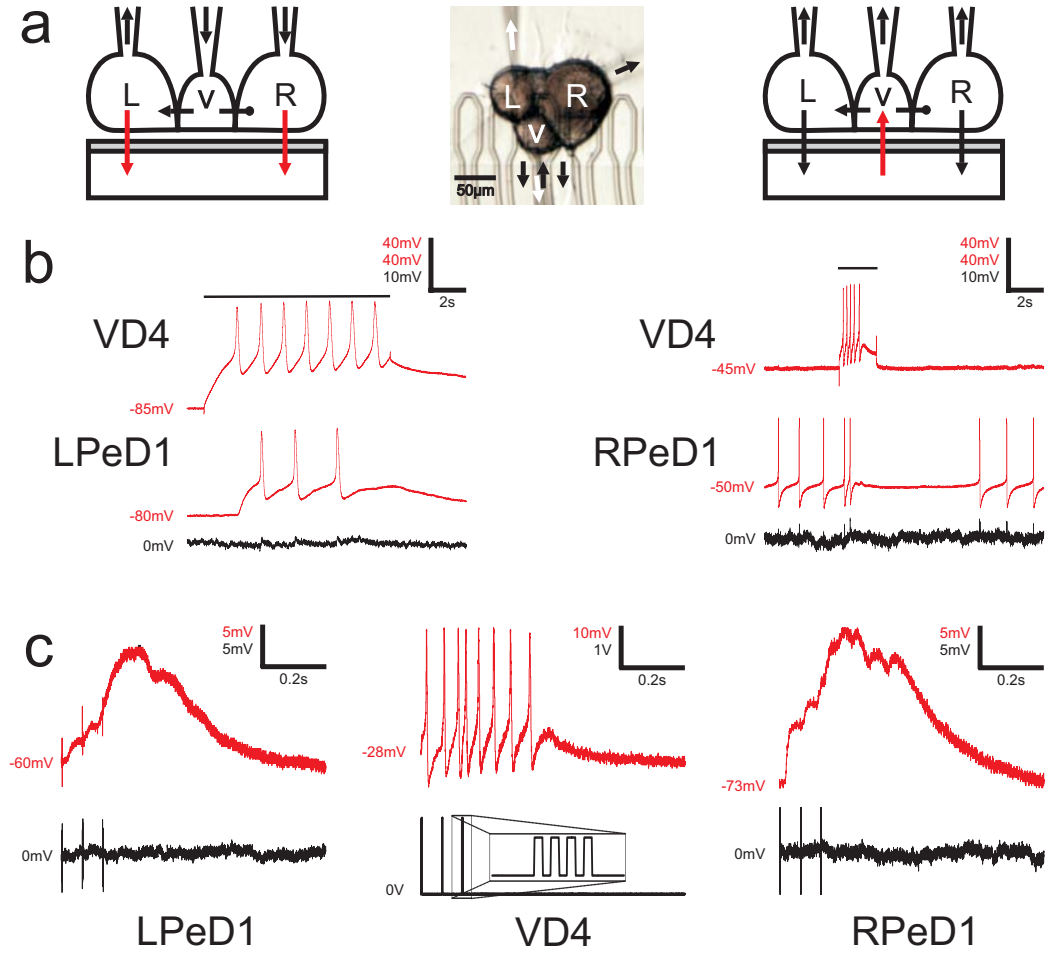

Figure 3.23: *Verifying coupling to chip.*

(a) schematic of the two conducted experiments as well as a micrograph of the investigated neurons. Arrows indicate signal flow. The left hand side depicts the recording of postsynaptic activity (b), while the right hand side shows the presynaptic stimulation (c).
In (b), the current injection (bar) into VD4 results in presynaptic activity, which is recorded intracellularly (top traces). On the postsynaptic side intracellular recordings (middle) pick up postsynaptic activity. In the case of LPeD1 (left) the activity increases, for RPeD1 in diminishes and picks up again. Transistor under each postsynaptic neuron records transient junction potentials during each action potential. Note, that an injected current drives RPeD1 into periodic activity throughout the recorded time.
In Panel (c) the layout has changed. Now the three columns represent the recordings for each neuron during a single experiment: A voltage stimulus (middle, lower trace) causes activity of VD4, which is recorded intracellularly (middle, top trace). The intracellular potentials (top trace) of the postsynaptic neurons LPeD1 (left) and RPeD1 (right) rise during presynaptic activity. The transistors underneath the postsynaptic neurons (bottom trace) record nothing apart from stimulus artifacts. Inset: shape of the stimulus.

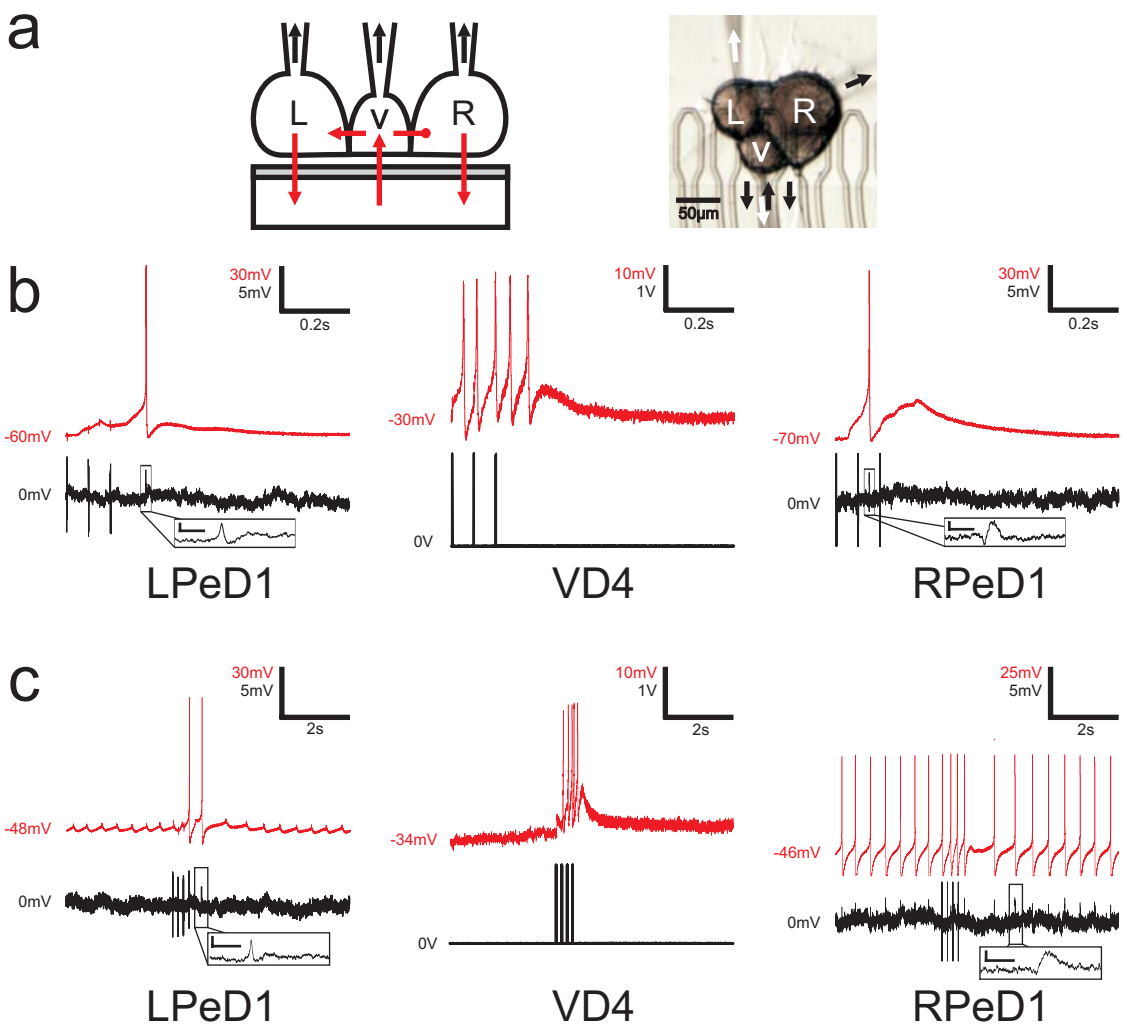

Figure 3.24: *A complete double loop experiment.*

(a) schematic of the conducted experiment as well as a micrograph of the investigated neurons. Arrows indicate the signal flow.
Panel (b) shows postsynaptic action potentials recorded intra- (top trace) and extracellularly (bottom trace) in LPeD1 (left) and RPeD1 (right) as response to the chip stimulation of VD4 (middle, bottom trace - stimulus, top trace - electrophysiology). A transistor underneath LPeD1 as well as RPeD1 records each action potential as can be seen from the insets (scaling $1\ mV\ /\ 1\ ms$*).*
In panel (c) stimulation of the presynaptic neuron VD4 (bottom trace, middle) causes postsynaptic action potentials in LPeD1 (left) and slows RPeD1's (right) continuous activity, which is driven by injection of a small positive current (not shown). For both postsynaptic cells, the recorded traces show intra- (top trace) and extracellular voltage (bottom trace). The insets show close-ups of the recorded transistors' gate voltages (scaling $1\ mV\ /\ 1\ ms$*).*

LPeD1 and not to VD4, which had been driven into activity. When looking at the micrograph in panel (a) of Figure 3.22, thinking about creating larger neuronal networks must also raise the issue of making these groups fit onto a linear array of two-way contacts. Already for groups of three neurons, the yield of successful experiments similar to the one described above has been low: The main limitation was either not getting large enough extracellular recordings from the postsynaptic neurons or a "crosstalk"-effect showing both pre- and postsynaptic depolarizations when applying a stimulus to the capacitors underneath the triple. Any of the above cases renders an otherwise viable synaptic triple useless in terms of the desired interfacing experiment. Therefore larger groups of neurons can only be reliably contacted when using a planar field of two-way contacts which is currently under development. With the technology used herein, the limits has been reached.

It would have been desirable from a neurophysiological or computational point of view to look at a feed-forward network with two pre- and one postsynaptic neuron. Unfortunately the current knowledge in cell culture of *Lymnaea stagnalis* does not provide candidates for such a network from the pool of identified giant neurons. None the less, it has been remarkable to find that all members of this species contain a network of three neurons, that can be reproduced with high fidelity in cell culture without taking care of intermixing cells from different animals. This capability was a major prerequisite for a successful interfacing of three interconnected neurons. Finding an organism, that provides a similar versatility and connectivity while maintaining the same yields of different types of synaptic contacts, neurotransmitters and receptors, will be a difficult task when planning the next step: cell cultures of larger networks on planar arrays of two-way contacts.

When I sing it's a cyclone
I'm writing a raging sea
Searching for a sign of life
Is it safe to say it's me?

- Gnarls Barkley, *A Storm Coming* (2006)

Chapter 4

Summary & Outlook

Under an endless sky
Wish I could fly away forever (and ever)
And the poetry is so pure
When we are on the floor together (it's been a long time)

When was the last time you danced?

Gnarls Barkley, *The Last Time* (2006)

In the previous chapter results and conclusions derived from the investigation of single, pairs and groups of three *Lymnaea* neurons have been presented and discussed spanning the range from stimulating and recording ion channel populations to evoked and monitored intercellular communication on the synaptic level. The following list gives a concise review of the major findings. A final paragraph sketches the next possible steps along the lines of this research project.

4.1 Summary

The following list sums up the major observations with respect to the topics presented in the results part. A single item here represents a more detailed summary at the end of each given subsection.

Single Cell Recording Poly-L-lysine (PLL) diminishes the cell-substrate distance down to 20 nm and increases the adhesion area in such a manner, that FETs record signals up to 30 mV during single action potentials. Interpretation of the extracellular signal also explains the reduced excitability leading to oscillatory behavior of neurons cultured on this coating.

Single Cell Stimulation Given strong adhesion conditions, ramp-shaped pulses can increase the ion channel conductivity even on SiO_2. Since potassium currents dominate in the adhesion membrane - another putative effect of the PLL coating - the ramp shaped pulses do not elicit action potentials. A further analysis showed, that square-shaped pulses allow minimal invasive stimulation through transient electroporation.

Excitatory Synaptic Couple An excitatory Loop - the extracellular stimulation of presynaptic activity while monitoring postsynaptic responses with FETs - has been constituted. Potentiation of the synapse demonstrated full extracellular control of a learning paradigm through chip stimulation and recording.

Inhibitory Synaptic Couples Two different inhibitory Loops were presented on three different coatings, indicating towards alternative coating for future chip experiments instead of PLL. A double stimulation experiment for complete control of inhibitory synapses from chip failed due to competition between stimulation through electroporation and presynaptic inhibition.

An Excitatory-Inhibitory Triple A Double Loop experiment demonstrated full extracellular chip control over an excitatory and a mixed excitatory-inhibitory synapse.

In summary, the recording of neuronal activity with field-effect transistors has provided insight into the interaction of the substrate with the neurons at single cell level. The results on neuronal stimulation with electrolyte-oxide-semiconductor capacitors allowed not only passive monitoring but also active triggering of synaptic transmission whether excitatory or inhibitory in nature.
The full control over inhibitory synapses, especially regarding the postsynaptic spiking, remains a topic of active research. On the other hand, the storage and recall of a single bit of information in the synaptic memory of an excitatory synapses hinted at the capabilities of this approach.
Finally, the interfacing of a three neuron network proved the scalability of this technique up to larger networks.

4.2 Outlook

After establishing the individual components of cell-cell and cell-chip interactions, now more detailed experiments, which could provide new insights into the topics of neuroscientific interest, become feasible.
The extracellular, non-invasive chip interfacing of learning neuronal networks contains three major aspects that have not been emphasized yet:

Detection of Single Synaptic Events First observations did not rule out that the depolarization due to postsynaptic currents might be detectable by FETs. Experiments with outgrown *Lymnaea* neurons forming chemical synapses would help to separate pre- from postsynaptic contributions.

Long-term Measurements Due to its non-invasive nature, long-term recordings during synapse formation of *Lymnaea* neurons would allow a glimpse at the electrical fine-tuning of the synaptic apparatus. Stimuli applied during that critical time period might affect its outcome.

Multicellular Networks After three comes many: Extending this approach to a functional multicellular network like the central pattern generator for the breathing rhythm of *Lymnaea* along with up- and downstream targets might allow the reconstruction and monitoring of a full behavioural relevant network *in vitro*.

Although each experiment in itself would not shake the foundations of neurobiology, the whole package could help to rouse the attention of the neuroscience community to an emerging technique. Hopefully it can provide new insights into the function of neuronal networks and maybe ultimately into our own trains of thoughts.

Listen to our lives
The wind will whisper the way it is
I am going to happen, what a lovely day it is
Don't ask why
Just live, and, die

- Gnarls Barkley, *The Last Time* (2006)

Appendix A

Cell Culture

This Appendix should give a concise recipe of successful animal culture. This includes the preparation scheme, the involved cell culture media as well as the chip preparation and a list of the substances used for the recipes.

A.1 Animal Preparation

For the preparation itself one needs the following items:

For sterile work under laminar flow hood:
1 Sylgard-coated container with large insect pins
1 Sylgard-coated 60 mm dish with small insect pins
2 forceps Dumont Dumoxel type 5
2 finely sharpened forceps
1 pair of curved eye-surgeon scissors
1 pair of fine straight scissors
5 disposable 35 mm Falcon dishes
1 disposable 50 ml Falcon tube
1 disposable 10 ml syringe
1 Hamilton glass syringe with micrometer-precision piston
1 Hamilton luer tip
1 piece of flexible tubing that fits luer tip
1 3-D Micromanipulator mounted on a base
1 set of silanized and fire polished borosilicate glass pipettes with tip diameters 50-100 μm

For non-sterile work:

1 glass beaker, 250 ml

1 pair of blunt, curved forceps

1 bottle of Lysterine

The preparation proceeds as follows:

1. Disinfect preparation equipment under laminar flow hood with 70% ethanol.
2. Collect animals of adequate size and number on a paper towel.

2b. Optional: Collect hemolymphe.

3. Fill a 250 ml glass beaker with 80 ml normal saline (NS).
4. Deshell all animals with blunt forceps and drop then into beaker.
5. Add 20 ml Lysterine to beaker for anesthetization.
6. Wait for 10 minutes.
7. During these 10 minutes
   a.) fill anti-biotic saline (ABS) into Sylgard-coated preparation dish
   b.) fill three 35 mm Falcon dishes with 3 ml ABS
   c.) fill two 35 mm Falcon dished with 3 ml defined medium (DM)
   d.) fill 50 ml Falcon tube with 20ml defined medium
   e.) add 750μ l of 1 M D-Glucose solution to Falcon tube to create high-osmolarity DM (HODM)
8. After 10 minutes transfer animals into dish
9. Pin down all animals at tentacles with 2 pins and in the mid-body with 1 pin
10. For each animal
    a.) cut from mid-body to mouth with curved eye-surgeon scissors
    b.) take two extra pins to fix the sides and the penis to the base
    c.) transfer the needles to the inside to pin down the head's skin
    d.) remove the needle in the middle pin fix the gonads towards the rear
    e.) fix buccal mass to the base outside of the animal with a pin
    f.) remove stomach and yellow gland with the second cut close to buccal mass
    g.) cut the ganglionic ring between the central ganglia
    h.) cut the connective tissue at the dorsal side close to the pedal ganglia
    i.) cut the visceral nerve far from the ganglionic ring
    j.) lift the ring with the long piece of visceral nerve
    k.) cut the remaining nerves close to the brain
    m.) mind not to severe the buccal nerves
    n.) severe the buccal ganglia from the buccal mass
    l.) transfer the brain to 1st Falcon dish filled with ABS
11. Wash the brains in the 3 Falcon dishes for 10 minutes each
12. In the meantime prepare enzyme solution
    a.) weigh 6 mg of Trypsin and dissolve it in 1st Falcon dish with DM
    b.) weigh 6 mg of Trypsin inhibitor and dissolve it in second Falcon dish

13. After last wash transfer brains into enzyme solution for 20 minutes
14. Move brains to inhibitor dish for 10 minutes
15. During the enzyme treatment:
    a.) rinse Hamilton syringe with 70% ethanol and let it dry in laminar air flow
    b.) fill 60 mm dish with 10 ml HODM
    c.) fill 10 ml disposable syringe with HODM
    d.) use disposable syringe to back-fill Hamilton syringe and insert piston
    e.) wrap syringe's glass nozzle in thin layer of Parafilm
    f.) mount syringe on base with 3D micro-manipulator
    g.) rinse the interconnected luer tip and tubing as well as the glass pipette with 70% ethanol
    h.) rinse the tubing with HODM
    i.) fill the tubing with HODM
    j.) connect luer tip and Hamilton syringe
    k.) connect end of tubing to glass pipette
    l.) test system by filling glass pipette with medium

Remarks:

2b. To collect hemolymphe:
take a 5 ml syringe, an injection needle, and a 0.2 μm low-protein binding syringe filter unit;
connect needle to syringe, use needle's tip to irritate snails;
take up the fluid emitted from the retracting animal (0.5 ml);
after getting about 3 ml, filter hemolymphe into 30 mm falcon dish for coating;
reuse hemolymphe up to 3 times to coat multiple dishes.

4. The shell removal can be achieved without damaging the animal's skin

10. a.) always point the scissors' tip away from the organs when you cut
    k.) mind not to severe the buccal nerves

11. After each transfer of the brains shake the dish 3x clock- and counter-clockwise
12. Label enzyme dishes carefully to avoid maltreatment
13. Important: shake dish as in 11. before and after the transfer, and after 50% of the treatment's duration
14. same as 13.

15. d.) Important: avoid any bubbles
    g.) this helps to avoid bubbles
    j.) put extra HODM in tip and drive piston into syringe to have a drop at the nozzle to avoid air in the tubing
    l.) if test fails and air is caught in the tubing, repeat all steps to avoid cell damage during extraction

A.2 Cell Culture Media

This section presents the recipes for the solutions used for *Lymnaea* cell culture.

A.2.1 Normal and Anti-Biotic Saline

Recipe for 1 liter of 4x Stock solution for Normal Saline (NS):

Salt	Concentration/mM	Mass/g
NaCl	160.0	9.35
KCl	6.8	0.50
CaCl2	16.4	2.41
MgCl2	6.0	1.21
HEPES	40.0	9.53

- add salts to 1 liter of highest quality water
- use NaOH to titrate the final pH of 7.9.
- dilute 250 ml with 750 ml of highest quality water to obtain 1 l NS.
- sterilize by filtration into 500 ml bottles.

Recipe for 500 ml of Anti-Biotic Saline (ABS):
- take 500 ml sterile NS
- add 10 ml of Gentamicin stock solution and
- add 0.75 ml of Ampicillin stock solution
→ final concentration: 150 μg/ml of both Gentamicin and Ampicillin.
! Osmolarity of ABS should be around 110 mOsm.

For Gentamicin stock solution
- take 1 g of substance and dissolve it in 133.3 ml highest quality water
- store at 7°C
- use within 6 months

For Ampicillin stock solution
- take 100 mg of substance and dissolve it in 1ml highest quality water
- store in cryovial at −20°C
- thaw before usage and refreeze afterwards

A.2.2 Defined Medium (DM) and High-Osmolarity DM

Recipe for 1 liter of Defined Medium (DM)

Substance	Quantity	Unit
L-15 stock solution	500	ml
L-Glutamine	150	mg
D+ Glucose	54.05	mg
4x NS stock solution	250	ml
Highest quality water	246.4	ml
Gentamicin stock solution	3.3125	ml
Ampicillin stock solution	400	μl

- add all components in the order of appearance
- store at 7°C
- use before 4 weeks, since L-Glutamine decays into toxic products
! Osmolarity of DM should be around 145 mOsm

To increase the shelf life, add L-Glutamine, D+ Glucose and antibiotics prior to use. Note that either Gentamicin or Ampicillin was added to the medium.
At a late stage of the thesis DM with Ampicillin alone proved to be sufficient.

Recipe for 20 ml High-Osmolarity Defined Medium (HODM)
- add 750 μl of 1M D+ Glucose stock solution to 20 ml of DM

A.2.3 Brain-Conditioned Medium

Recipe for 6 ml of Brain-Conditioned Medium (CM)

Coating of Petri Dish

To prevent the adhesion and binding of the proteins secreted by the brains, the 60 mm glass Petri dishes used for the culture are coated with a silane. The coating process can be done once for several dishes and lasts for more than 30 uses. Make sure to work under a hood, since the solvent for the silane is mildly hazardous.

- fill one new dish with roughly 10 ml of silane solution
- shake the dish gently to promote contact of the silane with all sides
- transfer the silane to the next dish, while leaving the other to dry in the hood
- repeat the above step for all dishes at least three times
- store the remaining silane solution in a new, airtight glass container for reuse
- leave all Petri dishes in the hood for 24 hours
- after 24 hours clean them with a cell-culture proof detergent

- sterilize the clean Petri dishes, wrapped in autoclave foil)
- good for storage up to 4 weeks

Creation of CM

! Prior to animal dissection make sure that at least one sterile Petri dish is present
- select 12 healthy animals for brain extraction:
    + old animals (> 3 months) for CM suited best for synapse formation
    + younger animals ($\sim$ 1.5 months) for outgrowth
- take out whole brains (do not cut the cerebral connective)
- wash the brains thoroughly:
    + fill seven 30 mm plastic dishes with 3ml ABS each
    + each washing cycle takes 20 minutes
    + before, after 50% and 100% of the time shake the dish
- after the last washing cycle finished:
    + take 60 ml sterile Petri dish and fill it with 6 ml DM
    + transfer brains, shake once more and leave for conditioning
- leave brains in a dark place with 70% humidity and at room temperature

The brains can be used multiple times for the creation of CM:
    + 3 days for 1x CM (fresh brains)
    + 5 days for 2x CM (once in culture)
    + 7 days for 3x or 4x CM (more than once in culture)

- during the incubation time leave the brains undisturbed
- after the time is up, the brains
    + should be transferred into a 30 ml plastic dish filled with ABS
    + repeat the 20 minutes cleaning cycle with 7 dishes filled with ABS
    + cleaning is necessary if brains will be reused for another round of CM
- after the time is up, the fresh CM
    + should be poured into a plastic 10 ml tube
    + has to be sealed airtight wrapping the cap in Parafilm
    + has to be labeled carefully (number of incubations, date, name, ...)
    + can either be kept at 4°C for direct usage within a week
    + or frozen at -20°C for storage

A.3 Chip Conditioning

Generally, all chips (two-way contact chips, high-sensitivity arrays, FLIC chips) were cleaned using a 70°C warm 10% solution of a detergent with an undiluted pH of 12. To rinse the chip heat 1 l of high quality water.

- remove cell culture medium from chip
- add several mls of detergent solution to the chip chamber
- wrap a corner of a clean, soft paper cloth around a pair of forceps with blunt tips
- use mild force to remove cell remains from the chip surface
- use the warm water to remove the detergent from the chip chamber
- rinse the chip chamber 3 times with water
- leave chip for a few minutes
- rinse the chip chamber again 10 times with water
- use compressed air to blow chip surface dry

The Infineon chip was cleaned by Lambacher.

To coat the chips with poly-L-Lysine, 1 ml of a filtered poly-L-lysine solution dissolved in HEPES ($pH = 8.4$) at a concentration of 1 mg/ml was left for at least 30 minutes. After removal the chips were rinsed 3x with 1 ml cell culture tested water, 1x with 1 ml NS - which was left on the chip for 10 minutes - and another 3x with 1 ml cell culture tested water, then left to air dry in a cell culture hood. For the FLIC chips the amount of medium had to be tripled. The chips were then either used directly for strong adhesion conditions or left for at least 3 days at 7°C wrapped in Parafilm to prevent contamination.

For the β-Laminin coating of the two-way chips, a 5 μl droplet of stock solution (0.5 mg/ml in 10% acetate) was left on the sensor area of the chip to dry up under a sterile cell culture hood. These chips were used directly for plating cells without further rinsing steps.

Appendix B

Chip Post-Processing

Even though the processing of the chips made by Zeck and Bonifazi [Zec02] was done before the beginning of this thesis research project, none the less the chips had to be glued and bonded to ceramic packages. After the bonding Perspex chambers were fitted on top to separate the compartments for electronics and cell culture.

- heat ceramic package in bonder to 120°C
- put a drop of bonding wax on the package and carefully place die in the center[1]
- leave chip for 25 minutes to cool down
- connect each bond pad on the chip with a gold contact on the package according to the appropriate bonding schematic
- fit outer and inner ring of the perspex chamber onto the die
- glue the outer ring to the package using a syringe filled with Elastosil/MK3
- glue the inner ring to the chip with MK3 (no Elastosil!)
- after 24 hours of desiccation time, glue outer to inner ring to create waterproof environment for the electronics
- wait another 24 hours until the acetate in the glue has evaporated completely
- before the first time in culture put cell culture medium on the chip for 24 hours
- start cleaning-culture cycle as stated above (A.3)

[1] double check the correct orientation wrt to the bonding schedule!

Appendix C

FLIC Staining Protocol

The FLIC chips were fitted into 30 mm plastic dishes, coated with poly-L-lysine and filled with 1.5 ml medium for placement of neurons. See the above section regarding the treatment of the chips prior to culture. After 16 hours in culture, the staining protocol as shown below was applied:

- dissolve the dye $DiIC_{18}$ in ethanol (pA) yielding a concentration of 4.5 μg/μl
- fill culture chamber with additional 3 ml DM
- add 20 μl dye solution to the dish
- stir and shake medium to distribute dye evenly
- wait for 10 minutes
- remove 3 ml old medium and replace with new DM
- wait 2 minutes
- repeat the last 2 steps until background fluorescence gets washed out (total 3-4 times)

Appendix D

Chemicals & Equipment

D.1 Cell Culture Medium

Ampicillin Sodium Salt (Gibco 11593-027)
Calcium Chloride (Sigma C-3881), 500g
D-Glucose (Sigma G-5767), 500g
Gentamicin Sulfate (Sigma G-3632), 5g
L-Glutamine (Sigma G-3126), 5g
Leibovitz L15-Medium, modified (Gibco Formulation #04195557), 500ml
Hepes (Sigma H-3375), 25g
Magnesium Chloride (Sigma M-9272), 500g
Potassium Chloride (Sigma P-4504), 500g
Poly-L-Lysine (Sigma P-1274), 25mg
Tris [Hydroxymethyl] Aminomethane (Sigma T-6066), 100g
Trypsin, Lyophilized Powder (Sigma T-4665), 100mg
Trypsin Inhibitor (Sigma T-9003), 100mg
Sodium Chloride (Sigma S-5886), 500g

D.2 Preparation

Fine Forceps #5, 11cm length (FST #11251-20)
Spring Scissors, 6mm Cutting Edge (FST #15030-15)
Ultra-fine Tip Forceps, Manually Sharpened, 15cm length (donated by Wali Zaidi)
Spring Scissors, 2mm Cutting Edge (FST #15000-03)
30mm Round Plastic Dishes (Falcon 35-3001)
Cellulose Acetate 0.2μm Sterile Membrane Filter, Renner GmbH
Glass Capillaries, 6 In, 1.5mm Outer Diameter (OD), No Filament (WPI #TW150-6)
Silane (Sigma SL2)
Tygone Tubing, 1.78 mm OD, 1.27mm Inner Diameter (ID) (Kleinfeld #9205526)

Luer-Tip Needle N18, Gauge 18, 1.27mm OD, 0.84mm ID (Hamilton #91018)
0.5ml Gas-tight Glass Syringe with Micrometer Screw (Hamilton #81242)
Precision Micromanipulator MM-33 (FST #25033-10)
Stereo Microscope (Zeiss Stemi SV-11)
Movable Microscope Mounting (Zeiss Stativ DA)
Cold-Light Source (Zeiss KL-1500)

D.3 Electrophysiology and Synaptic Block

3x Single Electrode Bridge Amplifier (NPI BA1-S)
3x Micro-Electrode Holder for 1.5mm OD Capillaries (NPI EH-02)
Chlorated Ag Metal Wire, 0.2 mm Diameter (Generic)
3x 3D-Hydraulic Micro Manipulator (Narishige Water Robot WR-88)
Diamond Glass Cutter Pencil (Generic)
Glass Capillaries, 6 In, 1.5mm OD, With Filament (WPI #TW150F-6)
Potassium Sulfate (Sigma P-9458), 100g
Non-metallic Flexible Syringe Needle (WPI MF28G-5)
Horizontal Glass Capillary Puller (WZ DMZ Universal Puller)
Stereo binoculars, Continuous Zoom, 60mm Working Distance (Leica Wild M10)
2/3" Color CMOS Sensor C-Mount Fire-Wire Camera (Pixelink PL-A742)
Cold-Light Source (Zeiss KL1500)
Run-time Compiled Software Development System (NI Labview 7.1)
6x Analog-In, 3x Analog-Out Measurement Software (in-house)

Hexamethonium Chloride (HMC, Sigma H-2138), 5g
Methyllycaconitine Citrate (MLA, Sigma M-168), 5mg
Mecamylamine Hydrochloride (MEC, Sigma M-9020), 5mg

D.4 Chip Stimulation and Recording

2x 15 Mhz Function Generator (Hewlett-Packard HP33120A)
GPIB Interface Card (National Instruments GPIB-PCI)
64x Analog-In/2x Analog-Out/32x Digital In/Out (DIO) PCI Card (NI 6071E)
16x AI/2x AO/32x DIO BNC Break-Out Box (NI BNC-2090)
1x 2:1 AO:AI/3x AI:AO SMB Break-Out Box (in-house)
64-channel Opto-Coupled DIO PCI Interface Card (Kolter electronics OPTO PCI)
Run-time Compiled Software Development System (NI Labview 7.1)
48-channel AI, 2x GPIB-triggered AO Measurement Software (in-house)

Bibliography

[Bli73] T. V. P. Bliss, T. Lomo. Long-lasting potentiation of synaptic transmission in dentate area of anesthetized rabbit following stimulation of perforant path. *Journal Of Physiology-London*, 232(2):331–356, 1973.

[Bon02] P. Bonifazi, P. Fromherz. Silicon chip for electronic communication between nerve cells by non-invasive interfacing and analog-digital processing. *Advanced Materials*, 14(17):1190–1193, 2002. Article 0935-9648.

[Bre04] S. Breit, J. B. Schulz, A. L. Benabid. Deep brain stimulation. *Cell & Tissue Research*, 318(1):275–288, 2004. Review Review.

[Bri05] M. Brittinger, P. Fromherz. Field-effect transistor with recombinant potassium channels: fast and slow response by electrical and chemical interactions. *Applied Physics A-Materials Science & Processing*, 81(3):439–447, 2005.

[Bru91] A. B. Brussaard, J. C. Lodder, A. Termaat, T. A. Devlieger, K. S. Kits. Inhibitory modulation by FMRFamide of the voltage-gated sodium current in identified neurons in Lymnaea-stagnalis. *Journal Of Physiology-London*, 441:385–404, 1991.

[Buc01a] V. Bucher, B. Brunner, C. Leibrock, M. Schubert, W. Nisch. Electrical properties of a light-addressable microelectrode chip with high electrode density for extracellular stimulation and recording of excitable cells. *Biosensors & Bioelectronics*, 16(3):205–210, 2001.

[Buc01b] V. Bucher, M. Schubert, D. Kern, W. Nisch. Light-addressed sub-mu m electrodes for extracellular recording and stimulation of excitable cells. *Microelectronic Engineering*, 57-8:705–712, 2001.

[Col01] M. A. Colicos, B. E. Collins, M. J. Sailor, Y. Goda. Remodeling of synaptic Actin induced by photoconductive stimulation. *Cell*, 107(5):605–616, 2001.

[Col06] M. A. Colicos, N. I. Syed. Neuronal networks and synaptic plasticity: understanding complex system dynamics by interfacing neurons with silicon technologies. *Journal Of Experimental Biology*, 209(12):2312–2319, 2006.

[Eli94] L. S. Eliot, R. D. Hawkins, E. R. Kandel, S. Schacher. Pairing-specific, activity-dependent presynaptic facilitation at Aplysia sensory-motor neuron synapses in isolated cell-culture. *Journal Of Neuroscience*, 14(1):368–383, 1994.

[Eve03] B. Eversmann, M. Jenkner, F. Hofmann, C. Paulus, R. Brederlow, B. Holzapfl, P. Fromherz, M. Merz, M. Brenner, M. Schreiter, R. Gabl, K. Plehnert, M. Steinhauser, G. Eckstein, D. Schmitt-Landsiedel, R. Thewes. A 128x128 CMOS biosensor array for extracellular recording of neural activity. *IEEE Journal Of Solid-State Circuits*, 38(12):2306–2317, 2003.

[Fen97] Z. P. Feng, J. Klumperman, K. Lukowiak, N. I. Syed. In vitro synaptogenesis between the somata of identified Lymnaea neurons requires protein synthesis but not extrinsic growth factors or substrate adhesion molecules. *Journal Of Neuroscience*, 17(20):7839–7849, 1997.

[Fro91] P. Fromherz, A. Offenhausser, T. Vetter, J. Weis. A neuron-silicon junction - a Retzius cell of the leech on an insulated-gate field-effect transistor. *Science*, 252(5010):1290–1293, 1991.

[Fro95] P. Fromherz, A. Stett. Silicon-neuron junction - capacitive stimulation of an individual neuron on a silicon chip. *Physical Review Letters*, 75(8):1670–1673, 1995.

[Fro03] P. Fromherz. *Neuroelectronic Interfacing: Semiconductor Chips with Ion Channels, Nerve Cells, and Brain*. Nanoelectronics and Information Technology. Wiley-VCH Verlag, Berlin, 2003.

[Fro05] P. Fromherz. The neuron-semiconductor interface. In Willner I. E., Katz, editors, *Bioelectronics*, pages 339–394. Wiley-VCH Verlag, Berlin, 2005.

[Gho06] G. Gholmieh, W. Soussou, M. Han, A. Ahuja, M. C. Hsiao, D. Song, A. R. Tanguay, T. W. Berger. Custom-designed high-density conformal planar multielectrode arrays for brain slice electrophysiology. *Journal Of Neuroscience Methods*, 152(1-2):116–129, 2006.

[Gle06] R. Gleixner, P. Fromherz. The extracellular electrical resistivity in cell adhesion. *Biophysical Journal*, 90(7):2600–2611, 2006.

[God06] Y. Goda, M.A. Colicos. Photoconductive stimulation of neurons cultured on silicon wafers. *Nature Protocols*, 1(1):461–467, 2006.

[Gus76] B. Gustafsson, E. Jankowska. Direct and indirect activation of nerve-cells by electrical pulses applied extracellularly. *Journal Of Physiology-London*, 258(1):33–61, 1976.

[Ham81] O. P. Hamill, A. Marty, E. Neher, B. Sakmann, F. J. Sigworth. Improved patch-clamp techniques for high-resolution current recording from cells and cell-free membrane patches. *Pflugers Archiv-European Journal Of Physiology*, 391(2):85–100, 1981.

[Ham99] T. Hamakawa, M. A. Woodin, M. C. Bjorgum, S. D. Painter, M. Takasaki, K. Lukowiak, G. T. Nagle, N. I. Syed. Excitatory synaptogenesis between identified Lymnaea neurons requires extrinsic trophic factors and is mediated by receptor tyrosine kinases. *Journal Of Neuroscience*, 19(21):9306–9312, 1999.

[Hil01] B. Hille. *Ion Channels of Excitable Membranes*. Sinauer Associates, Incorporated, 2001.

[Hin06] M. J. Hinner, G. Hubener, P. Fromherz. Genetic targeting of individual cells with a voltage-sensitive dye through enzymatic activation of membrane binding. *Chembiochem*, 7(3):495–505, 2006.

[Ioa06] A. A. Ioannides. Magnetoencephalography as a research tool in neuroscience: State of the art. *Neuroscientist*, 12(6):524–544, 2006.

[Iwa87] Y. Iwamoto, F. A. Robey, J. Graf, M. Sasaki, H. K. Kleinman, Y. Yamada, G. R. Martin. YIGSR, a synthetic laminin pentapeptide, inhibits experimental metastasis formation. *Science*, 238(4830):1132–1134, 1987.

[Jen01] M. Jenkner, B. Muller, P. Fromherz. Interfacing a silicon chip to pairs of snail neurons connected by electrical synapses. *Biological Cybernetics*, 84(4):239–249, 2001.

[Jos00] R. P. Joshi, K. H. Schoenbach. Electroporation dynamics in biological cells subjected to ultrafast electrical pulses: A numerical simulation study. *Physical Review E*, 62(1):1025–1033, 2000. Part B.

[Kan00a] E. R. Kandel, L. R. Squire. Neuroscience: Breaking down scientific barriers to the study of brain and mind. *Science*, 290(5494):1113–1120, 2000.

[Kan00b] E.R. Kandel, J.H. Schwartz, T.M. Jessell. *Principles in Neuroscience*. McGraw-Hill, 2000.

[Kau04] R. A. Kaul, N. I. Syed, P. Fromherz. Neuron-semiconductor chip with chemical synapse between identified neurons. *Physical Review Letters*, 92(3), 2004. 038102.

[Kyr89] M. Kyriakides, C. R. McCrohan, C. T. Slade, N. I. Syed, W. Winlow. The morphology and electrophysiology of the neurons of the paired pedal ganglia of Lymnaea-stagnalis (l). *Comparative Biochemistry And Physiology A-Physiology*, 93(4):861–876, 1989.

[Lam02] A. Lambacher, P. Fromherz. Luminescence of dye molecules on oxidized silicon and fluorescence interference contrast microscopy of biomembranes. *Journal Of The Optical Society Of America B-Optical Physics*, 19(6):1435–1453, 2002. Article 0740-3224.

[Lam04] A. Lambacher, M. Jenkner, M. Merz, B. Eversmann, R. A. Kaul, F. Hofmann, R. Thewes, P. Fromherz. Electrical imaging of neuronal activity by multi-transistor-array (MTA) recording at 7.8 mu m resolution. *Applied Physics A-Materials Science & Processing*, 79(7):1607–1611, 2004.

[Lin49] G. Ling, R. W. Gerard. The normal membrane potential of frog Sartorius fibers. *Journal Of Cellular And Comparative Physiology*, 34(3):383–396, 1949.

[Log04] N. K. Logothetis, B. A. Wandell. Interpreting the BOLD signal. *Annual Review Of Physiology*, 66:735–769, 2004.

[May92] M. Mayford, A. Barzilai, F. Keller, S. Schacher, E. R. Kandel. Modulation of an NCam-related adhesion molecule with long-term synaptic plasticity in Aplysia. *Science*, 256(5057):638–644, 1992.

[Mer05] M. Merz, P. Fromherz. Silicon chip interfaced with a geometrically defined net of snail neurons. *Advanced Functional Materials*, 15(5):739–744, 2005.

[Mun00] D. W. Munno, M. A. Woodin, K. Lukowiak, N. I. Syed, P. S. Dickinson. Different extrinsic trophic factors regulate neurite outgrowth and synapse formation between identified lymnaea neurons. *Journal Of Neurobiology*, 44(1):20–30, 2000.

[Mun03] D. W. Munno, D. J. Prince, N. I. Syed. Synapse number and synaptic efficacy are regulated by presynaptic cAMP and protein kinase a. *Journal Of Neuroscience*, 23(10):4146–4155, 2003.

[Ola06] C. W. Olanow, J. A. Obeso, F. Stocchi. Continuous Dopamine-receptor treatment of Parkinson's disease: scientific rationale and clinical implications. *Lancet Neurology*, 5(8):677–687, 2006.

[Par02] M. K. Park, A. V. Tepikin, O. H. Petersen. What can we learn about cell signalling by combining optical imaging and patch clamp techniques? *Pflugers Archiv - European Journal of Physiology*, 444(3):305–316, 2002.

[Pri00] A. A. Prinz, P. Fromherz. Electrical synapses by guided growth of cultured neurons from the snail Lymnaea stagnalis. *Biological Cybernetics*, 82(4):L1–L5, 2000.

[Rid91] R. L. Ridgway, N. I. Syed, K. Lukowiak, A. G. M. Bulloch. Nerve growth-factor (NGF) induces sprouting of specific neurons of the snail, Lymnaea-stagnalis. *Journal Of Neurobiology*, 22(4):377–390, 1991.

[Rin94] T. Rink, H. Bartel, G. Jung, W. Bannwarth, G. Boheim. Effects of polycations on ion channels formed by neutral and negatively charged alamethicins. *European Biophysics Journal With Biophysics Letters*, 23(3):155–165, 1994.

[Rit06] P. Ritter, A. Villringer. Simultaneous EEG-fMRI. *Neuroscience & Biobehavioral Reviews*, 30(6):823–838, 2006.

[San97] M. T. Santini, C. Cametti, P. L. Indovina, G. Morelli, G. Donelli. Polylysine induces changes in membrane electrical properties of K562 cells. *Journal Of Biomedical Materials Research*, 35(2):165–174, 1997.

[Sch02] J. Scholz, C. J. Woolf. Can we conquer pain? *Nature Neuroscience*, 5:1062–1067, 2002. Suppl. S.

[Sch07] Ingmar Schoen, Peter Fromherz. The mechanism of extracellular stimulation of nerve cells on an electrolyte-oxide-semiconductor capacitor. *Biophysical Journal*, 92(3):1096–1111, 2007.

[Smi01] A. B. Smit, N. I. Syed, D. Schaap, J. van Minnen, J. Klumperman, K. S. Kits, H. Lodder, R. C. van der Schors, R. van Elk, B. Sorgedrager, K. Brejc, T. K. Sixma, W. P. M. Geraerts. A glia-derived Acetylcholine-binding protein that modulates synaptic transmission. *Nature*, 411(6835):261–268, 2001.

[Ste97] A. Stett, B. Muller, P. Fromherz. Two-way silicon-neuron interface by electrical induction. *Physical Review E*, 55(2):1779–1782, 1997.

[Sye89] N. I. Syed, W. Winlow. Morphology and electrophysiology of neurons innervating the ciliated locomotor epithelium in Lymnaea-stagnalis (l). *Comparative Biochemistry And Physiology A-Physiology*, 93(3):633–644, 1989.

[Sye90] N. I. Syed, A. G. M. Bulloch, K. Lukowiak. Invitro reconstruction of the respiratory central pattern generator of the mollusk Lymnaea. *Science*, 250(4978):282–285, 1990.

[Sye91] N. I. Syed, W. Winlow. Respiratory behavior in the pond snail Lymnaea-stagnalis.2. neural elements of the central pattern generator (CPG). *Journal Of Comparative Physiology A-Sensory Neural And Behavioral Physiology*, 169(5):557–568, 1991.

[Sye92] N. I. Syed, R. L. Ridgway, K. Lukowiak, A. G. M. Bulloch. Transplantation and functional-integration of an identified respiratory interneuron in Lymnaea-stagnalis. *Neuron*, 8(4):767–774, 1992.

[Sze98] S.M. Sze. *Modern Semiconductor Devices*. Wiley-Interscience, 1998.

[Tas89] K. Tashiro, G. C. Sephel, B. Weeks, M. Sasaki, G. R. Martin, H. K. Kleinman, Y. Yamada. A synthetic peptide containing the IKVAV sequence from the A-chain of Laminin mediates cell attachment, migration, and neurite outgrowth. *Journal Of Biological Chemistry*, 264(27):16174–16182, 1989.

[Ulb01] M. Ulbrich, P. Fromherz. Neuron-silicon self-excitation: A prototype of iono-electronics. *Advanced Materials*, 13(5):344–347, 2001.

[Ulb05] M. H. Ulbrich, P. Fromherz. Opening of K+ channels by capacitive stimulation from silicon chip. *Applied Physics A-Materials Science & Processing*, 81(5):887–891, 2005.

[Ver06] A. Verkhratsky, O. A. Krishtal, O. H. Petersen. From Galvani to patch clamp: the development of electrophysiology. *Pflugers Archiv-European Journal Of Physiology*, 453(3):233–247, 2006.

[Voe05a] M. Voelker. *Detektion von Aktionspotentialen einzelner Säugetierneurone mit rauscharmen Feldeffekttransistoren nahe der thermodynamischen Messgrenze*. PhD thesis, Technical University Munich, 2005.

[Voe05b] M. Voelker, P. Fromherz. Signal transmission from individual mammalian nerve cell to field-effect transistor. *Small*, 1(2):206–210, 2005.

[Voe06] M. Voelker, P. Fromherz. Nyquist noise of cell adhesion detected in a neuron-silicon transistor. *Physical Review Letters*, 96(22), 2006. 228102.

[Wal06] F. Wallrapp, P. Fromherz. TiO2 and HfO2 in electrolyte-oxide-silicon configuration for applications in bioelectronics. *Journal Of Applied Physics*, 99(11), 2006. 114103.

[Wei96] R. Weis, B. Muller, P. Fromherz. Neuron adhesion on a silicon chip probed by an array of field-effect transistors. *Physical Review Letters*, 76(2):327–330, 1996.

[Wei97] R. Weis, P. Fromherz. Frequency dependent signal transfer in neuron transistors. *Physical Review E*, 55(1):877–889, 1997.

[Won81] R. G. Wong, R. D. Hadley, S. B. Kater, G. C. Hauser. Neurite outgrowth in molluscan organ and cell-cultures - the role of conditioning factor(s). *Journal Of Neuroscience*, 1(9):1008–1021, 1981.

[Woo99] M. A. Woodin, T. Hamakawa, M. Takasaki, K. Lukowiak, N. I. Syed. Trophic factor-induced plasticity of synaptic connections between identified Lymnaea neurons. *Learning & Memory*, 6(3):307–316, 1999.

[Woo02] M. A. Woodin, D. W. Munno, N. Syed. Trophic factor-induced excitatory synaptogenesis involves postsynaptic modulation of nicotinic acetylcholine receptors. *Journal Of Neuroscience*, 22(2):505–514, 2002.

[Zec01] G. Zeck, P. Fromherz. Noninvasive neuroelectronic interfacing with synaptically connected snail neurons immobilized on a semiconductor chip. *Proceedings Of The National Academy Of Sciences Of The United States Of America*, 98(18):10457–10462, 2001.

[Zec02] G. Zeck. *Halbleiterchip mit einfachem biologischen neuronalen Netz*. PhD thesis, Technical University Munich, 2002.

[Zec03] G. Zeck, P. Fromherz. Repulsion and attraction by extracellular matrix protein in cell adhesion studied with nerve cells and lipid vesicles on silicon chips. *Langmuir*, 19(5):1580–1585, 2003.

[Zei04] R. Zeitler. *Elektrisches Interfacing von Schneckenneuronen an CMOS Chips*. PhD thesis, Technical University Munich, 2004.

[Zre02] E. Zrenner. Will retinal implants restore vision? *Science*, 295(5557):1022–1025, 2002. Editorial Material.

The author would like to thank:

Prof. Peter Fromherz for the challenging, yet rewarding project,

Prof. Naweed Syed from the *University of Calgary* for his willingness to share his skills and expertise on *Lymnaea* cell culture,

Doris Eckerlein for support and fruitful discussion regarding cell culture,
Alexander Kunze for design and assembly of the chip amplifier and multiplexing boards,
Carool Popelier from the *Vrije Universiteit Amsterdam* for multiple trips to Munich and a legion of donated snails,

Günther Zeck for a tutorial in snail cell culture and physiology,
Matthias Merz for his boldness to instigate a cooperation between Dr. Naweed Syed and Prof. Peter Fromherz,
Dr. Raimund Gleixner for the tutorial about the FLIC experimental setup and data analysis,

Dr. Moritz Völker, Dr. Armin Lambacher, Dr. Ingmar Schön, Dr. Frank Wallrapp & Ralf Zeitler for various contributions to the success of this project
The whole Membrane and Neurophysics Department for critical observations and fruitful discussions,

My family for their continuing support and faith in me,

Sonja Golla for her direct, yet charming way of keeping me going.